Summer 2011

Molecular and Immunohistochemical Identification of a Sodium Hydrogen Exchanger-2C (Nhe2C) Paralog in the Gills of Marine Longhorn Sculpin (Myoxocephalus Octodecemspinosus)

Demi Brett Rabeneck

MOLECULAR AND IMMUNOHISTOCHEMICAL IDENTIFICATION OF A SODIUM HYDROGEN EXCHANGER-2C (NHE2C) PARALOG IN THE GILLS OF MARINE LONGHORN SCULPIN (*MYOXOCEPHALUS OCTODECEMSPINOSUS)*

by

DEMI BRETT RABENECK

(Under the Direction of James B. Claiborne)

ABSTRACT

Sodium hydrogen exchanger proteins (NHEs) are members of the cation proton antiporter superfamily (CPA) and are thought to function in fish for maintaining physiological ion concentrations and acid-base balances by excreting excess H^+ ions from the body in exchange for Na^+ ions. There are many more types of these proteins in teleost fish than in mammals due to putative genome duplication. This study describes a new form of NHE2 in the gills of marine longhorn sculpin, *Myoxocephalus octodecemspinosus*, designated NHE2c. Sequencing revealed that the NHE2c nucleotide-coding region transcribes a peptide 795 amino acids in length with an estimated molecular weight of 89.2 kDa. Data shows that NHE2c is a unique peptide from previously described NHE isoforms, including the NHE2 family. A polyclonal antibody made against NHE2c and used in double and triple labeled immunohistochemical experiments detected the peptide on the apical edge of gill cells that also contained Na^+-K^+-ATPase and NHE2b. Western blot analysis detected two protein bands at approximately 45 kDa and 75 kDa. These extra copies of NHE2 in the sculpin genome pose an intriguing question of why the proteins are synthesized in the first place. While, in the future, studying syntenic NHE paralogs in the NHE2 family of longhorn sculpin could give us an evolutionary perspective to homologous NHEs in higher vertebrates.

INDEX WORDS: Sodium hydrogen exchangers, NHE2c, Marine longhorn sculpin gills, *Myoxocephalus octodecemspinosus,* Frenchman Bay, ME

MOLECULAR AND IMMUNOHISTOCHEMICAL IDENTIFICATION OF A SODIUM HYDROGEN EXCHANGER-2C (NHE2C) PARALOG IN THE GILLS OF MARINE LONGHORN SCULPIN (*MYOXOCEPHALUS OCTODECEMSPINOSUS)*

by

DEMI BRETT RABENECK

B.S., University of Central Arkansas, 2007

A Thesis Submitted to the Graduate Faculty of Georgia Southern University in Partial Fulfillment of the Requirements for the Degree

MASTER OF SCIENCE

STATESBORO, GEORGIA

2011

MOLECULAR AND IMMUNOHISTOCHEMICAL IDENTIFICATION OF A SODIUM HYDROGEN EXCHANGER-2C (NHE2C) PARALOG IN THE GILLS OF MARINE LONGHORN SCULPIN (*MYOXOCEPHALUS OCTODECEMSPINOSUS)*

by

DEMI BRETT RABENECK

Major Professor: James Claiborne
Committee: Laura Regassa
Danny Gleason

Electronic Version Approved:
July 2011

DEDICATION

I dedicate this thesis and the time that I've spent in graduate school to my pawpaw, whose presence is always with me and who finally understands what I've been doing. Time is precious and life is short.

ACKNOWLEDGMENTS

Thank you to the scientists of the Claiborne and Evans 2009 and 2010 Mount Desert Island Biological Laboratory for teaching me about molecular biology and fish physiology. These things I would have never learned without their instruction. These people include: Dr. Claiborne, Andrew Diamonduros, Dr. Edwards, Dr. Evans, and Hana Kratochvilová.

Thank you to all the people who have helped me along the way to receiving my M.S., including, but not excluded to: my committee, Dr. Gleason and Dr. Regassa, as well as LaToyna Wilson and Cynthia Chan. John Riggs, you are much appreciated, too.

TABLE OF CONTENTS

LIST OF TABLES

LIST OF FIGURES

CHAPTER 1

Introduction

All animals must overcome internal acid-base imbalances caused by metabolic, respiratory and environmental factors. If homeostatic mechanisms fail to regulate pH, then metabolic acidosis may be induced. Respiratory acidosis occurs when less than normal amounts of CO_2 are expired from the animal. Environmental acidosis results from the presence of more CO_2 in the organisms' ambient surroundings then what it is acclimated to, and in the case of aquatic organisms, more acidic H^+ ions upon CO_2 hydration:

$$CO_2 + H_2O \Leftrightarrow HCO_3^- + H^+$$

In terrestrial animals metabolic acidosis commonly develops from the breakdown of proteins, fats and carbohydrates, dysentery, diabetes mellitus ketoacidosis, increased organismal activity and renal failure, where by the body cannot rid itself of even baseline levels of H^+ ions (Sherwood et al., 2005). As described below, homeostatic challenges in the extracellular fluid are even greater for aquatic organisms.

Challenges to maintaining homeostasis in fish

Unlike most terrestrial animals, fish have a limited capacity to combat extracellular acid-base imbalances by respiratory and renal mechanisms. Oxygen concentration in water at 12°C is approximately 6 mL/L; in air the oxygen concentration is approximately 210 mL/L (Weiss, 1970). So fish ventillatory rate is high in order to extract as much oxygen from the water as possible. Therefore, CO_2 is excreted at a high rate, and is highly soluble in water. This makes internal pCO_2 too low to be expired at any significant amount that will shift the Henderson-Hasselbalch equation to the right, in turn lowering extracellular pH by means of the bicarbonate buffering system.

Marine fish must work to retain water since it is lost to the hyperionic environment by osmosis. To counteract this water loss, marine teleosts drink water and have low urine flow rates of 0.03 to 0.45 mL kg^{-1} h^{-1} (Marshall and Grosell, 2006). The urine is not hyperosmotic to the blood, but marine teleosts do increase salt wasting in order to

copious amounts of urine to counteract the large volume of water that is absorbed by osmosis, but like the marine teleosts, the gills are their main sites for ion uptake in these animals as well.

Gills as a homeostatic organ

The gills, in contrast to the kidneys, experience a flow rate of seawater over the gill that is 100 to 400 mL kg^{-1} min^{-1}, making this tissue a more suitable site for waste excretion, in the form of ammonia, and for direct ion and acid-base transfers with the environment.Gills provide a vital regulatory boundary between the hypersaline marine environment and the animal. They not only serve as waste removal organs, but also regulate ion balance and cell integrity. Acid/base, ion, and water regulation are primarily branchial functions, as opposed to renal actions in humans (Evans et al., 1982). Fish have similar ammonia renal excretion to mammals, but the magnitude of waste removal by the kidneys is two-orders of magnitude less than that of the gills (Janis and Farmer, 1999). Renal excretion of Na^+, Cl^- and NH_4^+ when marine sculpin were transferred to a dilute seawater environment was less than 1% of branchial excretion rates (Claiborne et al., 1994). Even air-breathing fish like the African and South American lungfishes utilize their gills for CO_2 and nitrogen excretion, reinforcing the concept that gills play a vital role in waste removal (Janis and Farmer, 1999).

Gills have a thin integument and a large surface area in relation to body size that increases diffusion rates of ions like Na^+, Cl^-, H^+, and HCO_3^-. Extending from the gill arch are long filaments, from which primary and secondary lamellae branch (Figure 1, Figure 2), all of which are in contact with the ambient water environment. Lamellae, the respiratory organs of the gill, allow the fish to acquire adequate concentrations of O_2 through a countercurrent flow mechanism, in an environment where oxygen concentration is low (Figure 1) (Weiss, 1970). Diffusive permeability to ions across the gills, along with constant drinking of the seawater, introduces large amounts of salt to the intracellular and extracellular compartments of the marine fish. However, despite Na^+ entry via sodium-hydrogen exchanger proteins (NHEs), for example, it has been shown in the marine toadfish, *Opsanus beta*, that the branchial NHEs account for only 10% of the total Na^+ uptake of this ion (Evans, 1982).

Deoxygenated blood from the ventral aorta of the fish flows through the gill filament into the afferant filamental artery. This blood in the afferant filamental artery branches off into the lamellae via the pre-lamellar arteriole where it meets oxygenated water moving in the countercurrent direction. Oxygen diffuses from the water into the pre-lamellar arteriole and the oxygenated blood is pooled in the post-lamellar arteriole, where it travels through the efferent filamental artery and returns to aerate deoxygenated tissue (Figure 1) (Evans et al., 1999). In fish, the region of the filament that contains the afferant filamental artery is referred to as the afferant edge, and the side where the efferent filamental artery collects the oxygenated blood is called the efferent edge.

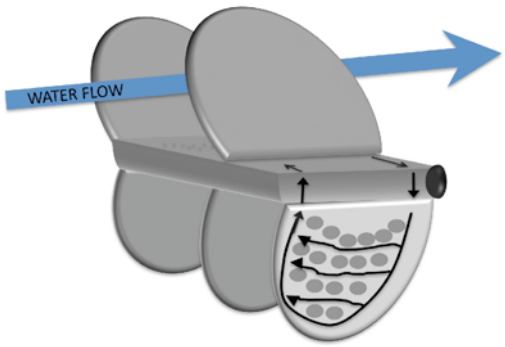

Figure 1: Diagram of a single filament and five lamellae showing the countercurrent direction of water to the flow of blood within a lamella. Deoxygenated blood from the ventral aorta of the fish flows through the gill filament into the afferant filamental artery and branches off into a lamella via the pre-lamellar arteriole. Blood in the prelamellar arteriole flows between pillar cells. Oxygen diffuses from the water into the pre-lamellar arteriole and the oxygenated blood in the post-lamellar arteriole travels through the efferent filamental artery and returns to aerate deoxygenated tissue. Mitochondira-rich cells (MRCs), indicated by a concave ovule, which possibly contain sodium hydrogen exchanger proteins (NHEs), are thought to be more concentrated along the afferent edge of the interlamellar region. Redrawn from Evans, 1999

There are several types of cells in the gill epithelium. Pillar cells are arranged on the gill filament between lamellae to regulate the width available for water flow (Evans et al., 1999). Mitochondria-rich cells (MRCs) are the main cells where osmoregulatory transfers take place and where NHEs have been located (for a review see Evans 2005). MRCs are most abundant on the afferant edge of the gill filament, in the region between lamellae, the interlamellar region, and rarely found on the lamellae of marine species (Evans et al., 2005). MRCs extend across the width of the gill epithelium, from the blood compartment at the basolateral membrane to the apical membrane that is in contact with the ambient water. MRCs are adjacent to accessory cells where a leaky paracellular pathway is thought to be the site of passive extrusion of Na^+ ions to the environment (Figure 3). Pavement cells surround these latter two cell types and make up the majority of the cell population on gill epithelia, but are thought to play a passive role in osmoregulation (for review of fish gill anatomy see Evans, 2005).

Figure 2: Light micrograph of branchial filaments and lamellae that extend perpendicularly, like rungs on a ladder. Claiborne, unpublished data.

Mitochondria-rich cells: Evidence and function

Currently accepted ideas concerning marine teleost osmoregulation strategies were first published in the 1930s. These studies concluded that marine teleosts drink salt water to replace the water lost by osmosis to their hyperosmotic environment; that components of the ingested seawater, including Na^+, Cl^- and K^+, are absorbed by the intestine, which facilitates the uptake of water into these tissues; and that the divalent ions, including Mg^{2+} and SO_4^{-2}, are eventually excreted in the urine. Na^+, Cl^-, and K^+ are extracted from the ingested seawater extrarenally, as these ions are present in very low concentrations in urine and the blood (marine teleost blood is hypotonic to seawater) (Smith, 1930). Apart from ingesting salt, evidence for Cl^- movement across the gills of freshwater teleost was provided by a series of isolated fish experiments in which Cl^- was depleted from the aquarium solution of a known Cl^- concentration (Krogh, 1937). Marine fish have an even thinner gill integument that freshwater fish, making it even more suitable for salt uptake.

The sites for active chloride secretion were thought to take place in "chloride cells," and were first described by microscopic investigation as being large, ovoid and mostly located at the base of the lamellae (Keys and Willmer, 1932). This interlammelar region for chloride cells is an ideal location, he postulated as to not deplete the oxygen in the efferent blood supply. Evidence that "chloride cells" were the site for NaCl absorption and H^+ excretion first came when euryhaline killifish, *Fundulus heteroclitus,* gills were perfused with an autoradiographic ouabain, an inhibitor to Na^+ uptake, that specifically and densely stained "chloride cells" (later named "mitochondria rich cells" [MRC]) (Karnaky et al., 1976). Chloride cells extend the entire width of the gill epithelium from the basal lamina to the apical membrane, so it was also interesting when this work isolated Na^+-K^+-ATPase to the basolateral membrane of MRCs. In a parallel experiment, it was determined that adding ouabain, an inhibitor of Na^+-K^+-ATPase, to the serosal side of gills, caused Na^+ influx to nearly cease (Silva et al., 1977). Thus Na^+-K^+-ATPase drives Na^+ movement from seawater by maintaining an intracellularly directed Na^+ gradient. The Silva model refuted earlier predictions that Na^+ -K^+ -ATPase should be located on the apical membrane of marine teleosts as to rid the animal of excess salt (Maetz, 1971). Sophisticated eletrophysiological studies from isolated killifish opercula

epithelium revealed a chloride current present in MRCs and not in pavement or accessory cells of the branchial tissue, concluding that these were the sites for active salt excretion (Karnaky et al., 1977; Foskett and Scheffey, 1982).

Once the mitochondria-rich cells were established as the main site for ion and acid-base regulation, many studies followed that sought to identify the cellular proteins responsible for maintaining these ion transfers. Na^+-K^+-ATPase creates an electrochemical gradient that drives the movement of Na^+ and K^+ across the basolateral membrane into the cell via a Na-K-2Cl cotransporter (Figure 3) (Pelis et al., 2001). Cl^- subsequently leaves the cell through apical Cl^- channels, termed cystic fibrosis transmembrane channels (CFTR), while some Na^+ is reabsorbed into the blood by Na^+-K^+-ATPase for extracellular fluid absorption, ion recycling, and maintenance of a low intracellular Na^+ concentration. Plasma HCO_3^- is recycled from the blood via a Na^+–HCO_3^- cotransporter. There is evidence for a Cl^- /HCO_3^- antiporter in the apical membrane of epithelial gill cells that aids in lowering pH of an alkaline cellular compartment (Claiborne et al., 1997) or functions in raising the bicarbonate concentration during internal acidosis (Toews et al., 1983; Claiborne and Heisler, 1986). The reversal of this protein depends on if either more Cl^- or more HCO_3^- is initially bound (Knauf et al., 2002).

Cl^- exit from the cell creates a greater positive transepithelial potential that causes the movement of Na^+ out into the seawater via paracellular Na^+ leak channels located between the MRC and accessory cells (Evans et al., 1999). The low intracellular Na^+ concentration drives the movement of Na^+ into the cell, via apical sodium hydrogen exchangers (NHEs), that is coupled to the extrusion of H^+ in order to raise intracellular pH (Claiborne et al., 2002). When stenohaline and euryhaline fish are transferred from seawater to freshwater, Na^+ and Cl^- influx rates are sharply decreased, indicating NHE dependence on external Na^+ and Cl^- concentrations (Maetz, 1971; Bentley et al., 1976; Claiborne et al., 1994; Edwards et al., 2005). If external Na^+ concentrations, which are typically around 35 g/L (500mmoles/l) in seawater, are lower than intracellular Na^+ concentrations, normally 55-80mmol/L, then passive sodium entry with NHE may cease (Morgan et al., 1994), although NHEs can also be powered by increased pH gradient.

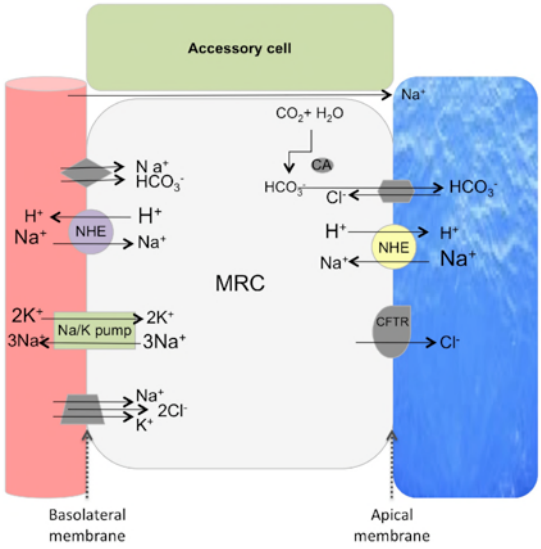

Figure 3: Current gill acid-base- and ion-regulatory model in seawater fish. Na^+-K^+-ATPase drives Na^+ movement via NHEs from the higher concentrated seawater by maintaining a low intracellular Na^+ gradient. The NHE antiporters transport excess H^+ ions to the ambient environment.

Sodium-hydrogen exchanger proteins (NHEs)

NHEs, also called solute carrier 9A proteins (SLC9A), are in the superfamily of monovalent cation proton antiporters (CPA). The electroneutral exchange of one extracellular Na^+ ion for one intracellular H^+ ion by NHE is one of the main mechanisms cited in the maintenance of intra- and extracellular pH regulation (Claiborne et al., 1999). Perhaps this is because of the ubiquitous presence of NHEs in organisms from all kingdoms and phyla, its diverse role in many physiological and pathological processes, or because of the inherent energy efficiency of NHEs, established by the passive sodium gradient in a marine environment (Brett et al., 2005; Malo and Fliegel, 2006). NHEs have been reported in various tissues from all eukaryotic lineages, including polarized cells of slime mold, *Dictyostelium discoideum* (Patel and Barber, 2005), sea urchin eggs (Johnson et al., 1976), myocardial cells (Fliegel and Dyck, 1995), kidney and intestinal epithelium, as well as in prokaryotic organisms. Studies have shown that NHEs, along with other regulatory proteins, have a role in acclimating organisms to stressful environments

(Orlowski and Grinstein, 2004). For example, the identification of a NHE 3 isoform on the apical gill membrane of Osorezan dace, possibly indicates that this protein allows this teleost to live in the 3.5-pH Osorezan Lake of Japan (Hirata et al., 2003). The sodium hydrogen antiporter (NHA) in bacteria, part of the CPA superfamily along with NHEs, allows *E. coli* to live in diverse environments (Orlowski and Grinstein, 2004). Also, various NHE isoforms in the euryhaline killifish (*F. heteroclitus*) may be differentially expressed and regulated in response to varying salinities (Edwards et al., 2005).

In the absence of extracellular sodium and in the presence of amiloride, a Na^+-K^+-ATPase inhibitor, Na^+/H^+ antiport activity nearly ceases. Therefore the uphill extrusion of H^+ ions from the cell via NHE is energized by the passive diffusion of Na^+ into the cell (Evans, 2008). An allosteric binding site in some NHEs is made apparent by the acceleration of Na^+ entry with decreasing intracellular pH (Aronson et al., 1982). Since the Na^+/H^+ exchange is electroneutral, there must be multiple H^+ ion binding sites in which NHE stays activated for continuous H^+ extrusion until the cell has returned to its physiological pH. Thus, two components may be needed to fully activate NHEs: an intracellularly directed Na^+ gradient and a high internal acid concentration (McDonald et al., 1982).

There is evidence for multiple NHE isoforms based on observations that these different antiporter versions respond to pharmacological inhibitors with different sensitivities; have completely different amino acid sequences in non-conserved regions; and are regulated differently depending on growth factors, protein kinases and cellular location (Wakabayashi et al., 2000). Additional NHEs are present in the teleost genome as a result of a genome duplication that is thought to have occurred after the divergence of teleosts from the tetropod lineage (Figure 4) (Volff, 2004). New genes can arise from mutagenic gene duplications in which homologous chromosomes achieve functional diversification and become unique homologues (Ohno, 1970). NHE1-NHE11 have been described in humans and there are at least 16 unpublished NHEs in the human genome based on sequence data (Diamonduros, personal communication). These isoforms are separate gene products and not the result of differential gene splicing from a single gene (Coupaye-Gerard, B. 1996).

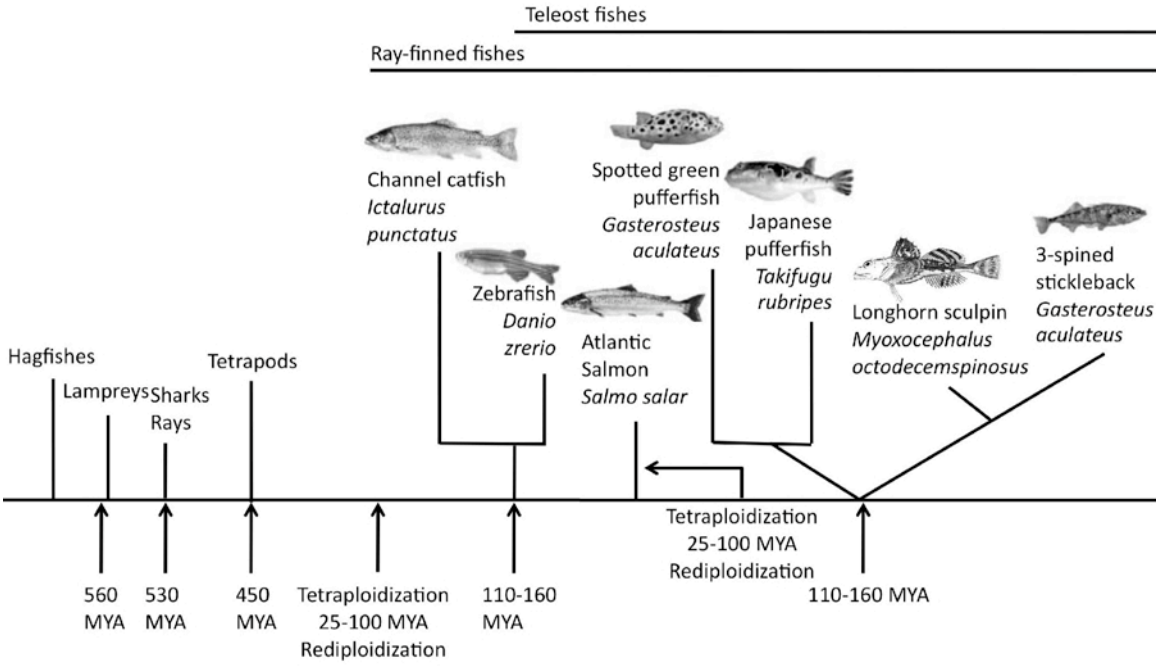

Figure 4: Genome duplications that may have occurred in the ray-finned fish lineage before the evolution of the teleost lineage. Because of the close evolutionary relationship between longhorn sculpin and 3-spined stickleback, cross-compatible NHE2c primers were designed based on the 3-spined stickleback genome, which has been sequenced, and used to amplify the unknown sculpin NHE2c sequence. Redrawn from Volff, 2004.

.

NHE1

NHE1 has a ubiquitous expression in nearly all vertebrate tissue (Yun et al., 1995; Coupaye-Gerard et al., 1996; Claiborne et al., 1999). Maybe this is the reason it was the first NHE isoform to be cloned (Sardet et al., 1989). Cellular expression has been targeted to the basolateral membrane by way of a pulse chase experiment and subsequent anti-NHE antibody labeling that detected a 110 kDa, N-glycoslyated protein in amphibian kidney cells (Coupaye-Gerard et al., 1996).

In general, NHE1 protects the blood from alkalinization by moving H^+ from the cytoplasm into the extracellular fluid by way of the basolateral membrane. If the plasma is too acidic, NHE1 expression is downregulated. In this sense, NHE1 is referred to as the "housekeeping" NHE. NHE1 is the predominant NHE isoform in mammalian sarcolemmal tissue of myocardium and may help to raise intracellular pH to overcome inadequate blood supply brought on by ischemia (Fliegel and Dyck, 1995). A NHE1 driven increase in cellular pH transitions the cell from G2 phase to the mitotic cycle so that cell proliferation occurs in a timely fashion (Putney and Barber, 2003). Northern blot analysis using a human anti-NHE1 probe detected an 8.0 kb NHE1 mRNA in the branchial tissue of marine longhorn sculpin with a lower expression in the small intestine, kidney, red blood cells and bladder of this same species (Claiborne et al., 1999). In this same study, Western blot analysis using human NHE1 antibodies identified an 80 kDa gill protein in mummichog and a 90 kDa in sculpin. NHE1 protein expression in *M. octodecemspinosus* decreased in response to 0.1mol/L HCl stimulated acidosis (Claiborne et al., 1999) and in hypercapnic, fresh water adapted *F. heteroclitus*. They speculated that this protein downregulation was possibly to increase the efficiency at which apical NHEs excreted H^+ out of the fish.

Even though NHE isoforms have different physiological roles depending on cellular location, NHEs share a conserved protein structure (Malo and Fliegel, 2006). The majority of all NHE structures have been deduced from the ubiquitously expressed NHE1. NHE proteins have 2 distinct domains. An N-terminal domain of approximately 450-500 amino acids comprised of 11-12 transmembrane spanning units, that create extra- and intracellular loops, and a C-terminal domain of approximately 130-450 amino acids that resides in the cytoplasm. Approximately 60% nucleotide homology exists

between transmembrane segments 2-12 (Coupaye-Gerard et al. 1996) in isoforms NHE 1-NHE 5 but there is only 30% homology in the C-terminal of these membrane bound NHEs. Despite the nucleotide sequence homology in the N-terminal region of NHE isoforms, the first transmembrane segment and the first extracellular loop differ completely in their amino acid sequence (Wakabayashi et al., 1997). The N-terminal alone was shown to be sufficient for NHE insertion into the plasma membrane and for 25% Na^+ transport when C-terminal deletion mutants were expressed in a transporter-deficient fibroblast cells (Wakabayashi et al., 1992). Deletion of the cytoplasmic domain shifted the pK value for the intracellular H^+ to an acidic range, which implies that the C-terminal domain controls the pH set point value while a H^+ allosteric modifier site is present in the amino-terminal domain. Deletion mutants without the C-terminal domain completely abolished growth factor induced NHE activation. In this NHE-1 domain analysis it was concluded that activation of NHE occurs through reversible phosphorylation-dependent coupling of the C-terminal cytoplasmic domain to the H^+ modifier site (Wakabayashi et al., 1992).

Two different NHE 1 membrane domain structural topologies exist to date. One study incorporated cysteine residues into a cysteine-free NHE1 to determine the accessibility of those cysteines with a biotinylated antibody. If the antibody could not bind, this section of the protein was determined to be located within the cytoplasm. The second study used the recently described crystal structure of NHaA in *Escherichia coli* (Hunte et al., 2005) as a template to construct a computational model of NHE-1, which is based on the assumption that these two proteins, even though part of two different families (CPA1 and CPA2), are evolutionary related. The two models do not agree on the exact transmembrane spanning region that forms the Na^+ channel of NHE-1, but a third study which evaluated each transmembrane unit with nuclear magnetic resonance (NMR) suggests that transmembrane regions VII and XI of the cystein-free model and transmembrane region 4 and 11 of NHaA in *E. coli* are equivalent, possibly meaning they share the same Na^+ transport function. It is thought that NHaA activation induces a conformational change that allows transmembrane regions 4 and 11 to expose the Na^+ receptive sites (Olkhova et al., 2006).

NHE2

NHE2 was first identified from rat colon RNA via cross reactivity with a NHE1 cDNA probe (Wang et al., 1993); NHE2 has 42% nucleotide sequence homology with NHE1. This same study further showed that NHE2 expression was greatest in the small intestine, large intestine and stomach. It was minimally expressed in the brain, kidney, testis, uterus, heart and lungs. This is different from rabbit NHE2, which has equal expression in the kidney and intestine. Within the mammalian kidney, NHE2 is predominantly expressed in the cortical thick ascending limb, macula densa and distal convoluted tubules (Orlowski and Grinstein, 2004). Within the intestine, NHE2 is found in the jejunum, ileum and colon (Malo and Fliegel, 2006). This isoform is thought to be subapically and apically expressed (Chow, 1999). NHE2 in PS120 cells, a fibroblast cell line that lacks all endogenous NHE expression, exists as 2 isoforms: a 75 kDa isoform that is netheir O- nor N-glycosylated and an 85 kDa protein that is O-glycosylated (Cavet et al., 1999). The majority (64%) of the glycosylated, 85 kDa protein is found on the cell surface, while only a small proportion (20%) of the non-glycosylated form of NHE2 protein resided at this location.

Within both the kidney and intestine, NHE2 is thought to function in electrolyte absorption and acid secretion. In NHE3 null mice, HCO_3^- is not reabsorbed by NHE3 in the proximal tubule and is carried to the distal tubule, where systemic acidosis causes NHE2 to facilitate absorption of Na^+ along with HCO_3^- (Bailey et al., 2004). Immature mice with NHE2 mutant genes possessed parietal cells of the gastric mucosal epithelium capable of acid secretion, but these intestinal mucosal cells were in various stages of degeneration (Schultheis et al., 1998). They speculated that the presence of NHE2 in early stage parietal cells were critical for their viability.

NHE2 was detected in marine longhorn sculpin gill tissue using PCR and RT-PCR with degenerative primers for homologous, mammalian NHE proteins; this was the first non-mammalian species to which this isoform was assigned (Claiborne et al., 1999). Sculpin NHE2 of the branchial tissue had 76% amino acid homology and 61% nucleotide homology to mammalian species in which NHE2 had been cloned. Claiborne et al. (1999) proposed that NHE2 might have a comparable role in acid excretion as in the renal and intestinal epithelium of rat, rabbit and human. Mammalian NHE2 antibodies

were used to probe tilapia gill homogenates and detected a double band on Western blots at approximately 87 kDa (Wilson et al., 2000). No bands were detected in basolateral membrane fractions. In euryhaline mummichog adapted to fresh water, NHE2 was detected at 85 kDa on Western blots and expression increased after exposure to 1% hypercapnia. NHE2 was not consistently detected in saltwater adapted animals (Edwards et al., 2005).

The first study to use fish-specific NHE2 antibodies for immunocytochemical labeling detected a NHE2 peptide on the subapical and apical membrane of branchial MRCs, along the interlammelar region, in marine longhorn sculpin (Catches et al., 2006). Although NHE2 was mostly found in MRCs, exhibiting a punctate staining pattern, the cotransporter covered a smaller area than sodium potassium ATPase in the cell. They postulated that baseline NHE2 expression was sufficient to control an increase in metabolic pH, since there was no detectable, immunohistochemical difference in gill control and acidotic groups. Western blot analysis with fish-specific antibodies bound to an 85 kDa protein and showed no significant difference between controls and fish subjected to acid exposure. To date, only one type of NHE2 had been demonstrated in fish, though the multiple copies due to genome duplication may indicate that additional NHE2 isoforms exist in some teleost species (Edwards et al., 2010).

NHE3

NHE3 was the second Na^+/H^+ antiporter to be cloned in mammals (Tse et al., 1992) and is thought to have changed little in the evolutionary time period from the elasmobranchs to the divergence of the tetrapod lineage, but evolved quickly in teleosts, so may possibly least related to other NHEs (Choe et al., 2005). In mammals, NHE3 has been identified in the intestine, and in the proximal tubule and thick ascending limb of the kidney, where in both anatomical locations the protein is crucial for Na^+ and water reabsorption (Vallon et al., 2000). Disruption of the NHE3 gene in the mouse intestine results in diarrhea, low blood pressure and mild metabolic acidosis. However, deletion of NHE1 and 2 showed little effect (He and Yun, 2010). Similarly, in renal cells, Ledoussal (2001) suggests that NHE3 expression may be indispensable for Na^+ absorption in the kidney, since mice with null copies of NHE3 and with wild-type NHE2 were not able to transport Na^+ across the epithelial cells, and increased amounts of Na^+ were found in the

urine (Ledoussal et al., 2001). NHE3 was the critical exchanger for renal Na^+ absorption and acid-base balance, since NHE3 null mice died. However, Bailey et al. (2004) suggests that this double knock-out experiment activated other renal acid-base compensatory mechanisms that could have accounted for the Na^+ uptake despite a mutant copy of NHE2.

In mammals, there is much evidence presented that shows the NHE3 isoform has an apical and an intracellular location on the apical membrane of recycling endosomes (Chow, 1999). NHE3 is neither N- nor O-glycosylated, which may explain its recycling plasma membrane and intracellular location, since glycosylation signals peptides to the cellular plasma membrane (Cavet et al., 1999).

With immunohistochemistry techniques using NHE3 fusion antibodies made against rabbit, NHE3 expression was located in the brachial epithelium of a marine blue-throated wrasse displayed in cuboidal cells that covered a large surface area along the apical membrane (Edwards et al., 1999). However, using the same mammalian NHE3-specific antibody, the isoform was expressed in freshwater fish on the basolateral side, similar to the saltwater fish in that the expression was mainly in the interlammelar region, but a few freshwater fish also expressed NHE3 on the lamellae (Edwards et al., 1999). NHE3 was always located in cells that coexpressed basolateral Na^+-K^+-ATPase in the Atlantic stingray, and was upregulated upon transfer from salt water to freshwater (Choe et al., 2005). NHE3 was also found to be located on the apical membrane of Osorezan dace that live in a highly acidic (3.5 pH) lake, suggesting this protein helps acclimate this fish to the acidic water that it ingests (Hirata et al., 2003). NHE3 was thought to be the predominant isoform responsible for Na^+/H^+ exchange in the marine longhorn sculpin, and has been located to the apical membrane of gill MRCs (Claiborne lab, unpublished data).

NHE4

NHE4 has a basolateral expression, and is located in most epithelial of mammalian renal cells, including the medulla, especially in cells lacking NHE1 (Bookstein et al., 1997; Orlowski and Grinstein, 2004). NHE4 regulates gastric acid secretion in the stomach, its predominant location in the gastrointestinal tract (Nakamura et al., 2005). NHE4 is a distinct isoform from NHE1 as it does not have the same sensitivity to

pharmacological inhibitors as does NHE1 and it has less affinity for intracellular H^+. This isoform is possibly better suited for ammonium exchange (NH_4^+) across the basolateral membrane of the thick ascending limb (Chambrey et al., 2001). The mammalian isoform is evolutionary similar to NHE2, since phylogenetic analysis shows that mammalian NHE2 always groups with NHE4, and the genes colocalize to the same chromosome region (Brett et al., 2005; Choe et al., 2005).

NHE5

NHE5 expression is restricted to the brain and may modulate the acidity of neurotransmitters, although its immunocytochemical localization and functional characterization has not been reported (Orlowski and Grinstein, 2004). NHE5 is most closely related to NHE3, with 53% amino acid identity in mammalian isoforms (Malo and Fliegel, 2006). NHE5 has even been found in endosomal compartments of fibroblast and neuronal cells (Brett et al., 2005). This isoform was found ubiquitously expressed in an 11-week-old human fetus (Brett et al., 2005).

NHE6-NHE11

pH and ion homeostasis is important throughout an organism, including transport vesicles in which proteins are carried to their final location. NHE6-NHE9 are positioned on the membranes of organelle compartments, such as the endoplasmic reticulum (ER) and trans-Golgi network, as well as recycling endosomes and late endosomes. Unlike NHE1-NHE5, and NHE10, that occur in specific patterns, in delimitative tissue types, orgenelle NHEs are ubiquitously and concurrently expressed in single cells.

Cells transfected with the full-length human NHE6 protein were probed with synthetic antibodies corresponding to the C-terminus of human NHE6 and located to the ER and plasma membrane (Miyazaki et al., 2001; Brett et al., 2002). Proteins are sent to the ER before being sorted into transport vesicles for relocation. Mutations in the NHE6 gene cause some forms of X-linked mental retardation (Gilfillan et al., 2008). This is due to the plausible role NHE6 has in regulating lumen pH. Thus a possible consequence of NHE6 inactivity could be lowered endosomal pH and decreased monovalent ion content, both of which might affect protein folding and trafficking. Recycling endosome trafficking is essential for growth of dendritic spines, a process considered to be the molecular basis of learning and memory.

NHE6 and NHE7 are ubiquitously expressed in tissues, but mainly distributed in skeletal muscle and brain (Ohgaki et al., 2010). Chimeras with C-terminal membrane-proximal regions of NHE7 indicated that this section of the isoform is required for localization to the trans-Golgi network (Fukura et al., 2010). NHE8 is located intracellularly in recycling endosomes and in the epithelial cells of intestine and kidney of rodents (Ohgaki et al., 2010). In mammalian kidneys, this NHE is present in renal brush boarder of renal proximal tubules (Goyal et al., 2003). Mammalian NHE8 is 25% identical to mammalian NHE1-NHE7 at the nucleotide level, and the NHE8-like clade, first seen in slime mold, is the oldest derived eukaryotic NHE (Piermarini et al., 2009). Preliminary studies in longhorn sculpin show that NHE8 is expressed throughout the cytoplasm and found in a wide array of gill cell types (Kratochvilova et al., 2009).

NHE9 localizes to late endosomes. In human tissue it is ubiquitously expressed, with the highest levels in heart and skeletal muscle and lower levels in liver, placenta, and kidney (Nakamura et al., 2005). Disruption of the NHE9 gene is a plausible foundation for neurological developmental disorders characteristic of Attention Deficit Hyperactivity Disorder (ADHD) per observation that this gene is disrupted in patients with this disease (de Silva et al., 2003).

NHE10 has been localized to the principle piece of the sperm flagellum with immunofluroescence microscopy, after finding the novel protein with an unbiased signal peptide trap screen, where a cDNA sequence of interest is fused to a reporter gene that targets the cell surface (Wang et al., 2003). Mice lacking this NHE were infertile, possibly due to the impediment of sperm motility by decreased intracellular pH. In fact, addition of ammonium chloride, which raises internal pH, improved sperm motility (Wang et al., 2003).

NHE11 function and immunocytochemical location are not known, but the NHE is located on human chromosome 1q25.1, is 1124 amino acids long and has a molecular weight of 12.9 kDa (Uniprot, 2007).

CHAPTER 2

Objective

Previously, NHE2 in sculpin was found to lack apical staining, implying that NHE3 is the predominant isoform during apical Na^+/H^+ exchange (Catches et al., 2006). The possibility of three paralogs of sodium hydrogen exchanger 2 (NHE2) in sculpin was first discovered on *Ensembl* when searching for a human ortholog of NHE2b, named solute carrier 9A2 (SLC9A2) (Diamonduros, personal communication). There were three NHE2s for the three-spined stickleback (*Gasterosteus aculeatus)*, an evolutionary descendant of longhorn sculpin, which were homologous to human SLC9A2 gene. The three stickleback paralogs were arbitrarily named 2a, for the first that was sequenced in the mummichung, *Fundulus heteroclitus*, the next 2b, the most synetic with humans and characterized in sculpin by Catches et. al. 2006, and finally 2c. The latter two are most similar in gene sequence. Since the stickleback and sculpin genomes are highly conserved, cross-compatible primers were made against the three-spined stickleback NHE2 paralogs for sculpin cDNA PCR amplification. LaRue et al. 2008 amplified a 1500 bp segment of sculpin NHE2c using primers that were designed based on the three-spine stickleback genome (LaRue, 2009). This sculpin amplicon was used to design forward and reverse gene specific primers as well as forward and reverse nested gene specific primers for the NHE2c RACE PCR. This is where the quest to sequence the protein and begin to unveil its functionality in sculpin began.

We hypothesize that the NHE2c RNA/cDNA transcript will be present in marine longhorn sculpin gill, that the protein will be located in mitochondria rich cells (MRCs), along with Na^+-K^+-ATPase and other previously described NHEs, and that the paralog will be further identified in gill homogenates. If NHE2c is located in MRCs by immunohistochemnical techniques, then it can be predicted that NHE2c may play an additional role in acid-base- and ion-homeostasis. To our knowledge, until now, NHE2c has never been molecularly characterized in a fish.

The first objective was to sequence the NHE2c of longhorn sculpin. NHEs are highly conserved, but unique isoforms have a distinct 3' nucleotide region (Brett et al., 2005). 3' RACE was performed to sequence this variable NHE domain. NHE proteins have been

successfully sequenced with RACE PCR methods in the Atlantic stingray (*Dasyatis Sabina*) (Choe et al., 2005), the spiny dogfish shark (*Squalus acanthias*) (Claiborne et al., 2008), the mummichog (*Fundulus heteroclitus*), and the longhorn sculpin NHE2 cDNA fragment (Gunning et al., 2001). Once the 3' nucleotide region was obtained, the cDNA was translated into amino acid sequence and an antigenic epitope of the carboxy-terminal was used to design a peptide-specific antibody.

Mammalian antibodies used against NHEs in the gills of fish have proven unsuccessful in detecting discriminatory binding of NHE2 (Edwards et al., 2005) and NHE3 (Edwards et al., 1999; Wilson et al., 2000), so the use of species-specific antibodies may be the most conclusive approach to characterizing sculpin NHEs. Accordingly, once the NHE2c antibody was made against the appropriate antigenic epitope of the –COOH terminus, the second objective of this study was to locate the peptide within intact gill sections of the longhorn sculpin, and to describe the location of the protein on the branchial filament and the proximity of NHE2c to two other proteins that are in support of the current acid-base- and ion-regulatory model (Choe et al., 2004; Catches et al., 2006). The α5 antibody binds to one of the α isoforms of Na^+-K^+ -ATPase, a likely indicator of a MRC, as this protein is highly expressed in these cells (Evans et al., 2005). A second antibody was used in colocalization, immunohistochemistry experiments in order to see how the location of the NHE2c paralog compares with the subapical NHE2b paralog, previously identified in the gills of longhorn sculpin (Catches et al., 2006).

(3) The third objective was to be able to detect NHE2c protein in gill homogenates from multiple fish, with the same autologous NHE2c antibody, in Western blotting. This second protein detection method provides further evidence that the NHE2c antibody is specific to its respective antigen (Choe et al., 2004).

Originally, a fourth objective of this project was to characterize the pH of Frenchman Bay, a habitat to the marine longhorn sculpin, and to simulate these values in aquaria in hopes of assessing the impact of environmental hypercapnia on NHE2c. Unfortunately while this objective was not completed, the pH of a small transect in Frenchman Bay was characterized (Appendix A).

Methods

Obtaining NHE2c cDNA sequence

Sculpin were caught by fishermen from Frenchman Bay, ME, and maintained in tanks with running seawater from the Bay. Within 1 week of capture, sculpin were anesthetized in MS-222 and terminated by spinal pithing. After sculpin sacrifice, holobranchs were homogenized for RNA extraction. Tissue for immunohistochemistry and Western blots were dissected from the same fish:1, 2 and 4 holobranchs from the right gill arch and 4 from the left were preserved overnight for immunohistochemistry with chilled 4% paraformaldehyde in 10mmol-l^{-1} phosphate buffered saline (PBS) adjusted to 7.4 pH; holobranch 1, 2 and 3 from the left gill arch were snap-frozen in liquid nitrogen for preservation until Western blotting.

RNA Isolation. Total RNA from gill tissue was isolated from longhorn sculpin using the Tri-Reagent RT method of extraction (Molecular Research Center, Inc., Cincinnati, OH). Before homogenizing the gill tissue in Tri-Reagent RT, the workstation and equipment, including homogenization probe and forceps, were cleaned with RNAase Zap, followed by 1% SDS, multiple washes in DEPC water, and finally Tri-reagent. Approximately 50-100mg of gill tissue in 1ml Tri-reagent was homogenized in a round-bottom 15ml Falcon tube on ice. The procedure separated the mixture into three layers: RNA (top, aqueous phase), DNA (interphase), and protein (lower, organic phase). The aqueous RNA phase was collected and transferred to a new tube for precipitation. RNA grade glycogen was added along with isopropanol so that a white-opaque pellet could be visualized at the bottom of the tube. The pellet was washed two times with EtOH before sterile DEPC water was added to the pellet, 10µl at a time, until it dissolved.

The total RNA was quantified and checked for purity with a Nanodrop 1000 Spectrophotometer (Thermo Scientific, Rockford, IL). Any background in the molecular biograde water was detected by first adding 1µl of the water to the pedestal. It was reblanked with 1µl of 1:1 molecular biograde water to phosphate buffer (Molecular Research Center, Inc., Cincinnati, OH). In the same volume ratio, 1µl of the RNA sample was added to 1µl of the phosphate buffer and 1µl of this solution was pipetted onto the pedestal. The RNA sample was measured for impurities by reading the A260/280 ratio

of the absorbance of nucleotides by the absorbance of proteins.

Reverse transcription. The RNA was reverse transcribed into first-strand complimentary DNA (cDNA) with SuperScript III RT (Invitrogen, Carlsbad, CA). Total RNA was added at 2μg per reaction along with dNTPs and GeneRacer Oligo dT Primer, in order to create a known 3' priming site, and then heated to 70°C for 5 minutes to eliminate secondary structure. The reaction was cooled at 4°C for ≥1 minute. The reverse transcriptase enzyme (SuperScript III RT) along with other optimizing reagents (5X First Strand Buffer, DTT, and Superase-Inh) were added and incubated at 50°C for 60 minutes. The reaction was terminated at 70°C for 15 minutes, and finally cooled to 4°C.

Primer design. Gene-specific, oligonucleotide primers were designed to amplify the first-strand cDNA so that the NHE2c cDNA product could be visualized with gel electrophoresis and sequenced (Table 1). Since the sculpin NHE2c sequence was unknown, an evolutionary descendant, 3-spined stickleback (*Gasterosteus aculeatus*), NHE2c sequence was used to design cross-compatible, gene-specific primers, and isolate a small part of the sculpin NHE2c sequence (LaRue, 2009). Once the sculpin amplicon was obtained, gene-specific primers were designed from the species-specific NHE2c sequence and were used to obtain the 5' and 3' ends of the transcript. Sculpin NHE2c gene-specific primers were also used to double-strand sequence the entire nucleotide transcript by primer walking its length. Primers were designed with Oligo 6 software (Molecular Biology Insights, Inc., Cascade, CO). The primers were ordered from Integrated DNA Technologies (Coralville, IA).

To obtain the 5' and 3' ends with the Marathon protocol, antisense 5' gene specific primers and 5' nested gene specific primers, along with sense 3' GSP and 3' nested GSP were designed with optimal parameters indicated in the Marathon protocol. The primers needed to be between 23-28 nucleotides in length for highest binding specificity, have 50-70% GC content to reach high annealing temperatures (Tm ≥ 65°C; best Tm ≥ 70°C), and preferably a GC clamp at the 3' end. Primers with self-complementary sequences that could fold back and form intramolecular hydrogen bonds were avoided. Similarly, primers that had complementarity to the Marathon Adaptor Primer (AP1 and AP2), particularly in the 3' ends, were avoided.

In addition to the 5' and 3' GSPs and nested GSPs, positive control primers that were

complimentary to either the 5' or 3' gene specific primers were designed to create overlapping PCR products. This positive control should have amplified a single band. This would confirm that the cDNA was present in the adaptor-ligated double stranded DNA and that it could be amplified.

Polymerase Chain Reaction and Agarose Gel Electrophoresis. Polymerase chain reaction (PCR), using cross-compatible and gene specific, oligonucleotide primers, to amplify NHE2c sculpin cDNA was performed using FastStart *Taq* Polymerase (Roche,Indianapolis, IN) and a Px2 Thermo Cycler PCR machine (Thermo Electron Corporation) in a 50μl reaction. The components of the 50μl master mix along with sculpin cDNA were centrifuged briefly to mix. The PCR cycles were specific to the primer annealing temperatures and expected product size (Table 1). In general, the first stage cycled once at 95°C for 3 minutes to denature the double stranded cDNA, then the optimal primer annealing temperature plus 5°C for 30 or 45 seconds, and 72°C for 2 minutes for elongation. During stage two, the PCR reaction was first heated to 95°C for 30 seconds, then decreased to the primer annealing temperature for 30 to 45 seconds, and finally elongated at 72°C for 1 minute/kilobase. The second stage cycled 35 times. The third stage gave the amplified cDNA extra extension time at 72°C for 10 minutes. Finally the reaction was cooled to 4°C for holding.

After completion of PCR, the products were mixed with 1.0μl of 6X loading buffer and electrophoresis was performed on a 1% or 2% agarose gel (Fisher Scientific, Waltham, MA; 200-600 bp resolution on 1% agarose; 700-1500 bp with 2% agarose) in 1X TAE (Tris-acetate-EDTA) stained with eithidium bromide (0.01%, .5 μl/45 ml gel) for visualization under UV light. The voltage used for electrophoresis was usually set at approximately 60-90 V for 25-45 minutes depending on the gel size and dimensions. If there was a significant background smear or multiple DNA bands in the range of expected size, the masked PCR fragments were resolved with low-melt gel electrophoresis and excised from the gel. The excised fragments were either sequenced or used as a DNA template in subsequent PCRs with internal, nested primers.

Low-meltAgarose Gel Electrophoresis. Many times the PCR product would not be comprised of a single band, so the DNA fragments from one product would be slowly separated from each other with Seaplaque agarose (Fisher Scientific) in 1X TAE at 1%,

2% or 3% concentration (using a higher concentration for good resolution under 500 bp). NuSieve GTG Agarose in 1X TAE, a low melting temperature agarose (Lonza, Fisher Scientific Company), was used for resolution down to 50 bp or less. The great sieving capacity of low-melt gels yields separated band products that can be sliced out of the gel with a sterile razor, followed by preparation for sequencing. Low-melt agarose has been modified so that the boiling point is lowered from over 90°C to around 65°C. This makes the recovery of undamaged DNA from the extracted gel slice possible since the melting temperature for the gel is lower than the nucleic acid denaturing temperature.

Marathon RACE cDNA Amplification. The Marathon RACE (Rapid amplification of cDNA Ends) kit included an adaptor sequence that was blunt-end ligated to the end of the unknown 5' and 3' NHE2c nucleotide sequence, along with adaptor primers (AP1 & AP2) that primed to this adaptor sequence. The 1500 bp amplicon that was obtained from LaRue et al. 2008, in the middle of the sculpin NHE2c sequence, was used to design gene specific primers that flanked the unknown, 3' region of sculpin NHE2c. Together, the adaptor primers and gene specific primers were used to PCR amplify the unknown transcript.

Marathon RACE cDNA Synthesis and Adaptor Ligation. Starting with Poly-A RNA, the first-strand cDNA was synthesized from a modified lock-docking oligo(dT) primer with two degenerate nucleotide positions at the 3' end. The modified oligo(dT) primer positions itself at the beginning of the polyadenylation rather than at random points in the poly-A tail. This eliminates most of the 3' heterogeneity inherent with conventional oligo-dT priming (Borson et al., 1992).

To the first-strand cDNA, a second-strand enzyme cocktail is added which includes *E.coli* DNA polymerase I, RNase H, and *E.coli* DNA ligase. These enzymes degrade the RNA and synthesize the second cDNA strand. T4 DNA polymerase creates blunt ends on the cDNA for adapter ligation. All reagents were added according to manufacturer's protocol.

Following ds cDNA synthesis and blunt end formation with T4 DNA polymerase, according to manufacturer's protocol, the ds cDNA was ligated to a Marathon cDNA adaptor (Figure 5). Blunt end ligation is more efficient than ligation to single-stranded cDNA by T4 RNA ligase as in the GeneRacer method (for attempted GeneRacer RACE

reaction see Appendix B). Undiluted adaptor-ligated cDNA was stored at -20°C and 1 µl each was diluted to 1/50 and 1/250 for Phusion High-Fidelity PCR amplification. At this point in time a library of adaptor-ligated cDNA was created. There was enough material to perform the rest of the protocol using gene specific primers for several different gene transcripts if desired.

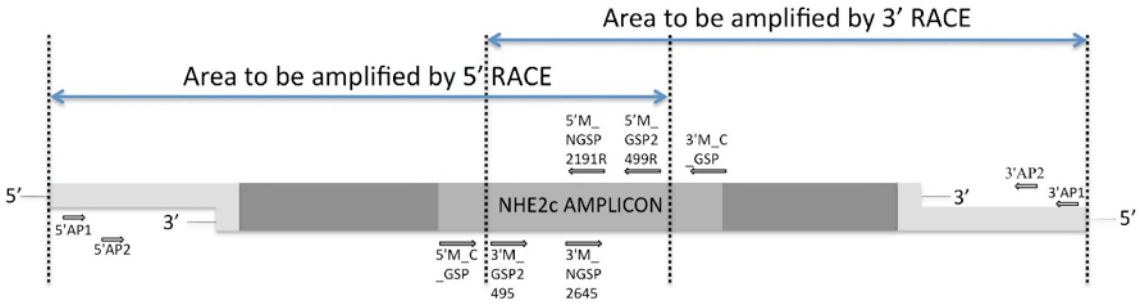

Figure 5: The 5' and 3' ends of Marathon adaptor-ligated double stranded cDNA is amplified using 5' and 3' gene specific primers (5'M_GSP2499R, 5'M_NGSP2191R, 3'M_GSP2495and 3'M_ NGSP2645) along with 5' and 3' Marathon Adaptor Primers in RACE PCR (Rapid Amplification of cDNA ends).

RACE with Phusion High-Fidelity PCR. The Phusion High-Fidelity PCR Master Mix (New England Biolabs, Ipswich, MA) was used to amplify the NHE2c sequence from the Marathon library of adaptor-ligated cDNA using GSPs. The method was designed to create optimal conditions for the amplification of any sequence, so 4 different procedures were used simultaneously, A, B, C, and D. For A and B, 10µl of High Fidelity (HF) 5x PCR buffer, 1µl dNTP (10mM), and 1µl of cDNA were added (concentration varies), as well as 5µl of upstream and downstream primer for solution A (10µM), and .5µl of upstream and downstream primer for solution B (10µM), along with .5µl of Phusion DNA polymerase (1.0 units/50µl PCR) and brought up to 50 µl with molecular grade water. The master mixes were prepared in the order listed according to protocol (New England BioLabs). For C and D, 10µl of 5x GC PCR buffer (for GC rich sequences), 1µl of dNTP (10mM), 1µl of cDNA, and 1µl of 2% TMSO, with 5µl of upstream and downstream primer for C (10µM), and .5µl of upstream and downstream primer for D

(10μM), plus .5 μl of Phusion DNA polymerase (1.0 units/50μl PCR) and molecular grade water was added to bring the mix up to 50 μl. The Phusion PCR mixes for the 3' end of NHE2c were ran with a stepdown PCR protocol that began at 98°C for 1 minute, and 75°C for 3 minutes, for 1 cycle. Next, at 98°C for 30 seconds, 72°C for 3 minutes, for 5 cycles. The third stage was ran at 98°C for 30 seconds, 70°C for 3 minutes, for 5 cycles. Then 98°C for 30 seconds, 68°C for 3 minutes, for 25 cycles. Then it ran at 72°C for 5 minutes, for 1 cycle, and finally was held at 10°C. The same step-down PCR cycle was used as for the 3' Phusion RACE PCR, except the initial annealing temperature was lowered by 1°C to 74°C.

For 3' RACE, the upstream adaptor primer 1 (3'AP1) was paired with the downstream 3' Marathon gene specific primer (3'M_GSP2495) in a first RACE PCR reaction, then this PCR product was used as the DNA template in a nested RACE PCR reaction with adaptor primer 2 (3'AP2) and 3' Marathon nested gene specific primer (3'M_ NGSP2645). Likewise, 5' RACE was performed with the combinations of outer upstream and downstream primers, 5'AP1 and 5' Marathon gene specific primer (5'M_GSP2499R), respectively, followed by nested primers 5'AP2 and 5'M_NGSP2191R. The nested RACE reaction offered a more specific NHE2c PCR product that could then be sequenced and cloned.

PCR controls were set-up to determine if there was a problem with one of the GSP or AP primers. Along with the experimental PCR reactions containing Adpator-ligated ds cDNA, diluted to 1/50 and 1/250, along with AP primer and a gene specific primer, a negative control PCR reaction without cDNA was run in parallel. To make sure the gene specific primer bound to the cDNA sequence in the right place and could produce a product, a complimentary gene specific primer that anneals to the opposite cDNA strand was used as a positive control along with the experimental GSP used to amplify adapter-ligated ds cDNA (3'M_C_GSP2710R, 3'M_C_NGSP3058R, 5'M_C_GSP2023, 5'M_NGSP2191R). The two GSPs should have produced a single band that showed overlap between the primers. To make sure the AP primer was not binding to both ends of the adaptor-ligated cDNA, and producing a smeared product, the AP1 and AP2 primers were used alone along with water to amplify the cDNA.

Cloning NHE2c Plasmid Insert. If the correct size PCR product (Table 1) and

sequence was obtained from 5' and 3' Marathon RACE PCR, it was cloned into a pCR®4-TOPO® plasmid vector and transformed into One Shot® TOP10 Chemically Competent E. coli, according to the TOPO TA cloning kit for sequencing manufacturer instructions. The PCR product obtained from Marathon RACE was incubated at 72°C with *Taq polymerase* in order to place over-hanging (A) nucleotides on the 3' end so that the PCR product ligated easily with the linear vector that had overhanging 3' (T) nucleotides.

The pCR®4-TOPO® plasmid contains the lethal *ccd*B gene fused to the C-terminus of the LacZα fragment. Ligation of a PCR product disrupts expression of the *lac*Zα-*ccd*B gene fusion permitting growth of only positive recombinants upon transformation in TOP10 cells. Cells that contain non-recombinant vectors are killed upon plating. Therefore, blue/white screening is not required and direct selection of recombinants can be done.

As the cloning reaction was incubated on ice, 2 vials of One Shot Top10 chemically competent *E.coli* were thawed from -80°C. From one of the vials, bacteria cells were transferred to a clean vial for the negative, bacteria-only control. To the second vial of competent cells, 1µl of pUC19 (10pg/µl) was added for the positive control. The TOPO cloning reaction was added to the third vial of *E.coli*. After one hour of shaking, 50µl of the bacteria alone and the pUC + bacteria were plated onto separate LB agar with carbenicillin (1ml of carbenicillin/25ml agar). Transformants were selected by separately plating the TOPO cloning reaction at high (50µl) and low (10µl) amounts onto the agar containing carbenicillin. To a fifth plate, LB agar without carbenicillin was added, to see if the plated *E.coli* could grow.

*PCR Screening and Incubation of Bacteria Transformants***.** Various sizes of transformed colonies were picked from the incubated plates. The colonies were circled on the bottom of the plate with a permanent marker and numbered. Aliquots of 9µl PCR master mix were distributed into each PCR tube and a small amount of transformed bacteria were directly transferred from the 50µl and 10 µl transformed plates into the PCR reaction tubes by touching a sterile, 100µl pipette tip to a bacterial colony then submersing the tip into the 9µl PCR master mix. The PCR tubes were numbered according to the colony chosen. Since the pipette tip had millions if not trillions of

bacteria cells still on it, the pipette tip was ejected directly into a 15ml Falcon tube with 3-4ml of LB broth containing 100µg/ml of carbenicillin at 1/1000 dilution for overnight culture at 37°C at 220 RPM.

PCR amplification of transformed colonies was executed with the Marathon RACE nested GSPs, and Adaptor Primer 2 (AP2) since this would give the greatest amount of sequence and was how the original DNA plasmid insert was obtained (see *RACE with Phusion High-Fidelity PCR*). In order to choose the transformed colony for sequencing, various controls were run to determine if the right size plasmid insert was obtained with all primer combinations. The controlled primer combinations were as follows: 3' Marathon Nested Gene Specific Primer (3'M_ NGSP2645) with Adaptor Primer 2 (AP2); 3'M_ NGSP2645 with 3' Marathon Complimentary Nested Gene Specific Primer (3'M_C_NGSP3058R); 3'M_ NGSP2645 and 3'M_GSP2495; and 3'M_GSP2495 with 3'M_C_GSP2710R. The PCR cycle used was an initial denaturation at 95°C for 3 minutes, annealing at 63°C for 30 seconds, and elongation at 72°C for 1 minute 30 seconds for 1 cycle, followed by 35 cycles of 30 seconds each denaturing at 95°C, annealing from 63°C, elongation at 72°C and a final one step elongation at 72°C for 10 minutes.

As previously described, the PCR products were separated with gel electrophoresis on a 2% agarose gel. If the correct size PCR fragments were obtained from the control primer pairs, then the colony that had the correct size plasmid insert after PCR amplification would be cultured overnight and then purified for DNA sequencing.

Sequencing preparation. Plasmids were isolated from the transformed bacteria using the High Pure Plasmid Isolation Kit (Roche), before being sent off for sequencing. The alkaline condition from the addition of NaOH in the Lysis buffer denatures the plasmid DNA into single strands and separates it from bacterial cells. The Binding buffer traps cellular debris along with the bacteria chromosome while the plasmid DNA remains in solution. After separating the plasmid DNA from bacteria, the plasmid DNA binds to glass fibers in High Pure Filter Tubes while in the presence of a Wash buffer with a chaotropic reagent, guanidine hydrochloride, which denatures bacterial DNA, proteins, and other macromolecule debris for removal. Bound DNA is released in a low-salt elution reagent. The procedure was performed according to protocol.

If general PCR amplification resulted in a PCR product of only a single band, the product could be prepared directly for sequencing according to the ExoSap-IT protocol (USB, Cleveland, OH). For 5µl of the PCR product, 2µl of ExoSap-IT was added. This mixture was incubated at 37°C for 15 minutes and at 80°C for 15 minutes. The incubated reaction was separated into 2µl volumes into two individual tubes. To each tube 21.2µl of molecular biology grade water (5 Prime, Fisher Scientific Company) was added, along with 0.8µl of the forward primer to one tube, and 0.8µl of the reverse primer to the other tube. The tube with a final volume of 24µl was sent to the Mount Desert Island Biological Laboratory for sequencing.

An excised gel slice from low-melt gel electrophoresis, withholding a potentially desired DNA fragment, was also prepared before sending off for sequencing. The gel slice was spun to the bottom of the tube and melted at 70°C for 10 minutes. The agarose was pipette up and down to get a uniform mixture. The melted gel slice was cooled to 45°C for 10 minutes and mixed. Into fresh tubes, 3µl of Agarase (Fermentas, Glen Burnie, MD) was added and warmed for a few minutes on a 45°C PCR plate (1 unit of Agarase per 100 mg [approx. 100 µl] of 1% agarose). The PCR machine was kept at 45°C with all tubes kept on the hot plate, then 100µl of melted gel was added to the agarase and mixed. The solution was digested at 42°C for 1.5-3 hours. After the sample remained liquid at room temperature, 23.2µl of the gel purified PCR product was pipetted into 0.8µl (10µM) of the forward PCR primer, and then again into a separate tube of 0.8µl of the reverse primer. If there was not 23.2µl of the gel purified product to work with, molecular biology grade water was added to the final tube to a volume of 24µl. The tubes were sent to the Mount Desert Biological Laboratory for sequencing.

Cellular localization of NHE2c peptide in gill tissue

*Antibodies***.** After the NHE2c 3' sequence was obtained with 3' Marathon RACE, cloning, and primer walking, the sequence was sent to Prosci Incorporated for affinity purified polyclonal rabbit antibody production. Peptide sequences were chosen based on highest antigenicity values and cross-reactivity with the other NHE antibodies. The antigenic index is an algorithm that produces a plot of surface contour, including immune accessible sites, by integrating protein flexibility with the degree of hydrophilicity and

solvent parameters (Jameson and Wolf, 1988). The rabbit NHE2c antibody was developed by ProSci against a sculpin-NHE2c-L511 peptide, from the COOH-terminal of the protein sequence in marine longhorn sculpin. The 14-residue, synthetic epitope was linked to Complete Freund's Adjuvant followed by Incomplete Freund's Adjuvant with booster injections before peptide injection: C-LQDERKEATRPKRK (amino acid sequence 576-588).

The mouse monoclonal α5 antibody used in this study was engineered by Dr. Douglas Fambrough and raised against the avian Na^+-K^+-ATPase α5 subunit. The antibody was obtained from the Developmental Studies Hybridoma Bank and developed with the support of the University of Iowa, Department of Biological Sciences, Iowa City, IA, 52242. The antibody recognizes fish Na^+-K^+-ATPase, including sculpin branchial cells (Choe et al., 2004).

The NHE2b paralog was detected with affinity purified rabbit polyclonal antibodies made against a synthetic epitope specific to NHE2b amino acid #694-708 (A94-APS: Ac-CVDNEHGSADNFRDGH-amide; GenBank accession number: AF159879) (Catches et al., 2006).

Alexa Fluor 488, 568 and 594 (Molecular Probes, Invitrogen) are fluorescent labeled secondary antibodies that are prepared from affinity-purified antibodies that react with IgG heavy chains. A goat anti-rabbit, Alexa Fluor secondary antibody that absorbed 568 wavelength was used to label anti-NHE2c and fluoresced red. A donkey anti-mouse secondary antibody, usually Alexa Fluor 488, was used to bind to the mouse anti-NKA antibody and it fluoresced green. Alexa Fluor 594 (donkey anti-rabbit) detected the primary antibody that bound to NHE2b and the resulting color was red. Prolong Gold Antifade Reagent with DAPI (Invitrogen, Carlsbad, CA) was applied to the tissue after incubating with the secondary antibody and washing to increase the amount of time before the fluorescent dyes faded and also to stain the nuclei in the cells blue.

Immunohistochemistry (IHC)

Following this incubation in 4% paraformaldehyde, fixative was rinsed from gill arches with PBS, and the bony gill rays were removed. Arches were swathed in filter paper and enclosed in plastic cassettes that were transferred to increasing ethanol solutions for dehydration (50%, 75%, 95%, 100% I, 100% II/ 45 minutes each), then

cleared in two CitriSolv solutions (also 45 minutes apiece). The tissue was prepped for paraffin embedment by first being incubated in three different solutions of the wax held in an oven kept at 60°C (1 hour individually). Next, the tissue was embedded into paraffin blocks and let harden before cutting 5μM sequential sections parallel to the lateral plain of the gill filaments, and perpendicular to the secondary lamellae, and set onto Superfrost®/Plus microscope slides (Fisher, Waltham, MA).

Slides were dewaxed in two different CitriSolv solutions then rehydrated in a series of decreasing ethanol solutions (100% I, 100% II, 95%, 75%, 50%) before incubating in PBS for 5 minutes. The slides were removed from the PBS, and the tissue was circled with a water repellent pen (Scientific Device Laboratory, Fisher) before being covered in Image-iT®FX Signal Enhancer for 30 minutes, rinsed in 1X PBS and subsequently blocked with 5% normal goat serum (NGS) in PBS for 30 minutes. The tissue was incubated overnight in primary antibody diluted in 5% NGS (1:250 for NHE2b, 1:750 for NKA, and 1:250 for NHE2c). The last and 3rd bleed from the rabbits injected with the NHE2c peptide was used as the primary antibody for IHC. The next morning, slides were rinsed 3 times for 5 minutes each in 1X PBS before being incubated for 1 hour in secondary antibodies diluted in PBS. Donkey anti-rabbit Alexa Fluor 594 or 568 (Invitrogen, Carlsbad, CA) bound to rabbit anti-NHE2b or -NHE2c (1:500 and 1:500, respectively). Donkey anti-mouse Alexa Fluor 488 bound to Na^+-K^+-ATPase, diluted to 1:500. After 1 hour had passed, tissue was rinsed 3 times for 5 minutes each in 1X PBS. Cover slips were mounted directly onto the tissue with Prolong® Gold. The tissue was then viewed under a Zeiss Axiovert 200 fluorescent microscope at Mount Desert Island Biological Laboratory, Salisbury Cove, ME. Some IHC tissue was documented under a single-photon laser scanning confocal microscope (Zeiss 510 Meta). At Georgia Southern University slides were viewed under a Laborlux 12 Trinoculuar Phase Contrast microscope (Leitz, Ontario, NY).

For colocalization IHC experiments, anti-NHE2c was applied to the tissue and incubated overnight at 4°C, then washed 3 times in 1X PBS for 10 minutes each time. Since the NHE2b antibody was also made in a rabbit, the existing C-region of the rabbit immunoglobulins (IgG) must be blocked before a secondary antibody that recognizes rabbit IgG C-region is added to the immune complex. Therefore, the tissue was

incubated in biotinylated goat anti rabbit (1:1000) for 1 hour at room temperature. Biotin-XX was washed from the tissue 3 times, each for 10 minutes. The slides were then incubated in steptavidin 555 (1:1000) for 1 hour at room temperature. Again the slides were washed for the 3 intervals of 10 minutes, and then finally the second rabbit primary antibody, rabbit anti-NHE2b, was applied to the gill tissue and incubated overnight at 4°C. If the tissue were to be tripled-labeled with anti-NHE2c, anti-NHE2b and anti-Na^+-K^+-ATPase (anti-NKA) then the α5 antibody that labels the α domain of NKA would be added to the antibody dilution along with anti-NHE2b, and incubated overnight.

Identifying NHE2c peptide in gill homogenates

*Western blots***.** Protein was homogenized for SDS-PAGE and immunoblotting in 2 mL of ice-cold homogenization buffer (1g of tissue/10mL homogenization buffer), 20µl PMSF (phenylmethylsulfonyl fluoride), and 10µl protease inhibitor cocktail (Research Products International Corporation, Illinois) with a Brinkmann EasyCare Generator Polytron-Aggregate (Luzern) on ice until all particles were dissolved. The homogenate was tranfered to 1.5ml microcentrifuge tubes and centrifuged for 10 minutes at 14,000 rpm at 4°C. The supernatent was transferred to a clean microcentrifuge tube and stored on ice. Protein was quantified with the BCA Protein Assay kit (Thermo Scientific, Rockford, IL) according to protocol. The protein sample concentrations were diluted 1:10 and 1:25 and pipetted onto a 96-well plate, along with BCA protein standards. The absorbance of each sample on the plate was read with a Sunrise plate reader (Tecan, Phenix Research Products, Switzerland), and protein concentrations calculated were based on the standard curve established by the BCA protein standards. At first enough protein for a final concentration of 25 µg/µl was added to individual lanes in the SDS-Page gel. However, this was not the appropriate sample concentration for most of the fish. By trial and error, these are the final protein concentrations for each fish: M1004, 30 µg/µl; M1005, 50 µg/µl; M1008, 12.5 µg/µl; M1009, 25 µg/µl; MJILL, 12.5 µg/µl.

Protein gel electrophoresis was ran in TRIS-HEPES-SDS Running buffer (NuSep) at 50V for 30 minutes and then 100V until the bottom blue line from the SDS sample buffer (NuSep) reached the end of the gel. The gels were removed from the holder, and

equilibrated in transfer buffer (NuSep, Bogart, GA) for 15 minutes. Scotch pads and blot paper were also equilibrated in transfer buffer, as well as the PVDF membrane, after dehydrating in methanol (Sigma) for 1 minute.

The blot sandwiches were removed from the blot container and the membranes immersed in blocking buffer (3% nonfat dry milk or Amersham ECL Blocking Agent) overnight at 4°C. The affinity purified NHE2c primary antibody was diluted in 1X TBST at 1/750 concentration, and the membrane was heat-sealed in plastic Ziplock bags, along with the diluted primary antibody, and rocked overnight at 4°C. The next day the membrane was washed three times for 10 minutes each and heat-sealed in a clean plastic Ziplock bag along with the hydrogen-peroxidase (HRP), goat anti-rabbit secondary antibody (Sigma, St. Louis, MO) for 1 hour at room temperature. After the incubation, the membrane was again washed 3 times for 10 minutes each.

The membrane was then placed on Saran wrap and covered with ECL Plus Western Blotting Detection system (Amersham, GE Healthcare, Piscataway, NJ) for 5 minutes according to protocol. The membrane covered by Saran wrap was placed in a developing chamber, within the dark room, and the Amersham Hyperfilm ECL was exposed for 30 seconds to 30 minutes. The film was then processed in Kodak Developer for 1 minute, or until the film became the right dark intensity when viewed under the red-light.

*Peptide competition controls***.** If the synthetic peptide from which the NHE2c antibody was made is pre-incubated with the antibody, then an immune complex should form, and the antibody should not be available to bind to the protein in the gill tissue. For peptide competition controls in both IHC and Western blots, a 200-fold molar excess of peptide was incubated with antibody based upon the dilution at which the antibody is used (IHC, 1:250; immunoblots, 1:750). However, some of the peptide could have degraded, so the amount of peptide to add to the reaction was estimated by incubating a 4:1 ratio of peptide:antibody at 37°C for 2 hours. The peptide-antibody solution was diluted in blocking agent. After the incubation period, the solution was centrifuged for 15 minutes at 10,0000 rpm at 4°C. A pellet formed and Western membrane was incubated with the supernatant overnight at 4°C. Approximately 200 µl of the solution was left in the tube so that peptide-antibody complexes were not pipetted onto the membrane.

Table 1: List of cross-compatible, gene-specific and manufacturer designed primers for amplification of the NHE2c nucleotide sequence. Astericks (*) indicate that that this amplicon is an estimated size.

Primer name	Primer sequence	Strand orientation	PCR	RACE	Sequencing	Amplicon	Anneal
CC570	GCGCCATCATGCACTCGGTCAAA	Sense			X	1500	61°C 45 sec
CC571	TGGCTGTCGTCGGGCAGATCGTAT	Antisense			X		
CC572	TCCGAACCGTCCCGCTCAACTT	Sense			X	600	56°C 30 sec
CC573	TGGCTGTCGTCGGGCAGATCGTAT	Antisense			X		
GR3'P	TGTCAACGATACGCTACGTAAC	Antisense		X		1220*	54°C 30 sec**
GR3'_C_GSP2506	CCCGATAACATCAACAG	Sense		X			
NGR3'P	GCTACGTAACGGCATGACAGTG	Antisense		X			
N_GR3'_C_GSP2580	GGGCATCAGCATCCGTCCAAT	Sense		X			
3'M_GSP2495	TCTTCACCTTACCCGATAACATCAACA	Sense		X		1600*	SD 72°C- 68°C
3'M_C_GSP2710R	CACACAAGTCCTCAACGCCACTG	Antisense	X	X			
3'AP1	GCCCTATAGTGAGTCGTATTAGGATGG	Adaptor		X			
3'M_ NGSP2645	ACATCAACGCGGAGGTTCACACCA	Sense		X	X		
3'M_C_NGSP3058R	GGCTGTCGTCGGGCAGATCGTATT	Antisense	X	X			
3'AP2	GCCGCTCGAGCCCTATAGTGAGT	Adaptor		X	X		
5'M_GSP2499R	TCCTGTTGATGTTATCGGGTAAGGTG	Antisense		X		900*	SD 74°C- 68°C
5'M_C_GSP2023	GGCCTCCTGTTCGGGTTCGTG	Sense	X	X			
5'AP1	CCATCCTAATACGACTCACTATAGGGC	Adaptor		X			
5'M_NGSP2191R	ACTTCATGGTGACGGCGCACGTA	Antisense		X			
5'M_C_NGSP1695	GAACAGCGTCGGCATCGGGATTT	Sense	X	X			
5'AP2	ACTCACTATAGGGCTCGAGCGGC	Adaptor		X			
P.walkGSP2924	AGGCGACTCGACCCAAGAGG	Sense			X	900	55°C 45 sec
P.walkGSP3832R	GGCCAATACCACAAAAACGCACAC	Antisense			X		
P.walkGSP3008	GACAGAAGACGATGGGCTACAC	Sense			X	475	61°C 45 sec
P.walkGSP3483R	CGGTGGTCGCACTGGTTCAGAGTC	Antisense			X		
P.walkGSP3021	GGGCTACACCACCAAATACAATCT	Sense			X	550	61°C 45 sec
P.walkGSP3574R	TCCCTGACCCCTATGACGAGTC	Antisense			X		
P.walkGSP3058	CGAGCCAGGGAGATTCTGA	Sense			X	755	55°C 45 sec
P.walkGSP3816R	ACGCACACAGACATAACATAGAAA	Antisense			X		
5'SP_1401R	GGGGACCTGGATCCGAGGGTAGTC	Sense			X	1400	
5'SP_1435R	AAGAGGCCAGCAGCACCCACAGAGTGAA	Sense			X		
5'GSP_1057	TCGGCCTAAATGACAACTAGTTGTTTTG	Antisense			X	650	60°C 30 sec
5'GSP_1709R	ATGCCGACGCTGTTCCACAGGGTTC	Sense			X		

Results

Obtaining NHE2c cDNA sequence

NHE2c RNA was obtained from longhorn sculpin. The validity of the RNA was determined after reverse transcription and amplification of first strand cDNA with gene specific primers (GSPs) using polymerase chain reaction (PCR) (Figure 9). An approximately 650 bp fragment was obtained using an annealing temperature of 56°C with cross compatible 572 (CC572) and CC573 stickleback primers; this product corresponded with the predicted size based on the primer annealing sites to the stickleback NHE2c transcript. A bold, NHE2c RNA/cDNA band was obtained from all sculpin subjects, not shown. This could indicate that NHE2c mRNA is present at high levels in the branchial epithelium of this fish species.

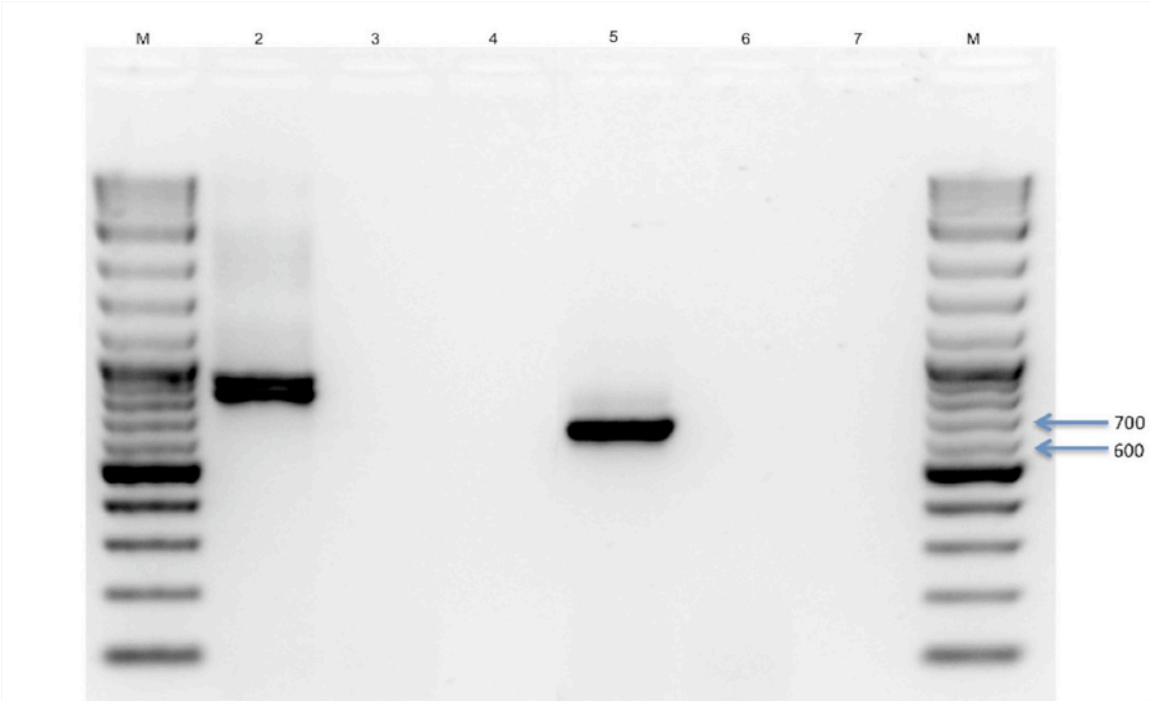

Figure 6: 2% agarose gel stained with 0.01% ethidium bromide showing PCR amplification of reverse transcribed NHE2c cDNA using CCF572 and CCR573 primers (lane 5). NHE2c cDNA fragment was of an expected 646 bp based on the predicted size of the primer annealing sites to the stickleback NHE2c transcript. Lane 2: positive control with NHE3; lane 3: - NHE3 RNA negative control; lane 4: -NHE3 cDNA negative control; lane 5: NH2c cDNA; lane 6: NHE2c RNA negative control; lane 7:- NHE2c cDNA negative control.

For RACE (Rapid Amplification of cDNA Ends) PCR, Gill total RNA was isolated from *M. octodecemspinosus* 48 (MOC48) sacrificed during summer 2009 (gill 3 = 0.09g, gill 4 = 0.02g) and first strand cDNA created with the Marathon kit according to protocol. Once the adaptor was ligated, a double-stranded cDNA library was created, and RACE PCR with Phusion DNA polymerase resulted in a gel electrophoresis band of 1196 bp (Figure 7, Lane 16). This PCR product was obtained with 3' Marathon Gene Specific Primer (3'M_GSP2495) and 3' Marathon Complimentary Gene Specific Primer (3'M_C_GSP2710R) using a stepdown PCR cycle with 1/50 cDNA concentration. Even though no band appeared to come from the PCR product with 3' Adaptor Primer 1 (3'AP1) or 3'M_GSP2495, the primers that should have amplified through the unknown 3' NHE2c sequence, the PCR products from Phusion reactions with High Fidelity, low primers buffer (B) and GC-rich, low primers buffer (D) were used for nested Marathon RACE PCR (Figure 7, Lanes 3 & 5). Nested RACE PCR amplification with High Fidelity, high primers (A) and GC-Rich, low primers (D), of outer Phusion reaction B and D PCR products, respectively, resulted in two, separate, bold bands that were approximately 1700 bp using the same touchdown PCR cycle (Figure 8, Lanes 1 & 8). This was the expected size fragment for the 3' RACE full-nested reaction (Table 1). Primers used were 3' Marathon Nested Gene Specific Primer 2 (3'M_ NGSP2645) and 3' Adapter Primer 2 (3'AP2). Three bands were resolved and extracted after low-meltgel electrophoresis of the nested PCR fragments from Phusion reaction B:A, and 2 bands were extracted from Phusion reaction D:D (low-meltgel not shown). The highest molecular weight band from reaction B:A and the lower band of D:D returned trace files with sequences that were homologous to stickleback NHE2c. PCR products of desired sequence were cloned, and then the colonies were selected for PCR amplification in order to determine which colonies should be cultured overnight in LB media.

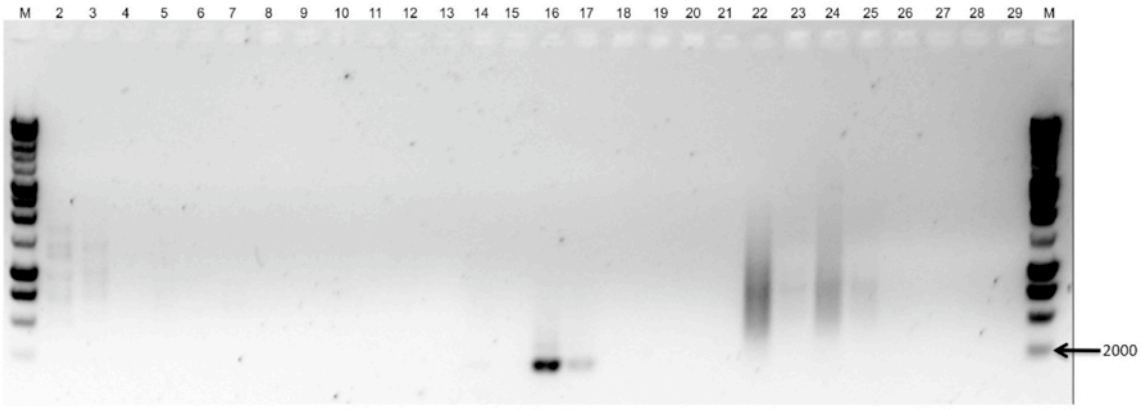

Figure 7: 2% agarose gel stained with 0.01% ethidium bromide of 3' Marathon RACE PCR with Phusion polymerase. Lanes are divided into groups of 4 and are primed with the same cDNA template and primers, the only thing that is different between the four lanes is that the first lane and second lane of each group is primed with High Fidelity Phusion buffer (high and low primer concentration) and the third and fourth lanes of each group are primed with the GC-Rich Phusion buffer (high and low primer concentrations, respectively). Lane 2- 5: 1/50 Marathon library cDNA template primed with 3' Marathon Gene Specific Primer (3'M_GSP2495) with 3' Adapter Primer 1 (3'AP1). Lane 6-9 is the same as lanes 2-5 except with 1/250 cDNA concentration. Lane 10-13 are negative controls without cDNA. Lane 14-17 are positive controls with 3'M_GSP2495 and 3' Marathon complimentary gene specific primer (3'M_C_GSP2710R). Lanes 18-21 are negative controls without cDNA, amplified with the 3'M_GSP2495 and 3'M_C_GSP2710R primers. Lanes 22-25 are negative controls *with* the Marathon adaptor-ligated cDNA but primed with 3'AP1 alone, in order to see if AP1 binds to both ends of the transcript. Finally, Lanes 26-29 are negatives of the previous reaction, that is without cDNA.

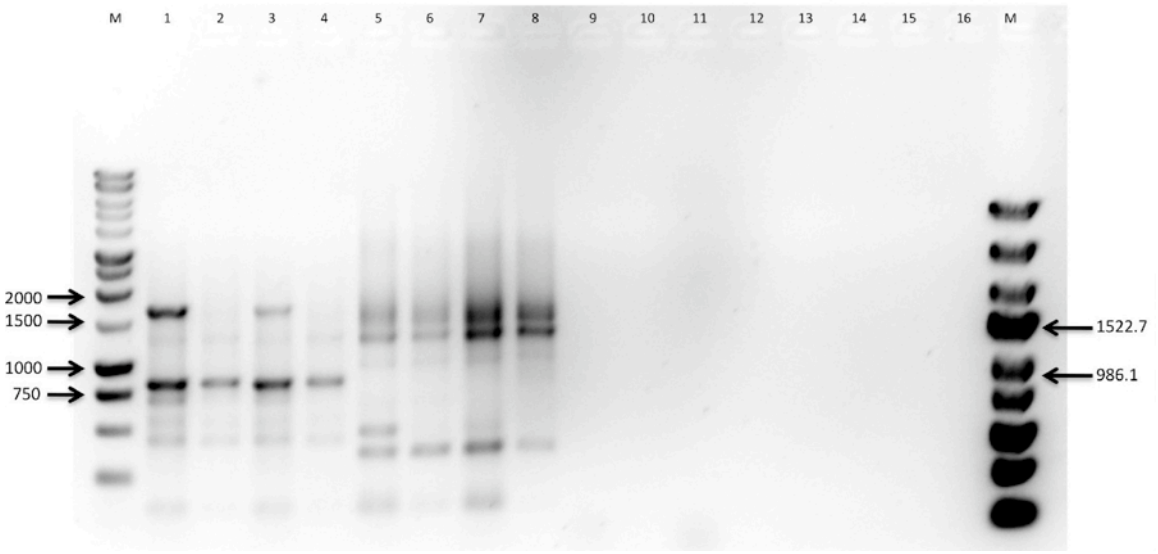

Figure 8: 2% agarose gel stained with 0.01% ethidium bromide of 3' Nested Marathon RACE PCR with Phusion polymerase. Primers used for all PCR reactions were 3'M_ NGSP2645 and 3'AP2. The first, outer RACE products of 1/50 cDNA content, primed by 3'M_GSP2495and 3'AP1 (Figure 7, Lane 3 & 5), did not have a visible band, but the outer RACE PCR products obtained with 3'Adaptor Primer 1 (3'AP1) and 3'M_GSP2495 along with Phusion High Fidelity, low primers buffer (B) and Phusion GC-rich, low primers buffer (D) were used for nested Marathon RACE PCR. Lane 1-4 are nested RACE PCR reactions of the outer RACE product obtained by using High Fidelity low primers buffer (B), with different Phusion buffers in each lane, including: High Fidelity-High and Low Primer buffer and GC-rich – High and Low Primer buffer, respectively. Lane 5-8 are products using the same 4 Phusion buffers, but are a nested reaction of the outer RACE product that was obtained with GC-rich, low primers buffer (D). Lane 9-12 are negative nested Phusion reactions without cDNA. Lanes 13 & 14 are positive controls with 3'M_GSP2495 and 3'M_C_GSP2710R. Lanes 15-16 are with the latter primer set but without cDNA.

Using the excised DNA fragment from the low-melt gel as the DNA template, along with the combinations of nested primers 3'M_ NGSP2645 and 3'AP2 from outer-nested reaction with 3'M_ NGSP2645 with 3'M_C_NGSP3058R primers, the estimated size fragments were obtained (approximately 1,600 bp and 400 bp; Figure 9, Lanes 5 & 6 and Lanes 8 & 9, respectively). Therefore, the transfomed colonies were picked and amplified with 3'M_NGSP2-AP2 primer pair to try to obtain the largest amount of 3' sequence (Figure 10). The transformed TOP10 *E. coli* colony with the putative 3' Marathon insert (Figure 10, Lane 9, D-D) was purified of its plasmid and sent off for sequencing since it was the only sharp, single band in the expected range of 1,300 to 1,600 bp, based upon the 3' region of NHE2c in 3-spined stickleback (*ENSGACG00000014986: sequence was fine-tuned by comparisons with one or more homologous ESTs; Edwards 2010). The 260/280-spectrophotometer ratio for assessment of DNA purity was 1.98. The sequence returned was a cloned contaminate.

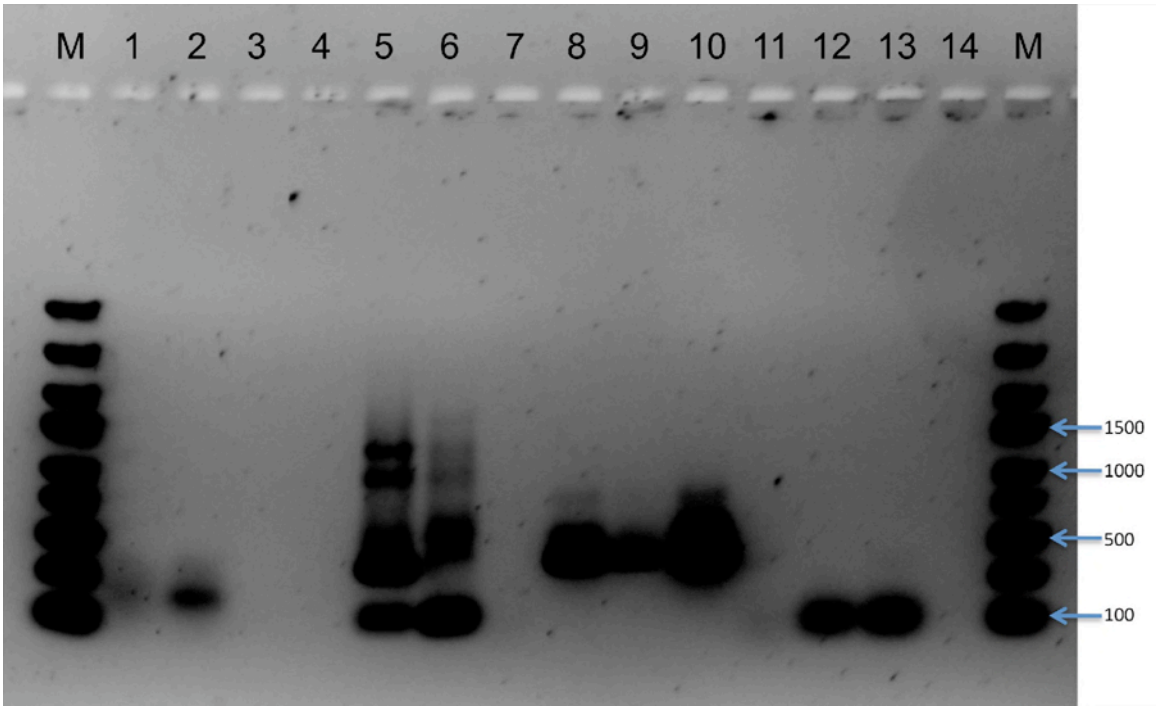

Figure 9: 2% agarose gel to see if the Marathon RACE NHE2c gel-purified inserts could be amplified with PCR. Lane 1 and 2 were positive controls to verify that Marathon Adaptor-ligated cDNA could be primed by 3'M_GSP2495 and 3'M_C_GSP2710R, to obtain an approximate size of 200 bp, indicating that the primers specifically bound to NHE2c. Lane 3 and 4 were negative cDNA of this same reaction. The cDNA template for lane 5 was the gel-purified, nested RACE reaction that used GC-rich, low primers buffer for both the outer RACE product and the nested RACE product (D:D). Lane 6 was cDNA of the gel-purified, nested RACE reaction using High Fidelity, low primers Phusion buffer for the outer RACE reaction (B) and High Fidelity, high primers buffer (A) for the nested RACE reaction. Both cDNA templates were primed with 3'M_ NGSP2645 and 3'AP2. The upper bands in lane 5 and 6 were of expected size (approximately 1,300 to1,600), and lane 7 was a negative control. Lanes 8 and 9 were of the same cDNA templates as lanes 5 and 6, respectively, but primed with 3'M_ NGSP2645 and 3'M_C_NGSP3058R and the expected size of 414 bp was obtained, which was the nucleotide signal corresponding to the NHE2c nucleotide transcript. Lane 11 was a negative control. Lanes 12 and 13 were again of the gel-purified inserts but this time primed with 3'M_ NGSP2645 and 3'M_GSP2495.

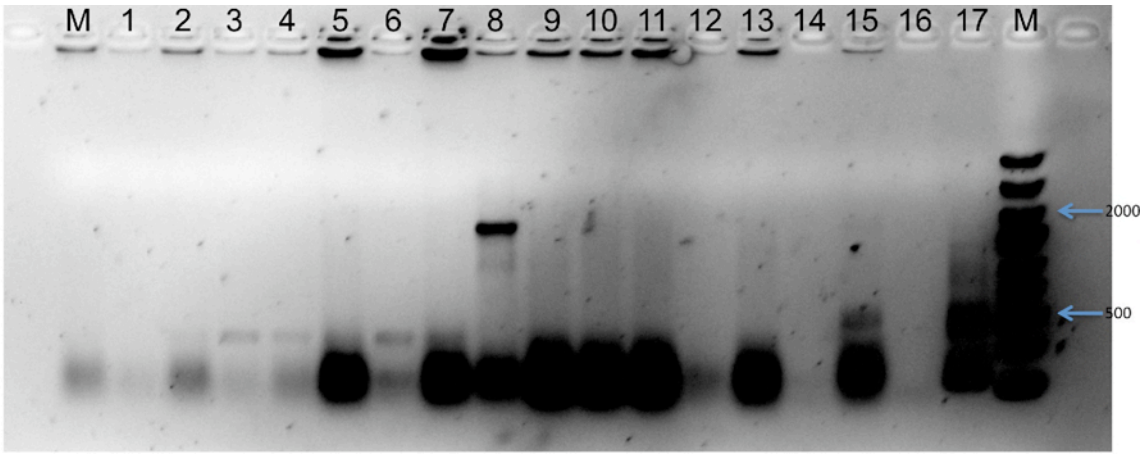

Figure 10: 2% agarose gel of *E. coli* colonies transformed with gel-purified, nested RACE reactions with Phusion DNA polymerase. Lanes 1-9 were clones with plasmid inserts from the gel-purified, nested RACE reaction that used GC-rich, low primers Phusion buffer for both the outer RACE product and the nested RACE product (D:D). The clones were primed with 3'M_ NGSP2645 and 3'AP2. Lanes 10-17 were clones with inserts from the gel-purified, RACE nested reaction using High Fidelity, low primers Phusion buffer (B) for the outer RACE reaction and High Fidelity, high primers buffer (A) for the nested RACE reaction using the same primers. Lane 8 was purified of its plasmid and sent off for sequencing since it had one of the largest size fragments, around the projected size of 1,300 to 1,600 bp.

After failing to identify a clone with the NHE2c sequence, different colonies from the original transformants were chosen, PCR amplified and cultured overnight (Figure 11). The PCR data showed that there were two faint bands (Figure 11, Lane 1 and 8) that were at the approximate size of the NHE2c insert, so these bands were cultured overnight in LB media. However, no colonies chosen had the NHE2c insert.

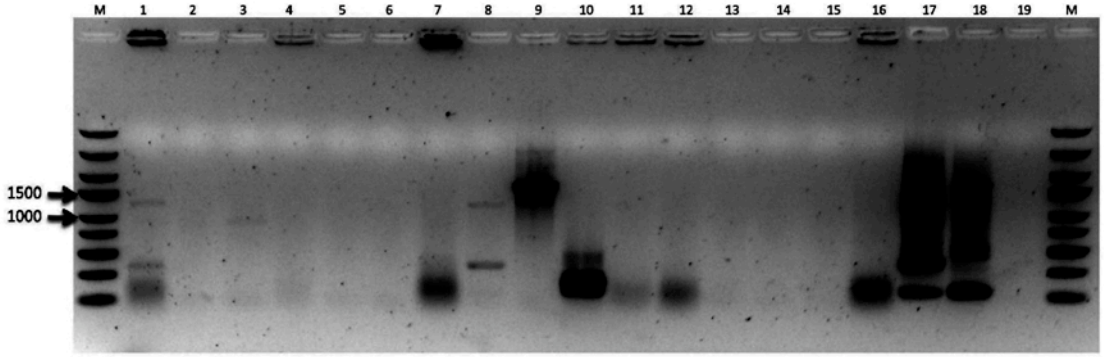

Figure 11: 2% agarose gel stained with 0.01% ethidium bromide of selected from *E. coli* colonies transformed with gel-purified, nested RACE reactions with Phusion DNA polymerase. Amplified colonies of bacteria transformants with a plasmid insert containing gel purified, 3' Marathon NHE2c nested RACE product. Lane 2-9: colonies transformed with 2nd nested Phusion PCR product with GC-rich, low primer buffer (D) along with 3'AP2 and 3'M_ NGSP2645 primers; lane 10-16 colonies transformed with 2nd nested Phusion PCR product with High Fidelity, high primer buffer (A) and 3'AP2 and 3'M_ NGSP2645 primers; lane 17 and 18 positive controls with gel purified 3' Marathon RACE PCR products, Phusion D and B, respectively; lane 19 negative control; M = GeneRuler Express DNA ladder. The black input level of this figure was increased with Graphic Converter so that the bands could be seen.

So the cloning process was repeated for the second time. RACE PCR products from outer Phusion reactions B (High Fidelity, low primers Phusion buffer) and D (GC-rich, low primer buffer) that had been stored at -20°C were again amplified with 3'AP2 and 3'M_ NGSP2645 along with Phusion buffers A (High Fidelity, high primer buffer) and D, respectively. Again, low-meltgel electrophoresis was performed to separate and extract the 1,300 to 1,600 bp fragment. The gel purified RACE products were then cloned, the colonies analyzed by PCR (Figure 12, lane 4), and the recombinant plasmid that generated a PCR amplification product of approximately 400 bp was plasmid purified and sent off for sequencing.

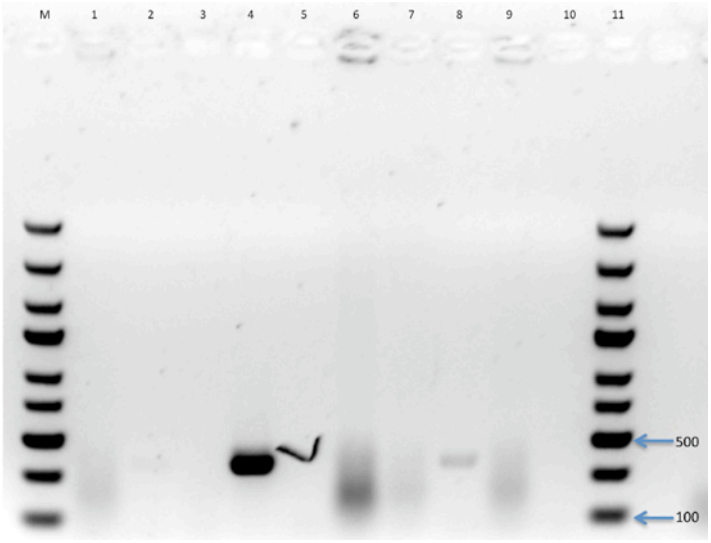

Figure 12: 2% agarose gel stained with 0.01% ethidium bromide of transformed *E. coli* colonies with gel-purified, nested RACE insert. Amplified bacteria recombinants (using whole cell template) with High Fidelity, high primer buffer (A) and 3'AP2 and 3'M_ NGSP2645 primers for the inner nested reaction and High Fidelity, low primers Phusion buffer (B) for the outer RACE reaction.

The 3' ends of NHE2c were eventually obtained by the second cloning reaction of the 3' Marathon RACE PCR product. Primers were designed based on the cloned template to sequence through the open reading frame (base pairs1180-3564) to the polyadenylation tail of the 3' untranslated region (Figure 13). Three different fish were sequenced and trace files were aligned with the cloned sculpin NHE2c sequence in MacVector to affirm the double-stranded sequence and to determine any new transcript.

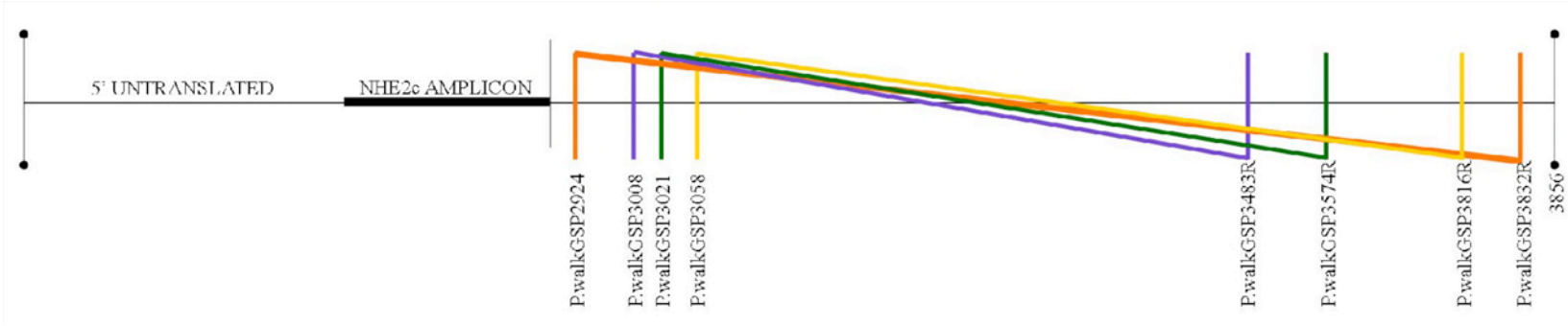

Figure 13: Longhorn sculpin, NHE2c gene specific primers were used to prime and "walk" along the gene in order to double-strand sequence the open reading frame as well as the 5' and 3' untranslated nucleotide sequence from 3 different fish.

Marathon 5’ RACE was used to complete the sculpin NHE2c DNA transcript. Positive controls indicated that primers 5’M_GSP2499R and 5'M_C_GSP2023 were possibly binding to NHE2c even though an unanticipated size band of 1,340 bp was obtained (Figure 14, lane 3). Products resulting from the PCR reaction with primers 5’M_GSP2499R and 5’AP1 were approximately the size expected, so the PCR products were low-melt gel purified and used as the cDNA template in the nested RACE reaction (Figure 15). Nested primer pairs 5'AP2 and 5’M_NGSP2191R amplified a fragment with approximately 900 bp (Figure 15, Lane 1). 5’ sequencing primers (5'SP_1401R, 5'SP_1435R), in addition to the Marathon primers, were sent along with the 5’ Marathon RACE products for sequencing at MDIBL. The result of the nested RACE reaction, using 5'AP2 and 5’M_NGSP2191R to prime the outer RACE reaction that was amplified with 5’M_GSP2499R and 5’AP1 returned considerable amount of NHE2c sequence (Table 2).

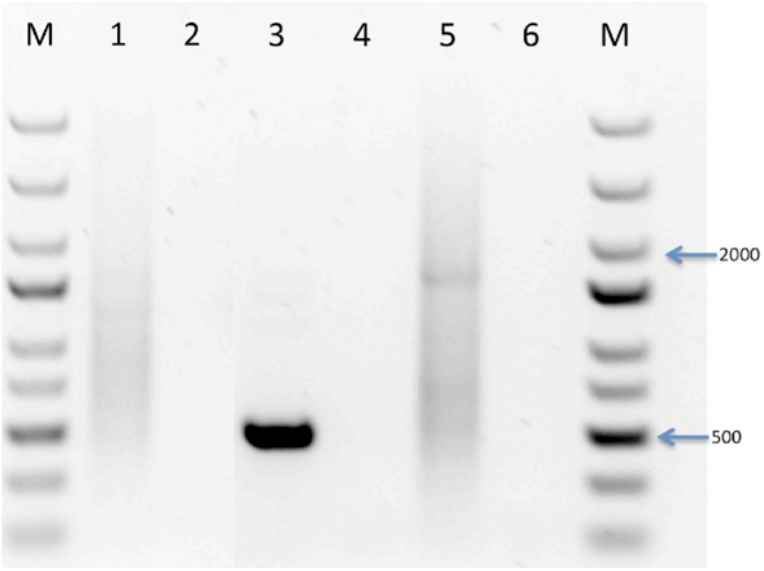

Figure 14: 2.0% agarose gel stained with ethidium bromide to show outer 5’ RACE products obtained with regular Phusion PCR protocol. cDNA template for all positive controls and experimental lanes is the Marathon Adapted cDNA library at 1/50 concentration. Lane 1 is primed with 5’AP1 and water, showing that AP1 was binding to both ends of various cDNA templates, not just NHE2c. Lane 2 and lanes subsequent to the following lanes mentioned are negative controls of the reaction. Lane 3 is primed with 5’M_GSP2499R and 5'M_C_GSP2023. The expected size fragment was obtained, with approximately 450 bp. Lane 5 is primed with 5’AP1 and 5’M_GSP2499R, with the expected size fragment of 1,100 bp.

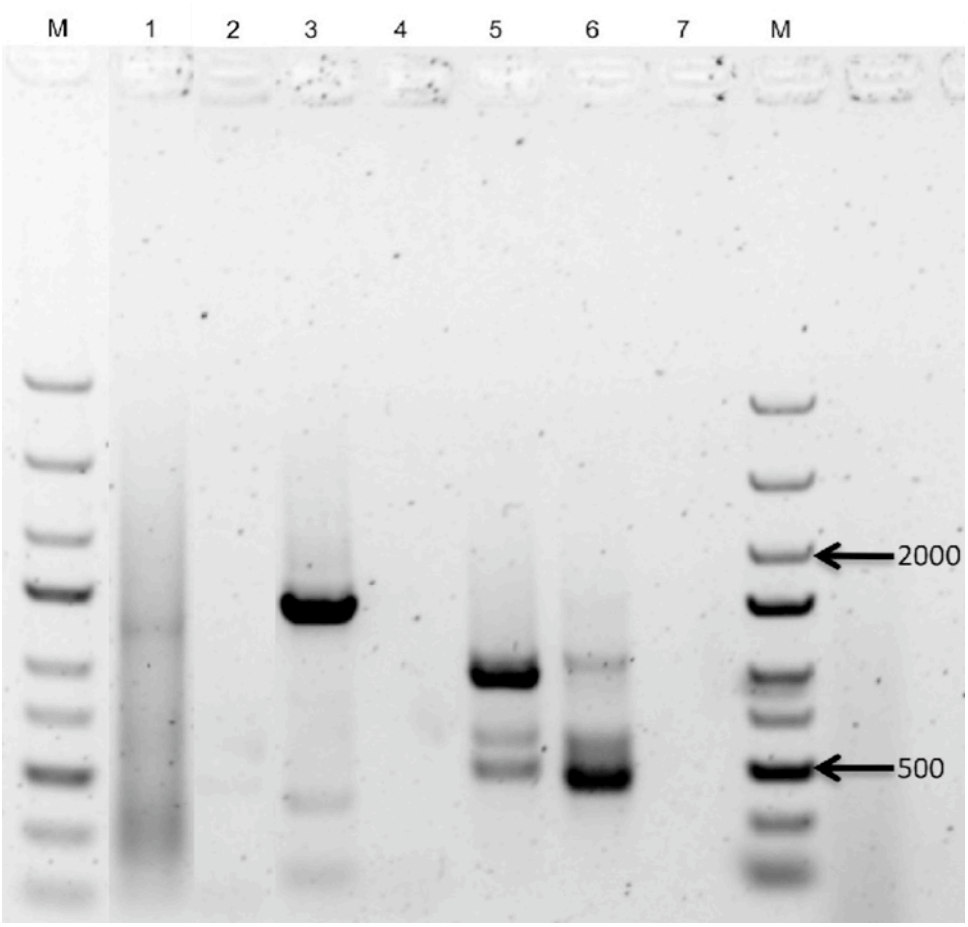

Figure 15: 2% agarose gel stained with 0.01% ethidium bromide to show Nested 5' RACE products using regular Phusion protocol (standard PCR buffer with $MgCl_2$). Lanes 1 is the nested RACE reaction primed with 5'M_NGSP2191R and 5'AP2 of the 5' outer RACE reaction using 5'M_GSP2499R and 5'AP1. Lane 3 is a positive control with M_5'GSP2 and M_5'GSP2, another combination of GSP primers, with the Marathon Adaptor-ligated cDNA template. Lanes 5 & 6 are amplifications of the first outer RACE reaction with AP2 and water. RACE PCR product from Lane 1 was removed of agar and sent off for sequencing at MDIBL

Table 2: Methods and primers used to obtain the full-length, double-strand sequenced, nucleotide transcript of NHE2c in 3 different fish.

METHOD	PRIMERS	SEQUENCE OBTAINED (based on final sequence contig)	FISH
PCR – CROSS COMPATIBLE PRIMERS	CC572, RCC573	2420-3050	MOC 48
3' RACE – MARATHON	3'M_GSP2495, 3'AP1 3'M_ NGSP2645, 3'AP2	2700-3170	MOC 48
CLONING – 3' MARATHON PRODUCT	T3, T7 (TOPO TA Cloning kit)	2640-poly-A tail (3880)	MOC 48
PRIMER WALKING - PCR	P.walkGSP3008 P.walkGSP3483R P.walkGSP3021 P.walkGSP3574R	2640-poly-A tail	MOC 48
PRIMER WALKING	P.walkGSP2924 P.walkGSP3832R P.walkGSP3058 P.walkGSP3816R CC570,CC571	1570-3830	MOC 74, MOC 75
5' RACE – MARATHON	5'M_GSP2499R, 5'AP1 5'M_NGSP2191R, 5'AP2 5'SP_1401R, 5'SP_1435R	1470-2140 1-1290	MOC 48
PCR	5'GSP_1057, 5'GSP_1709R	1054-1710	MOC 71, MOC 73

The sculpin NHE2c nucleotide sequence (GenBank accession #: JN252127) contains 1180 bp of 5' untranslated sequence, a 2,384 bp open reading frame and ending in 292 bp of 3' untranslated sequence followed by a poly-A tail (Figure 16). The Kozak sight begins at nucleotide position 1,177 with the sequence AAGATGG (Kozak, 1984). This consensus sequence is thought to be an initiator site for eukaryotic mRNA sequences. The ATG start codon is within this Kozak sequence. Flanking sequence up to 1,000 bp on either side of the Kozac sight needed to be verified, so primers were made to sequence through this region in 2 other fish (MOC71 & 73, Table 2). The open reading frame predicted from this sequence codes for a protein that is 796 amino acids in length with a molecular weight of 89kDa.

A ClustalW amino acid alignment indicates that sculpin NHE2c has a 44% identity with mouse NHE2 and a 61% identity exists between NHE2b (Figure 17). Sculpin NHE2c and a putative three-spined stickleback NHE2c sequence share 69% identity. Argos plots show that NHE2c has 11-12 transmembrane regions that are conserved among other mammalian NHE2s and sculpin NHE3 (Figure 19). Values greater than 1 in Argos plots indicate a likely transmembrane-spanning region. The phylogenetic neighbor-joining tree indicates that the longhorn sculpin NHE2c amino acid sequence groups with *G. aculeatus* NHE2c, and that similar NHE2 paralogs are arranged together (Figure 20). This best tree may also confirm that NHE3 is evolutionary distant to the NHE2 subfamily (Wang et al., 1999).

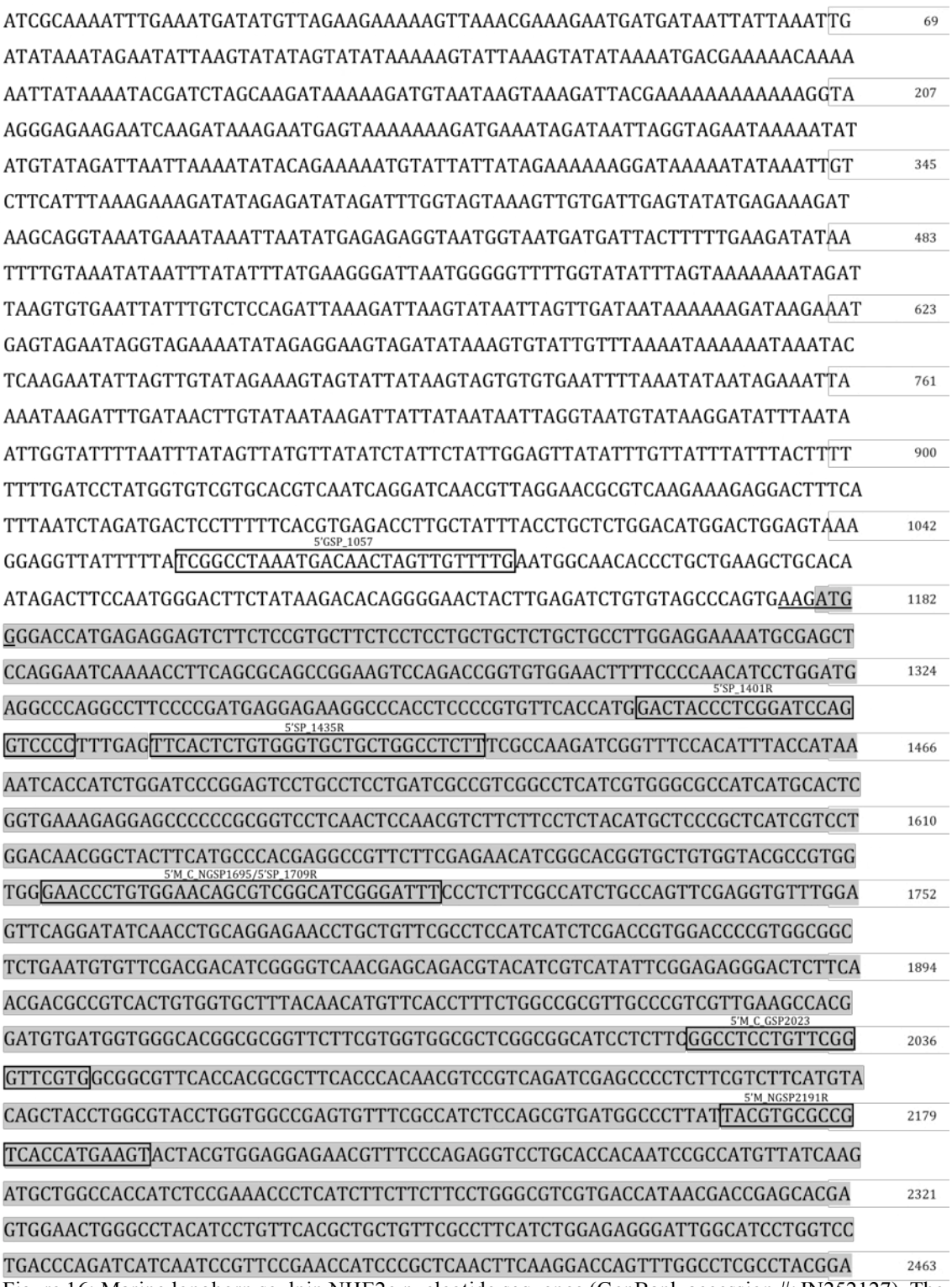

Figure 16: Marine longhorn sculpin NHE2c nucleotide sequence (GenBank accession #: JN252127). The NHE2c nucleotide sequence contains 1180 bp of 5' untranslated sequence, a 2,384 bp open reading frame and ending in 292 bp of 3' untranslated sequence followed by a poly-A tail. The open reading frame is highlighted in grey. The Kozak sequence that contains the start codon ATG is underlined. The stop codon is contained within the primer box for P.walkGSP3574R at base position 3562. The gene specific and cross compatible primers designed to prime to the NHE2c sequence are boxed.

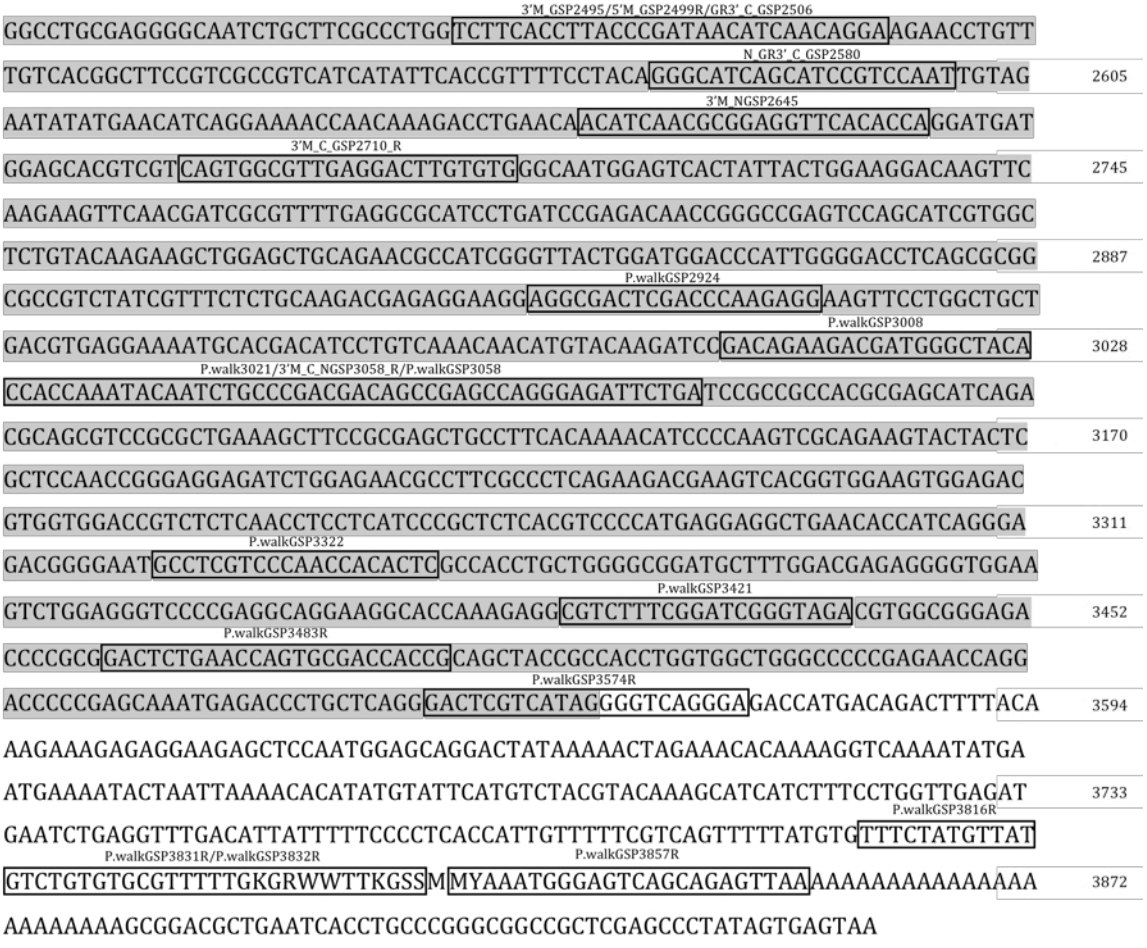
3'M_GSP2495/5'M_GSP2499R/GR3'_C_GSP2506
GGCCTGCGAGGGGCAATCTGCTTCGCCCTGGTCTTCACCTTACCCGATAACATCAACAGGAAGAACCTGTT
N_GR3'_C_GSP2580
TGTCACGGCTTCCGTCGCCGTCATCATATTCACCGTTTTCCTACAGGGCATCAGCATCCGTCCAATTGTAG
2605
3'M_NGSP2645
AATATATGAACATCAGGAAAACCAACAAAGACCTGAACAACATCAACGCGGAGGTTCACACCAGGATGAT
3'M_C_GSP2710_R
GGAGCACGTCGTCAGTGGCGTTGAGGACTTGTGTGGGCAATGGAGTCACTATTACTGGAAGGACAAGTTC
2745
AAGAAGTTCAACGATCGCGTTTTGAGGCGCATCCTGATCCGAGACAACCGGGCCGAGTCCAGCATCGTGGC
TCTGTACAAGAAGCTGGAGCTGCAGAACGCCATCGGGTTACTGGATGGACCCATTGGGGACCTCAGCGCGG
2887
P.walkGSP2924
CGCCGTCTATCGTTTCTCTGCAAGACGAGAGGAAGGAGGCGACTCGACCCAAGAGGAAGTTCCTGGCTGCT
P.walkGSP3008
GACGTGAGGAAAATGCACGACATCCTGTCAAACAACATGTACAAGATCCGACAGAAGACGATGGGCTACA
3028
P.walk3021/3'M_C_NGSP3058_R/P.walkGSP3058
CCACCAAATACAATCTGCCCGACGACAGCCGAGCCAGGGAGATTCTGATCCGCCGCCACGCGAGCATCAGA
CGCAGCGTCCGCGCTGAAAGCTTCCGCGAGCTGCCTTCACAAAACATCCCCAAGTCGCAGAAGTACTACTC
3170
GCTCCAACCGGGAGGAGATCTGGAGAACGCCTTCGCCCTCAGAAGACGAAGTCACGGTGGAAGTGGAGAC
GTGGTGGACCGTCTCTCAACCTCCTCATCCCGCTCTCACGTCCCCATGAGGAGGCTGAACACCATCAGGGA
3311
P.walkGSP3322
GACGGGGAATGCCTCGTCCCAACCACACTCGCCACCTGCTGGGGCGGATGCTTTGGACGAGAGGGGTGGAA
P.walkGSP3421
GTCTGGAGGGTCCCCGAGGCAGGAAGGCACCAAAGAGGCGTCTTTCGGATCGGGTAGACGTGGCGGGAGA
3452
P.walkGSP3483R
CCCCGCGGACTCTGAACCAGTGCGACCACCGCAGCTACCGCCACCTGGTGGCTGGGCCCCCGAGAACCAGG
P.walkGSP3574R
ACCCCCGAGCAAATGAGACCCTGCTCAGGGACTCGTCATAGGGGTCAGGGAGACCATGACAGACTTTTACA
3594
AAGAAAGAGAGGAAGAGCTCCAATGGAGCAGGACTATAAAAACTAGAAACACAAAAGGTCAAAATATGA
ATGAAAATACTAATTAAAACACATATGTATTCATGTCTACGTACAAAGCATCATCTTTCCTGGTTGAGAT
3733
P.walkGSP3816R
GAATCTGAGGTTTGACATTATTTTTCCCCTCACCATTGTTTTTCGTCAGTTTTTATGTGTTTCTATGTTAT
P.walkGSP3831R/P.walkGSP3832R
P.walkGSP3857R
GTCTGTGTGCGTTTTTGKGRWWTTKGSSMMYAAATGGGAGTCAGCAGAGTTAAAAAAAAAAAAAAAA
3872
AAAAAAAAGCGGACGCTGAATCACCTGCCCGGGCGGCCGCTCGAGCCCTATAGTGAGTAA

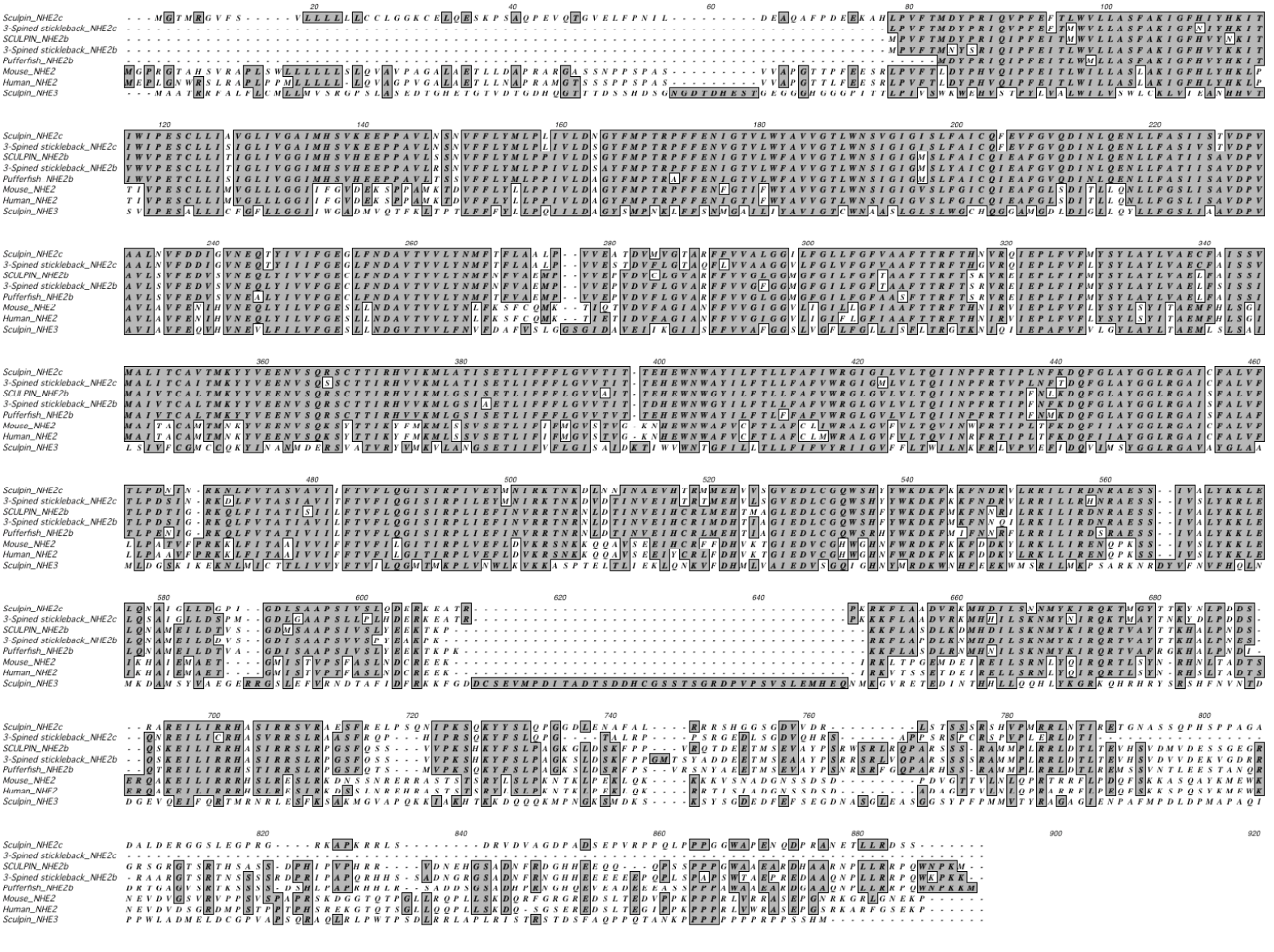

Figure 17: NHE amino acid alignments between teleostian and mammalian species.Grey boxes indicate homologous amino acid regions between the species. No box identifies protein-specific amino acid sequence.

Cellular localization of NHE2c in gill tissue/ Identification in gill homogenates

Once the 3' nucleotide region was verified in 3 different fish and translated into the amino acid sequence (–COOH -terminal), the antigenic regions were plotted with MacVector software (Figure 18). A greater antigenicity value indicates that the amino acid sequences are hydrophilic, and are potential regions for a protein-specific antibody to bind. An antibody that discriminately detected an epitope of the sodium hydrogen exchanger 2c (NHE2c) isoform was created from the carboxy terminal (–COOH) of the sculpin NHE2c protein. A NHE2c-specific epitope was chosen that had no similarity between other sequenced NHEs, so that the NHE2c antibody would not detect these related Na^+/H^+ antiporters. Then ProSci Inc. made a 14-residue synthetic peptide from residue 576 to 590 of the –COOH terminal and raised the NHE2c antibody in rabbits in response to injections with this peptide: C_LQDERKEATRPKRK.

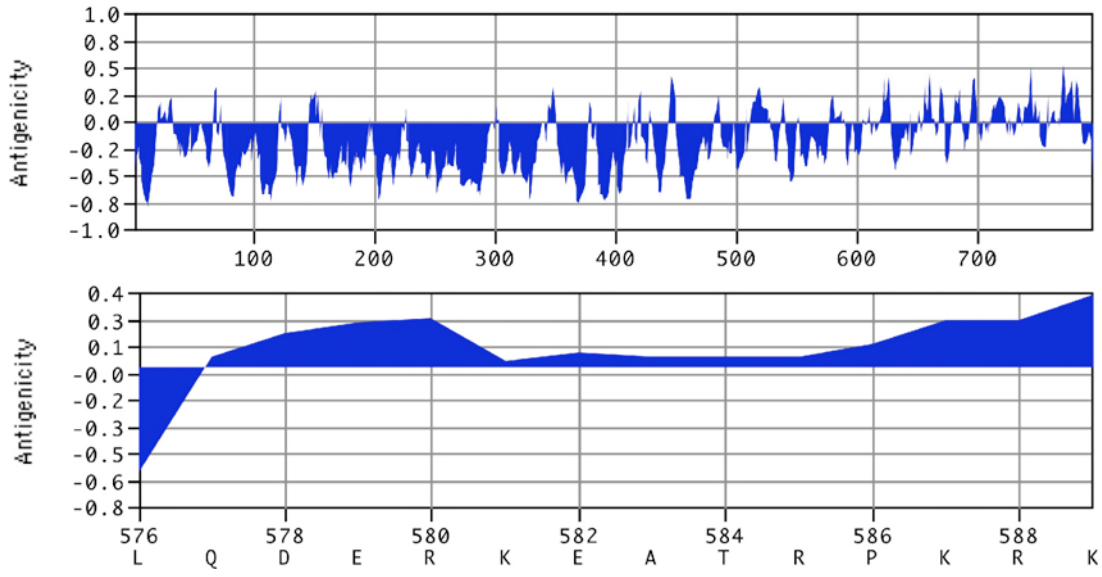

Figure 18: Antigencity plots of the NHE2c amino acid sequence with the unique, 14-residue epitope from the –COOH - terminal (amino acid sequence 576-588). Peaks >0 indicate a hydrophilic region that is accessible from the cytoplasm. ProSci Inc. made an antibody against this epitope in rabbits by injecting them with a synthetic sulfo-SMCC-linked peptide.

There is at least one area on the branchial epithelium where the NHE2c antibody may specifically bind. Using tissue from fish subjected to 0.1M HCl infusions (Catches et al., 2006), including *M. octodecemspinosus* (MOC) 34, 37, 38, 48 and 54, the NHE2c antibody consistently targeted crescent shapes along the apical edge of the filament (Figure 23; Figure 24, A&B, C&D). This staining pattern often colocalized with NHE2b (Figure 22) and the Na^+/K^+ cotransporter (Figure 23), indicative of mitochondria-rich cells (MRCs). NHE2c may also have a subapical expression, as a punctate pattern that does not come from anti-NHE2b labeling is sparingly seen (Figure 23). Control animals from summers 2009 and 2010 also appeared to express NHE2c in these apical locations, albeit more sparsely distributed (Figure 24, E & F). Peptide competition controls indicated that the NHE2c antibody successfully targeted the protein in immunocytochemically labeled gill tissue (Figure 25), and to gill homogenates by Western blotting (Figure 26). Antibody dilutions no longer appeared to bind to cellular locations with IHC or to the approximately 45 and 75 kDa bands on Western blots when pre-incubated with peptide. Specific staining is not as intense when gill tissue is incubated with pre-immune serum (Figure 33).

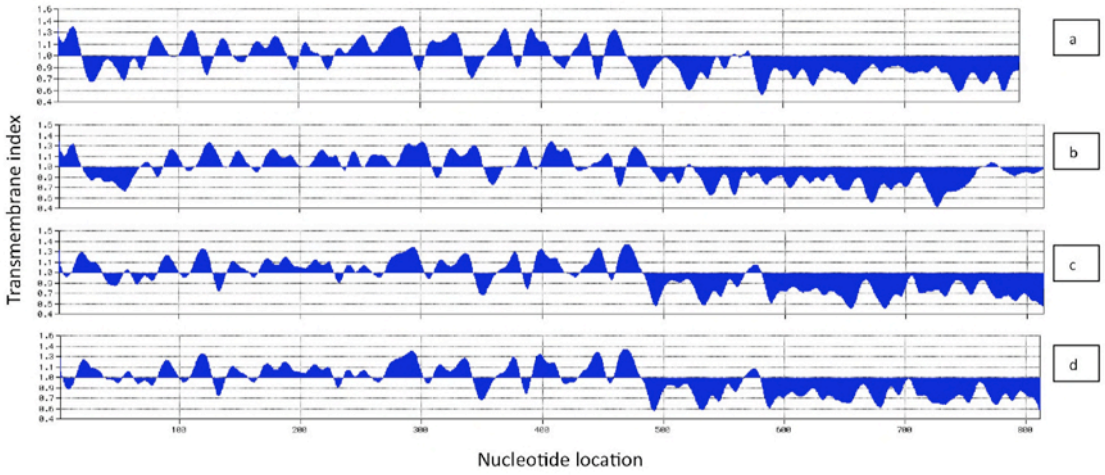

Figure 19: Argos transmembrane plot displaying *M. ocotdecemspinosus* NHE2c (a) and NHE3 (b), mouse NHE2 (c) and human NHE2 (d). Values >1 indicate likely transmembrane segments.

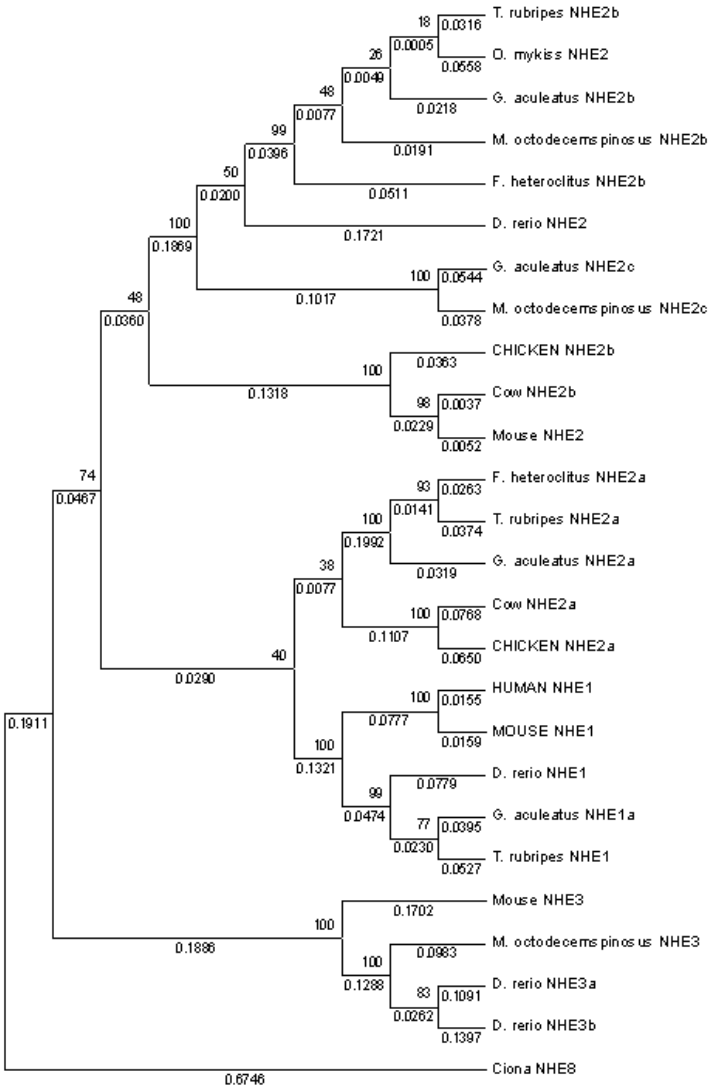

Figure 20: Phylogenetic best tree of selected vertebrate protein sequences from the NHE 1-3 family including *M. octodecemspinosus* NHE2c, rooted to *Ciona*. MEGA was used to construct the phylogeny based on neighbor-joining method. Branch lengths are printed below each branch and bootstrap percents are printed to the left of each node. Accession numbers, other than *M. octodecemspinosus*, were obtained from a recent publication that data-mined for sequences on Ensembl and compared them with an EST databases on NCBI (Edwards et al., 2010). Sculpin NHE2c groups along with the only other NHE2c found in *G. aculeatus*. Ciona NHE (*ENSCING00000009555), *F. heteroclitus* NHE2a (AAV68496), Mouse NHE2 (NP 001028461), Mouse NHE3 (XP 127434), Mouse NHE1 (NP 058677), *Danio rerio* NHE1 (NM 001113480), *Takifugu rubripes* NHE2a (*SINFRUG00000125906), *Gasterosteus aculeatus* NHE2a (*ENSGACG00000018550), *G. aculeatus* NHE2c (*ENSGACG00000014986), *D. rerio* NHE2 (*ENSDARG00000058780), *G. aculeatus* NHE2b (*ENSGACG00000002959), *T. rubripes* NHE2b (*SINFRUG00000153952), *F. heteroclitus* NHE2b (EU886295), *M. octodecemspinosus* NHE3 (EU909191), *Leuciscus leuciscus* NHE3 (AB055466), *D. rerio* NHE3a (NP 001106944), *D. rerio* NHE3b (NM 001113479.1), *M. octodecemspinosus* NHE2{b} (AF159879), *T. rubripes* NHE1 (AB200332), Human NHE1 (P19634), *G. aculeatus* NHE1b (*ENSGACT000000180), *G. aculeatus* NHE1a (*ENSGACT000000029),Cow NHE2{b} (XP 604493), Cow NHE2{a} (XP 597114), Chicken NHE2{b} (XP 416918), Chicken NHE2{a} (XP 420258), *Oxyrhinchus mykiss* NHE2 (EF446605.2).

Gill Diagram

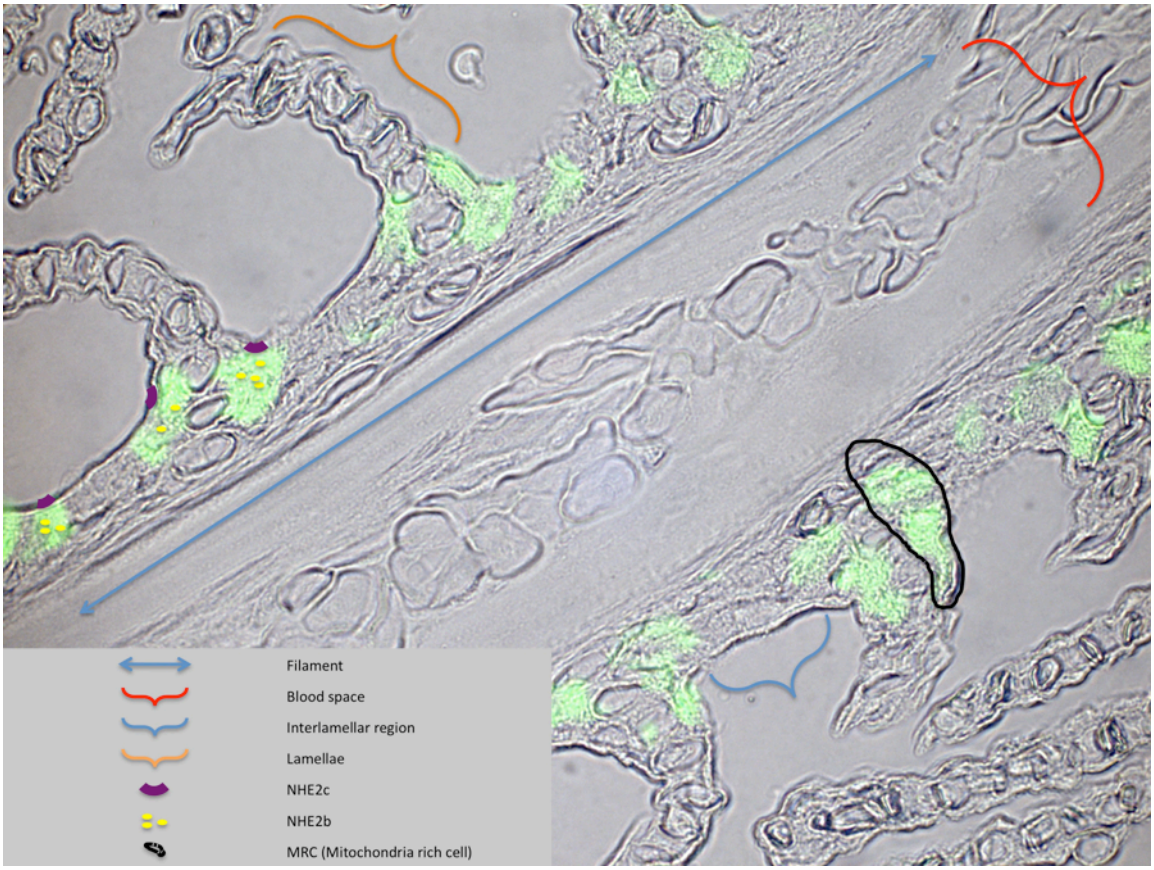

Figure 21: Diagrammatic, color-contrasting micrograph of mitochondria rich cells (MRCs), indicated by Na^{+}-K^{+}-ATPase labeled with the $\alpha 5$ antibody, merged with a gill micrograph taken over white light. Schematic positions of NHE2c are represented by purple, crescent shapes and the position of NHE2b by yellow, punctuate ovules. Notice that all three proteins reside within the MRCs. The MRCs span the entire width of the epithelium, from the basolateral to the apical membrane. The blue arrow indicates the length of the gill filament. The blood space lies in the center of the filament (specified by the red bracket). Just outside the blood space is the basolateral membrane boundary. The apical membrane is the boundary layer of the gill that juxtaposes the external, water environment. The interlammelar space, which lies between two, consecutive lamellae, is signaled by blue bracket, and the lamellae is designated by the orange bracket.

(*Myoxocephalus octodecemspinosus*) MOC 37

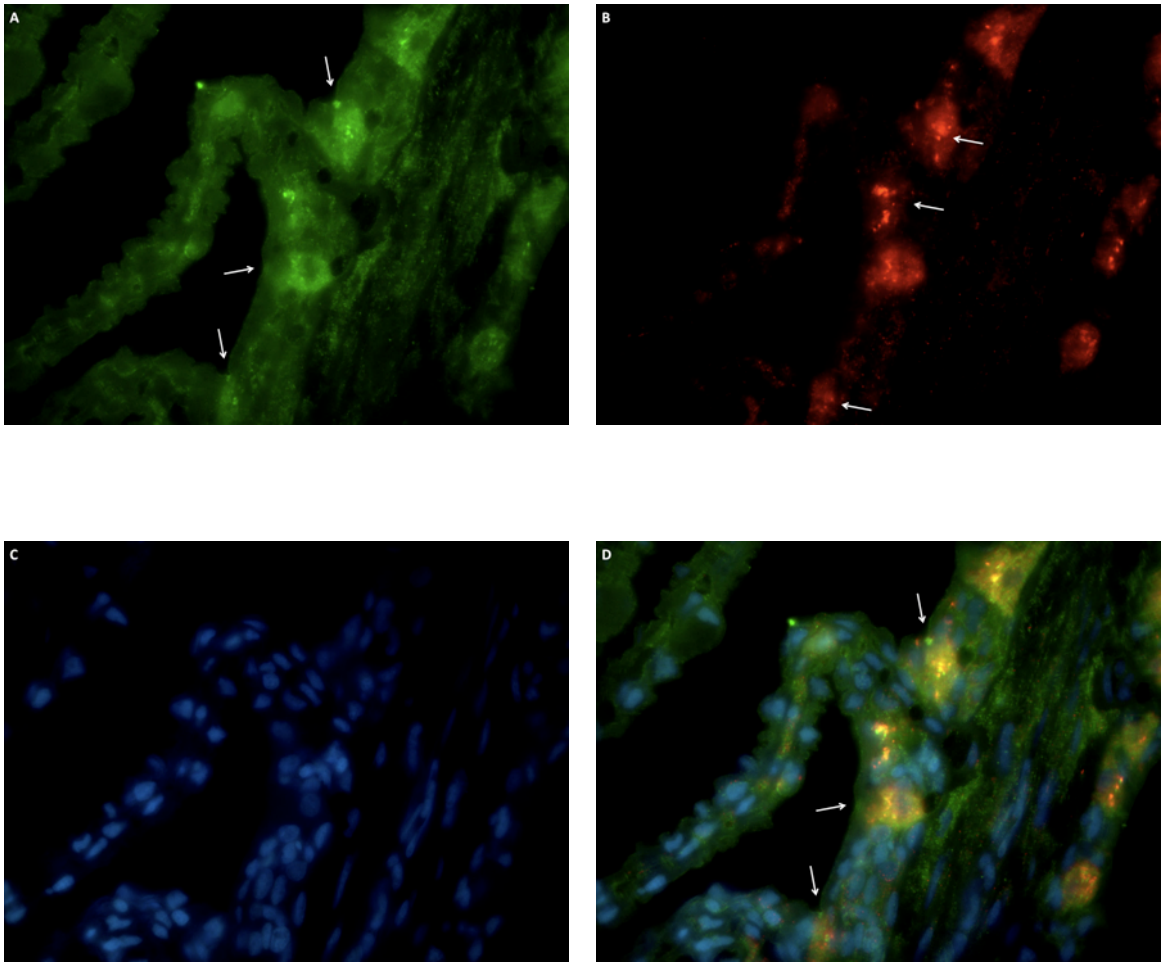

Figure 22: Contrasting micrograph images demonstrating the location of longhorn sculpin NHE2c (A) and NHE2b (B) along the interlammelar region of branchial tissue. The gill was double-labeled with rabbit anti-NHE2c, then rabbit anti-NHE2b, and stained with goat anti-rabbit 488 and 568, respectively. A composite image (D) is compiled of NHE2c and 2b, along with the gill nuclei stained with DAPI (C). The 2 antibodies are located in the same vicinity of the putative MRCs, and therefore may support the current gill acid-base- and ion-regulatory model. Although the NHE2c, bleed 3 antibody nonspecifically binds to areas within the gill tissue, the antibody highlights apical crescent regions of the MRCs that are distinguished from the lamellae, blood space and most parts of the lamellar region. 100x oil immersion.

MOC 34

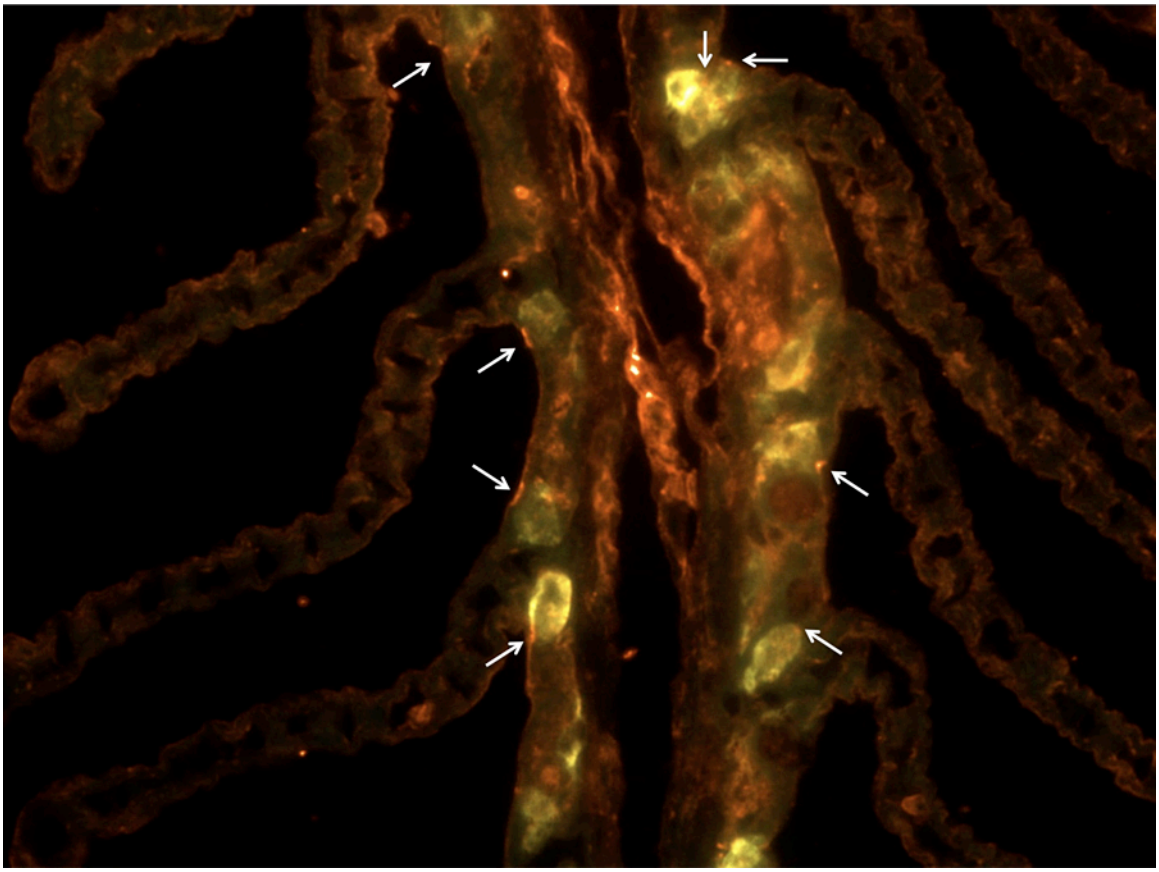

Figure 23: Fluorescent micrograph image of a immunohistochemical experiment in which NHE2c was colocalized to the same cells as Na^+-K^+-ATPase in the gills of marine longhorn sculpin. Oblong mitochondria rich cells (MRCs), whose location is signaled by the presence of Na^+-K^+-ATPase, extends the width from the basolateral membrane to the apical membrane. According to colocalization studes like this, with α5 and NHE2c antibodies, NHE2c is located on the apical tip of theα domain of Na^+-K^+-ATPase. 100X magnification.

NHE2c & NKA in other sculpin

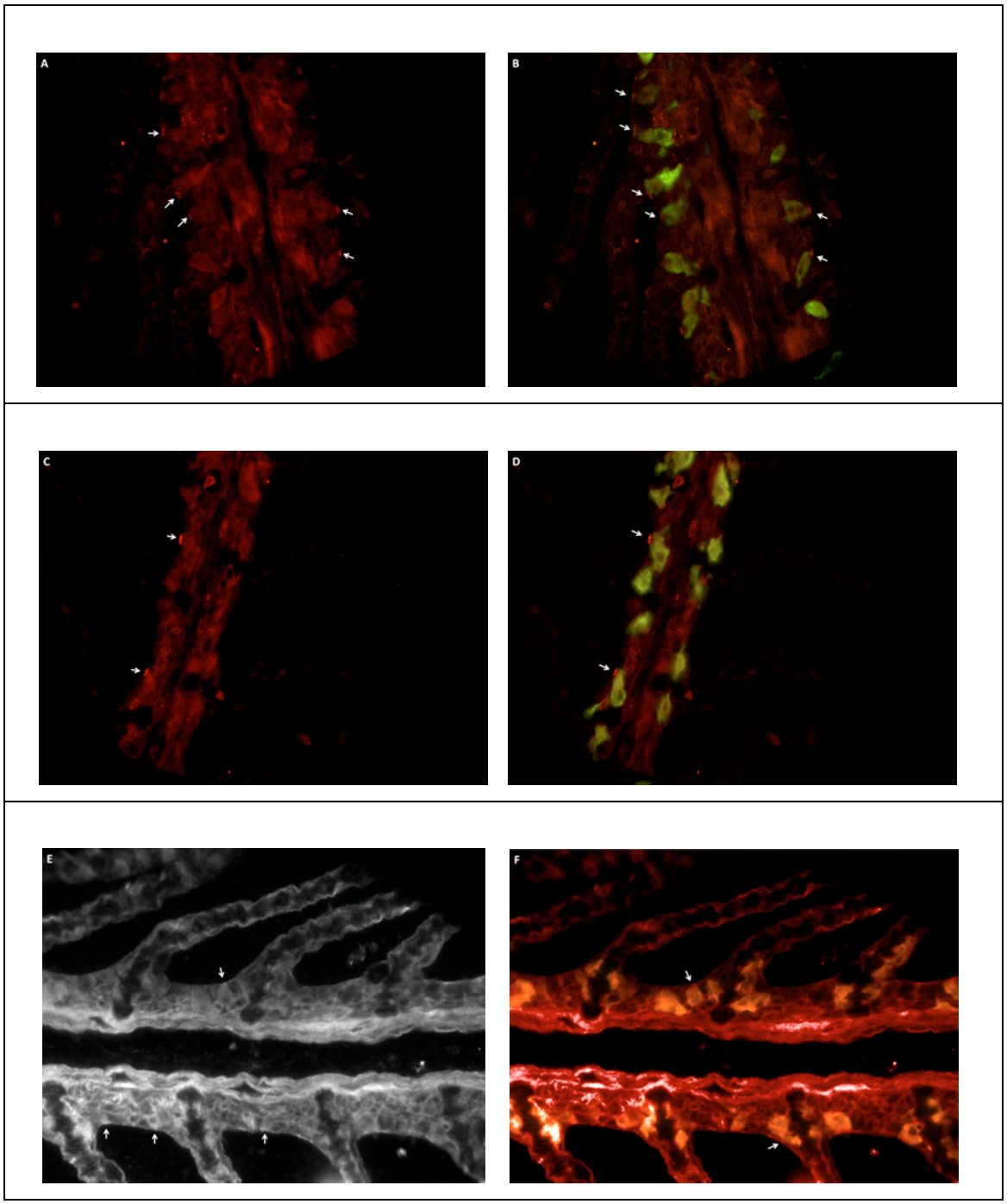

Figure 24: Fluorescent micrographs of longhorn sculpin gills that have undergone immunohistochemical colocalization experiments with NHE2c and Na^+-K^+-ATPase antibodies. These gills represent three different marine longhorn sculpin (A & B: MOC38; C & D: MOC54; E & F: MOC1006) that have not yet been presented for immunohistochemical data in this thesis. This IHC data further supports the hypothesis that NHE2c is located in MRCs, along with Na^+-K^+-ATPase and may be involved in acid-base and ion regulation in the animal. 100X oil immersion.

Peptide Competition Controls (MOC 37, 1009 & 48)

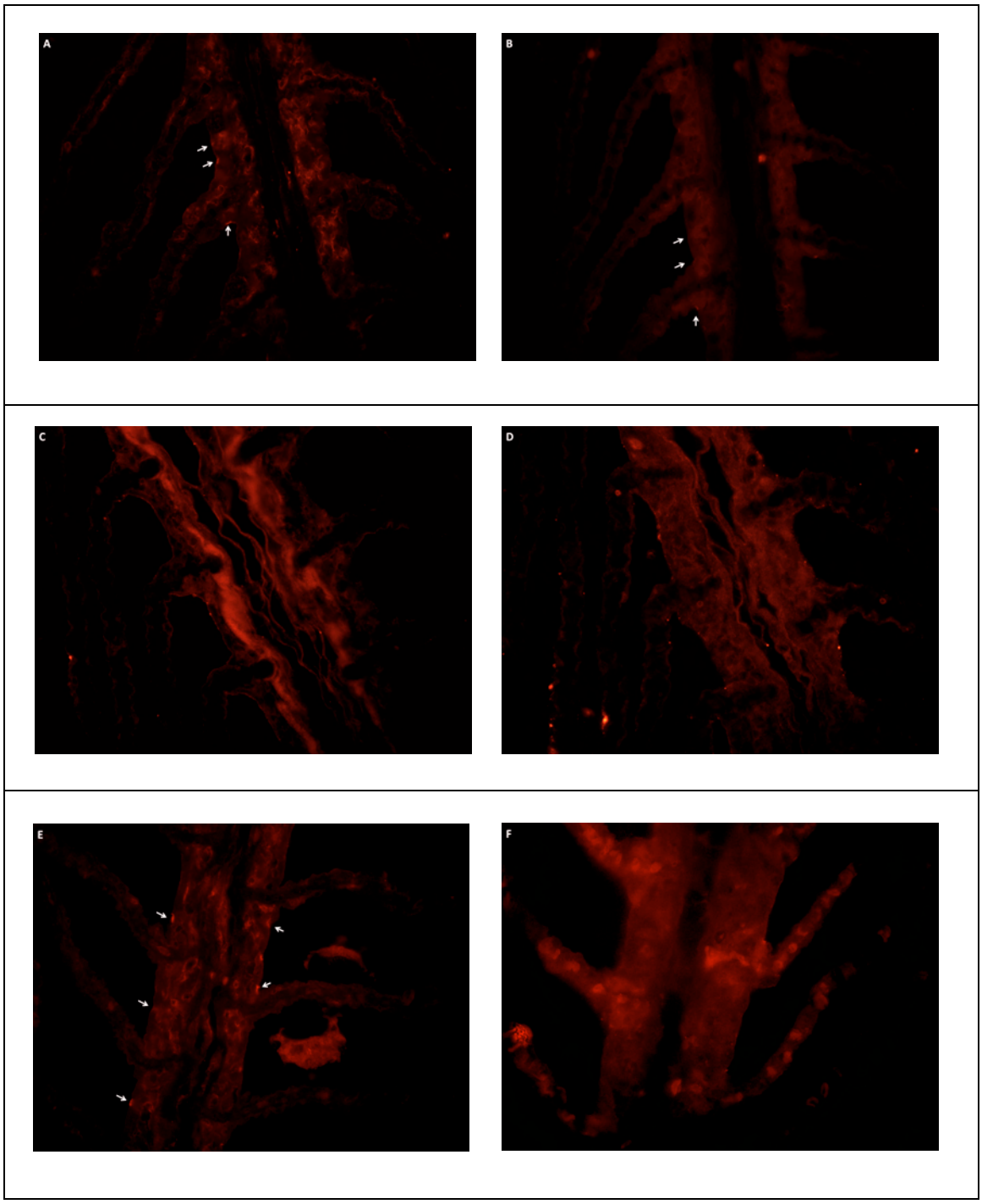

Figure 25: Peptide competition controls from pre-incubated NHE2c antibody with the synthetic NHE2c peptide (B, D & F). This control ensures that the antibody is specific for the peptide from which it was made. Each rectangle contains two consecutive gill slices from the same animal (A & B: MOC37; C & D: MOC1009; E & F: MOC48), in hopes of displaying how the apically crescent staining is removed when the antibody is preincubatd with the peptide (A & B; E & F). M1009 (C & D) lacks apical staining, but a basolateral labeling by the anti-NHE2c antibody does disappear when the antibody is precincubted with its peptide.

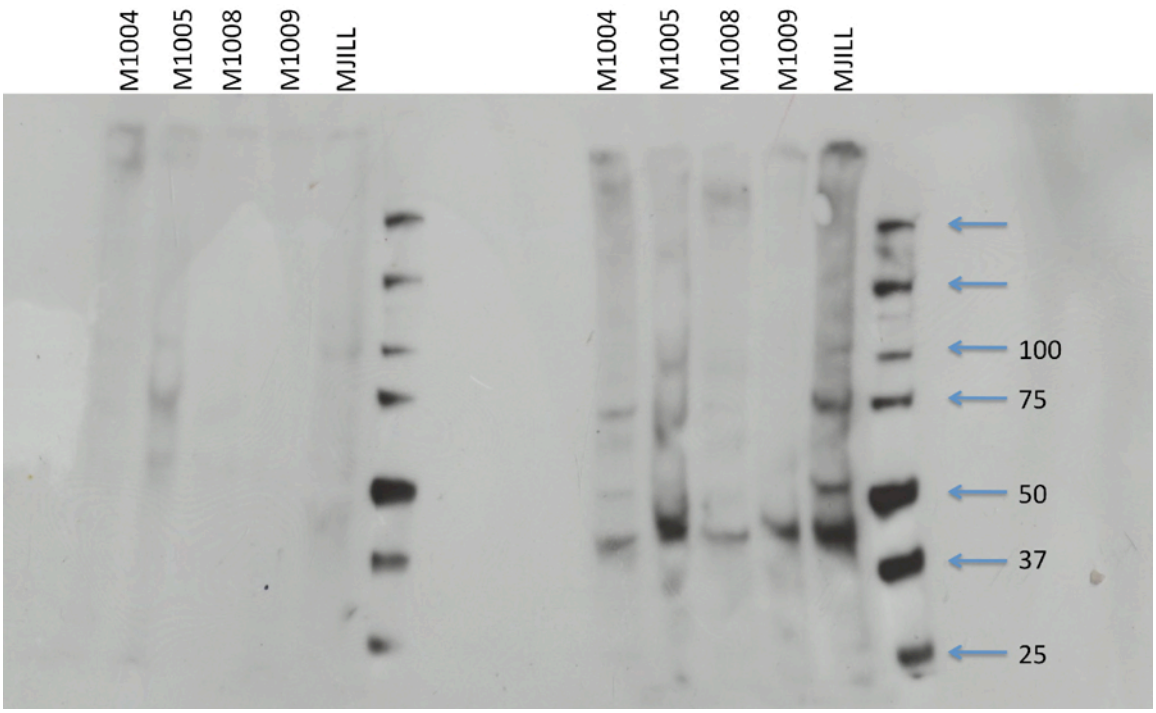

Figure 26: Western blot of five fish gill homogenates (from left to right: MOC1004, MOC1005, MOC1008, MOC1009 and MOCJ) probed with NHE2c affinity purified antibody on the right, and pre-incubated peptide competition control on the left. The antibody appears to bind to a protein that is approximately 45 kDa. In two fish, M1004 and MJILL, the antibody appears to target a 75 kDa protein. The protein may be degraded into a dimer when processed for Western blotting. MacVector and NCBI estimate the molecular weight of NHE2c to be around 89 kDa. The far right lane on each immunoblot is the protein standard.

Discussion

To our knowledge, this is the first time that a sodium-hydrogen exchanger 2c (NHE2c) paralog has been characterized in the gills of a fish. The presence of the NHE2c transcript is evident in RNA and cDNA, as only primers specific to the three-spined stickleback and sculpin NHE2c nucleotide sequence were used to amplify first-strand cDNA. Three-spined stickleback (Gasterosteiformes) follows the longhorn sculpin (Scorpaeniformes) in the evolutionary timescale (Figure 4). Therefore the whole-genome shotgun sequencing of the three-spined stickleback has proven useful in the design of gene specific primers that are cross compatible with sculpin Na^+/H^+ antiporters.

Based on this research, NHE2c is consistent with the ion – and acid-base – regulatory model in marine teleost gills. This model utilizes the low intracellular Na^+ concentration maintained by basolateral Na^+-K^+-ATPase to drive the inward flow of Na^+ ions while extruding acidic H^+ ions in a 1:1 electroneutral exchange (Claiborne et al., 1999). The NHE2c protein was detectable in MRCs, the presence of which is indicated by Na^+-K^+-ATPase labeled with the α5-antibody. Within MRCs, NHE2c also colocalized with NHE2b, although with a more apical position in the osmoregulatory cells.

The α5 labels all 4 α–subunit isoforms (Choe et al., 2004), so the exact isoform that is present in sculpin gills cannot be determined, but Na^+-K^+-ATPase is identified as ovule structures below the apical membrane. The α and γ subunits are the main catalytic domain of Na^+-K^+-ATPase, but the β subunit is responsible for anchoring the protein into the plasma membrane (McCormick et al., 2009). That this Na^+-K^+-ATPase antibody only labels the α subunit may be the reason why we do not observe Na^+-K^+-ATPase on the basolateral side of MRCs, which extend from the basolateral membrane of the gill epithelium to the interlamellar region positioned just before entry into lamellae (Figure 21, 23 & 24)). Na^+-K^+-ATPase positioning along the basolateral membrane of MRCs has long been accepted as the driving force for the ion regulatory and acid-base balances that occur in these epithelia cells (Maetz, 1971).

NHE2c is so far the 3rd NHE2 paralog to be located in the sculpin genome, and the 2nd to be molecularly characterized. NHEs are well conserved throughout the vertebrate lineage, so the fact that novel NHE paralogs (ex. NHE2a, b & c) are being discovered may indicate that other animals possess multiple paralogs within a NHE subfamily due to

genetic mutations (Zizak et al., 2000). Apart from being neutral mutations, unused genes within the genome, it is possible that these different paralogs within the NHE2 subfamily have become actived, specialized copies of the genes made available through genome duplication (Cutler et al., 2000; Cutler and Cramb, 2001). There are three fates to duplicated genes: the copied gene can be nonfunctional; the gene duplicate can acquire a new function that is passed on by natural selection; and both copies can acquire degenerative mutations that cause different functional losses, so that both genes are needed to fulfill the same function of the ancestral gene (Force et al., 1999). All three fates can be carried on into the next generation. In view of this research demonstrating that the NHE2c gene is translated into protein, it can be hypothesized that NHE2c may play a role in acid-base balance in longhorn sculpin, it could have additional functions that are currently unknown or it may share a complimentary role with other NHEs. According to our results, NHE2c is expressed as protein (Figure 23, Figure 26), which seems counteractive to the possibility of the NHE2c being a dormant gene in the genome. Further research is needed to know how NHE2c functions in sculpin gills.

The presence of multiple copies of NHE2 in higher vertebrates is not out of the question. In fact, a comparison of *F. heteroclitus* NHE2a and NHE2b paralogs with cow and chicken NHE2 proteins suggests that these two terrestrial animals possess multiple copies of NHE2 (Edwards et al., 2010). More evolved species of actinopterygii tend to lose structures (such as a glomerulus in some marine species) and have less genes (Hinegardner, 1968). One view is that the loss of genes could reflect the structures they lost, and consequently this is how the teleosts became specialized, because they are doing things more efficiently with the genes they kept (marine fish tend to produce small amounts of urine in order to retain water). If humans have retained these extra copies of NHEs within a subfamily, then it could be speculated that these NHEs helped humans to evolve more specialized functions. Prior to this research, NHE2b was found to be the most synetic paralog with human NHE2. So even if humans did not retain these extra copies of NHE2, the discovery of these NHE paralogs in a few teleosts gives evolutionary perspective to the obtainment of NHE2 in humans.

Regardless of the evolutionary reason why NHE2c exists in marine longhorn sculpin, according to this research, at least two copies of NHE2 exist in longhorn sculpin species.

The first full-length gill NHE2 in longhorn sculpin (Gunning et al., 2001) is most likely NHE2b, as indicated in a recent publication (Edwards et al., 2010), and verified by its grouping away from NHE2c (Figure 20). This research may give further support to the suggestion that the NHE2 subfamily should undergo phylogenetic rearrangement. NHE contigs like NHE2a, NHE2b and NHE2c could be compared, and an algorithm that takes into account genomic similarities and differences between the sequences could be used to reconstruct the phylogeny (Mandoiu et al., 2009). The NHE2 paralogs do group by similarity according to the phylogenic organization of members from NHE subfamilies 1-3 (Figure 20). Sculpin NHE2c is located closest to the three-spined stickleback NHE2c, with a 69% identity. Other NHEs also align together, including the 2b paralogs and the NHE3 subfamily.

NHE2c cDNA and Protein Sequence

Three-spined stickleback gene specific primers were first used to produce a partial sequence of NHE2c in sculpin from first-strand cDNA using reverse-transcription and PCR techniques (LaRue, 2009). For Rapid Amplification of cDNA Ends (RACE), an adaptor sequence was then ligated to the end of this fragment and NHE2c gene specific primers were added to extend the sequence to the characteristic 3' region of the NHE2c DNA transcript. After many trials of RACE, cloning to get more sequence, and finally primer walking with gene specific primers in multiple fish, the full-length sculpin NHE2c cDNA was assembled. The cDNA nucleotide transcript is 3,932 bp long (Figure 16) and codes for a protein that is 795 amino acids and 89kDa (Figure 17). This size is on the higher end of the molecular weights of NHEs, but the extra 5' coding sequence, when compared to other NHEs (Figure 17), could account for the added protein dimensions.

Sculpin NHE2c has 12 transmembrane spanning segments in the first 500 amino acids of the N-terminal, a conserved feature of NHEs (Zizak et al., 2000). The hydrophobic regions (< 0) in the antigenicity plot (Figure 18) correspond to the peaks that are >1 in the Argos transmembrane plot (Figure 19), since peaks greater than zero signify the regions that transverse the bipolar membrane (Argos et al., 1982; Jameson and Wolf, 1988). In both plots, the N- and C-terminal domains of the NHE proteins sharply contrast from one another, where the N-terminal is hydrophobic and has many transmembrane

segments, and the C-terminal domain is mostly hydrophilic and lacks membrane-spanning regions; indicative of separate transmembrane and cytoplasmic domains. The first transmembrane segment of NHEs is not conserved (Wakabayashi et al., 1997), and this is confirmed by looking at the NHE amino acid alignments (Figure 17) and Argos plots (Figure 19).

NHE2c Protein Characterization

A rabbit, anti-sculpin NHE2c polyclonal antibody was used in immunohistochemical techniques to visualize the protein in the gills, and in Western blots to estimate the size and validate its presence in gill homogenates. Immunohistochemical labeling with the NHE2c antibody revealed thin, crescent shapes, localized to extremely apical regions of the interlamellar gill filaments (Figure 21, 22, 23 & 34). On closer examination, the putative NHE2c peptide juts out from ovule-shaped Na^+-K^+-ATPase proteins (Figure 23). This is interesting because to date no member of sculpin NHE2 subfamily has been found in this area of the branchial epithelium. An earlier study of sculpin NHE2b located the majority of the peptide in subapical, intracellular regions, coexpressed in separate cells with either Na^+-K^+-ATPase or Vacuolar-H^+ -ATPase (Catches et al., 2006). Coexpression studies with V-H^+ -ATPase were not conducted in this project to make any conclusion regarding NHE2c colocalizatoin with this H^+ pump. Staining was more frequent on one side of the filament than the other, presumably the afferent edge where MRCs are more proliferate because of its position juxtaposing the arteriovenous circulation (Wilson and Laurent, 2002).

Positively stained tissue for NHE2c was verified by substituting the antibody with a preincubated, antibody with peptide solution and in a separate reaction pre-immune serum (Figure 25, Figure 33). In some cases, there is some nonspecific staining with the pre-immune serum. However, this does not affirm false-positive antibody specificity. The pre-immune serum could have a good amount of pre-existing, natural antibodies that recognize antigenic determinants, not molecules (Tips et al., 1997). In contrast the peptide-competition control showed that NHE2c antibody-specific staining was eliminated and is indicative that the antibody is specific for its peptide.

Immunohistochemical data shows that NHE2 location is complex, and this has been documented in other research as well. NHE2 has been found apically and basolaterally in

mammals (Tse et al., 1993; Soleimani et al., 1994), as well as subapically in branchial epithelium (Catches et al., 2006). An apical NHE2c location was not detected consistently in control sculpin from summer 2009 and 2010, but did show consistent apical staining in acidotic fish from summer 2003. However, it is doubtful that the branchial tissue was prepared any differently during these time periods. The Claiborne lab uses a standard IHC protocol, and Catches (2006) prepared the gill tissue no differently from the present study. Longhorn sculpin research is always conducted at the Mount Dessert Island Biological Laboratory in Bar Harbor, ME, so animal care and facilities should be fairly constant. However, in summer 2010, there was an air leak in a water valve that pumped seawater from Frenchman Bay to aquaria in the lab, causing hyper-gaseous air that resulted in a large number of animal deaths at the marine laboratory. It is not known how long this problem with the water pumps was occurring; so all the fish from summer 2010 could have been affected by increased concentrations of dissolved gases like oxygen and nitrogen. Hyperoxia induces respiratory acidosis in fish since their ventillatory rate slows and they retain CO_2, leading to hypercapnia (Wood, 1991). In contrast to metabolic acidosis, Na^+ /H^+ antiporter expression may not change in response to respiratory acidosis, as Cl^-/HCO_3^- cotransporters are hypothesized to be the dominant route to regain control of homeostatic pH in gills under hyperoxic conditions.

If metabolic acidosis cannot explain the lack of NHE2c immunohistochemical protein detection in some control fish, then there are a number of other reasons why the protein may not be consistently detected. NHE2c may be an ancillary protein that is a backup to other Na^+/H^+ antiporters. NHE2 was upregulated in the distal tubule of NHE3-null mice, perhaps as an alternative route for bicarbonate reabsorption that is normally performed by NHE3 in the proximal tubule of control animals (Aronson, 1983; Bailey et al., 2004). Conceivably NHE2c may have a complimentary role with NHE2b, since this study shows NHE2c cDNA and protein to be present in gills, but baseline levels of NHE2b in control sculpin may have been sufficient for recovery from metabolic acidosis (Catches et al., 2006). Still another explanation could be that salinity affects NHE2 expression. NHE2c mRNA expression increased 2-fold in 20% seawater adapted longhorn sculpin (Hyndman and Evans, 2009). In saltwater adapted mummichog, NHE3 but not NHE2 was consistently detected, but in fresh water adapted animals, NHE2 was the dominant

isoform (Edwards et al., 2005). Prior to data mining and the NHE2c paralog discovery in GenBank, NHE3 was thought to be the dominant apical isoform in marine longhorn sculpin (Claiborne, unpublished data), as NHE2 was located subapically in MRCs (Catches et al., 2006). In fact, NHE2c and NHE3 in the gills of marine longhorn sculpin have similar cresent-shaped immunocytomchemical patterns. But the NHE2c antibody is not binding to NHE3, because the antibody is specific for a unique epitope only found in the NHE2c sequence, plus, NHE2 and NHE3 are distantly related and therefore do not have a high amino acid similarity (Figure 17 & 20).

Since NHE3 and NHE2c have such similar apical locations in the interlammelar region of sculpin gills, it can be hypothesized that NHE2c is the dominant isoform in animals with a 5' or 3' trinucleotide repeat that was found in the NHE3 mRNA transcript of longhorn sculpin (Diamanduros, 2006; Lanier, 2007). mRNA nucleotide repeats usually leads to changes in gene expression or complete loss of it (Liu et al., 2001). More functional comparisons of NHE3 and NHE2c in sculpin could help solve these confounding results of NHE2c expression in gills.

Lastly, NHE2c protein levels may be too small for immunological detection. Although the NHE2c antibody consistently targeted protein bands at 45 kDa, and sometimes a second band at 75 kDa, in Western blots (Figure 26), the protein homogenate for immunoblots consists of filaments from 2 gill arches. Immunohistochemical protein detection was in a mere 5μm cross-section of the gill arch, and whether it was the afferent edge or efferent edge of the filament is not known. Also noteworthy is that sculpin gill tissue is inherently autofluorescent, and the secondary antibody used introduces a significant amount of background staining (Figure 32). Both of these fluorescent impediments could interfere with the NHE2c signal.

In summary, we have demonstrated that NHE2c RNA, cDNA and protein is present in the gills of marine longhorn sculpin (*M. octodecemspinosus*). This NHE2c paralog is unique from the previously described NHE2b paralog in sculpin, as shown by the dissimilarities in the two amino acid sequences, and by its novel location on the apical membrane of the branchial epithelium, compared to the subapical distribution of NHE2b. Therefore, NHE3 is not the only apical NHE isoform within sculpin, and NHE2c may play an important role in the extrusion of H^+ ions from the fish, by Na^+/H^+ antiport

activity. Mulptiple NHEs in sculpin and other teleosts may demonstrate the importance this antiporter has in fish physiology, possibly evolving for tolerance to fluctuating ambient surroundings (ex. Ocean acidity, Appendix A). Studying NHEs in fish gives us an evolutionary perspective to homologous NHEs in higher vertebrates. One of the NHE paralogs mentioned (either NHE2b or NHE2c) could possibly be an NHE isoform retained in humans. Studying these transporters in a fish model could in the future shed insight on how these transporters function in humans and even in their role in human diseases.

Appendix A: pH, TA, DIC and ancillary water sample data

Carbon dioxide absorption in the oceans liberates H^+ ions from carbonic acid (H_2CO_3) and bicarbonate (HCO_3^-) in a reversible and balanced reaction (Millero, 2006): $CO_2 + H_2O \leftrightarrow H_2CO_3 \leftrightarrow HCO_3^- + H^+ \leftrightarrow CO_3^{2-} + 2H^+$. However, due to the increased amount of carbon dioxide in the atmosphere from anthropogenic activity, 20%-30% of the gas is absorbed by the ocean surface, which amounts to more H^+ in the oceans, thus increasing ocean acidity (Palmer et al., 1998; Solomon et al., 2007). Recent data indicates that this increased acidity is especially prevalent in the surface waters of the Atlantic Ocean (Key et al., 2004). CO_2 first enters the ocean cycle from Southern oceans and is carried North by deep ocean currents, where high latitudes and cold waters enhance CO_2 solubility conditions (Khatiwala et al., 2009; Zeebe and Wolf-Gladrow, 2009). CO_2 saturated fog from New England industrial areas also often lingers in the areas of Maine and Nova Scotia (Sullivan, 2006). The current average ocean pH is around 8.1, and is predicted to decrease by 0.3-0.4 pH units by the end of the century (Orr et al., 2005). Currently there is little published data of the water pH in Frenchman Bay, ME, near the MDIBL. In this preliminary study we have begun to characterize the pH and associated water quality parameters, including temperature, salinity, dissolved inorganic carbon (DIC), and total alkalinity (TA) of a small transect in Frenchman Bay, ME.

Surface (within 1m) and bottom water samples were collected on three separate days (during the months of June and July) for summers 2009 and 2010 by lowering a Niskin bottle on a line at three coordinates along a South to North transect. The sampling sites began near the moorings off of the MDIBL (N44°26'02.3", W068°17'25.5"; 6m depth), through pelagic waters (N44°26'21.8", W068°17'21.8"; 20m depth) to Lamoine Beach (N44°27'00.4", W068°17'10.2"; 11m depth). After lowering the bottle to the target depth, a weighted messenger was released down the line to stopper both ends of the bottle. After retrieval of the bottle, the water was immediately analyzed at the surface for salinity and temperature (YSI-85 handheld dissolved oxygen/conductivity meter) and water was quickly transferred from the Niskin bottle through Silicone tubing to rinse a borosilicate glass bottle that was then filled with the water sample, from bottom to top and without any headspace or the introduction of air bubbles. Three replicates were collected from

each Niskin bottle sample. To each bottle a drop of mercuric chloride ($HgCl_2$) was added to stop any metabolic activity. The samples where stored at 4° C prior to shipping on ice to the Ocean Process Analysis Lab (OPAL) at the University of New Hampshire in Durham, for analysis of DIC, TA, and pH (using salinity and temperature measurements). DIC was measured in quadruplicate while TA and pH were measured in duplicate.

Overall surface and bottom ocean pH were significantly lower in 2009 than in 2010 (Table 1). Wootton et al. 2008 suggested that seawater pH can fluctuate by a full unit or more, year-to-year, and by as much as 0.24 units diurnally. For each year, surface pH was significantly higher than epibenthic pH (2009: $U=222$, $df = 1$; 2010: $t=4.96$, $df = 1$, $p<0.001$). pH was not statistically different between locations.

Salinity was significantly higher in surface waters during summer 2010 than in summer 2009. Salinity measurements taken at low tides on 7/21/10 and 7/28/10 were statistically different from each other by 0.3 ppt ($F=5.136$, $df=2,51$, $p=0.0093$, Tukey-Kramar for *a posteriori*). *In situ* water temperatures taken from the bottom of the bay were significantly higher in 2010 (Table 1). Temperatures measured with the YSI 85 Dissolved Oxygen and Conductivity Meter were significantly different for each day of measurement ($H=20.00$, $df=2$, $p<0.0001$). There was no significant difference between shipboard salinity (2009 and 2010) and temperature measurements (2010) taken at the surface and bottom of the water column. In 2009, temperature was significantly different between depths ($t=2.700$, $df=13$, $p=0.018$). Temperature and salinity measurements were not significant between locations in a single year.

We have used the average pH of each replicate in the data presented in Table 1. pH values in Table 1 and discussed in the text are directly measured pH with a probe. Extrapolating pH from dissolved inorganic carbon (DIC) and total alkalinity (TA) with CO2Sys Excel Macro (Lewis and Wallace, 1998) results in an average surface pH 8.09 ±0.01 and a bottom pH of 8.01 ±0.01 for 2010 (Table 2). This method was not employed for 2009 data because sufficient DIC and TA values were not obtained for that year.

Table 3: Mean water quality parameters measured in Frenchman Bay, ME, taken within 1 m of the surface and at the bottom of the bay at three different locations. pH surface and bottom measured in 2009 U=222, df = 1, p<0.001 (one-tailed test). pH difference between 2010 surface and bottom values when corrected for ties t=10.602, df = 1, p<0.001 (two-tailed). pH comparison between surface 2009 and 2010 when corrected for ties t=3.46, df = 1, p<0.001 (one-tailed). pH bottom 2009 and 2010 when corrected for ties t=6.046, df=1, p=0.0155 (two-tailed). Salinity F=7.2885, df=3, p<0.001, Tukey-Kramar test surface 2010 significantly different surface 2009. Temperature F=5.3410, df=3, p=0.0047. Mann-Whitney-U test for pH, 1-way ANOVA for salinity and temperature, mean ± SE.

Year	**Depth**	**pH**		**Salinity (ppt)**		**Temperature**	
		Mean	N	Mean	N	Mean	N
'09	Surface	7.87 ±0.01	13	31.0 ±0.1	7	14.9 ±0.5	7
	Bottom	7.76 ±0.02	19	31.4 ±0.2	8	12.6 ±0.7	8
'10	Surface	7.93 ±0.01	26	31.8 ±0.0	9	15.8 ±0.8	9
	Bottom	7.82 ±0.01	27	31.7 ±0.1	9	15.4 ±0.4	9

Table 4: Water quality parameters, including total alkalinity (TA) and dissolved inorganic carbon (DIC) were measured in Frenchman Bay, ME, and pH was extrapolated using the CO_2 Sys EXCEL Macro (Lewis, 1998). pH is significantly lower at the bottom of the bay than at the surface t=5.087, df=52, p-value<0.001.Student T-test, mean ± SE

Depth	**pH**		**TA (µmol/kg)**		**DIC (µmol/kg)**	
	Mean	N	Mean	N	Mean	N
Surface	8.09 ±0.01	27	2137 ±3.03	27	1974 ±3	27
Bottom	8.01 ±0.01	27	2154 ±1.78	27	2025 ±5	27

Perspective

Clearly, a two year "snap-shot" of water pH variability is not enough to show long term changes, but these base line measurements will provide a basis for comparison in future studies. Studies where teleost species have been exposed to 1% hypercapnia, which is equivalent to 10,000 ppm pCO_2, have resulted in increased excretion H^+ ions from the fish to the water (Edwards et al., 2005) and increased expression of NHE proteins (Wall et al., 2001; Ivanis et al., 2008). Throughout the brief history of ocean acidification research, most studies involve the classic levels of ambient pCO2 (~380 ppm) and future atmospheric pCO2 (usually 750 ppm) (Riebesell et al., 2009). Hypercapnic studies may indicate that some teleost species will be able to physiologically cope with rising ocean pH through NHE upregulation and Cl^-/HCO_3^- antiporters.

Figure 27: pH and ancillary data was measured from samples collected along a North to South transect in Frenchman Bay, ME. Surface (within 1m) and bottom water samples were collected on three separate days (during the months of June and July) for summers 2009 and 2010 by lowering a Niskin bottle on a line at three coordinates along a South to North transect. The sampling sites began near the moorings off of the MDIBL (N44°26'02.3", W068°17'25.5"; 6m depth), through pelagic waters (N44°26'21.8", W068°17'21.8"; 20m depth) to Lamoine Beach (N44°27'00.4", W068°17'10.2"; 11m depth).

Appendix B: Alternative RACE methods also tried

GeneRacer RNA Ligase-Mediated cDNA Amplification:

Once some of the sequence for sculpin NHE2c was obtained from cross-compatible *Gasterosteus aculeatus* primers, GeneRacer gene specific primers were designed with Oligo 6 software (Molecular Biology Insights, Inc., Cascade, CO) for positive control PCR and for performing rapid amplification of cDNA ends (RACE). The RACE PCR was performed using the GeneRacer (Invitrogen, Carlsbad, CA) kit. Gene specific primers were used in conjunction with a homologous GeneRacer 3' primer to amplify the 3' end of sculpin NHE2c (Table 1).

GeneRacer RACE cDNA Synthesis

Determination of unknown 5' and 3' ends is made possible by creating known priming sites with the GeneRacer RNA Oligo and GeneRacer Oligo dT primer. To obtain 5' ends, an RNA oligonucleotide is selectively ligated to decapped mRNA ends using T4 RNA ligase (Kazuo and Sumio, 1994).

In order to synthesize a protein specific antibody for immunofluorescent detection, the identity of the NHE2c 3' ends was foremost desired since this is the most variable region of the NHEs. For 3' end synthesis, total RNA was isolated as noted previously, then mRNA was reverse transcribed using SuperScript III RT and the GeneRacer Oligo dT primer to create first strand cDNA. The GeneRacer Oligo dT primer creates a known priming site at the 3'end of the first strand cDNA to create known priming sites at the 3′ ends (Figure 28).

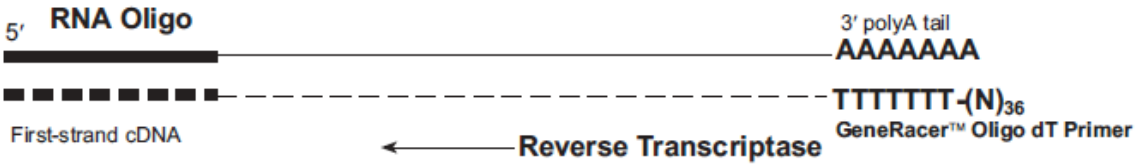

Figure 28: First-strand cDNA was created by reverse transcribing mRNA using SuperScript™ III RT and the GeneRacer™ Oligo dT Primer to create RACE ready cDNA with known 3' priming sites so that GeneRacer 3' Primer can be used in RACE PCR.

GeneRacer RACE PCR

Forward GSP and Forward nested GSP were designed for the sense cDNA strand to amplify the cDNA 3' ends once the homologous GeneRacer 3' Primer was primed onto first strand cDNA (Figure 29). Additional PCR with nested primers is used when a distinct RACE PCR product is not obtained or when high background PCR is detected from the first RACE PCR. For a positive control, two GSP that amplified a short segment of the cDNA were designed to verify that the cDNA was present.

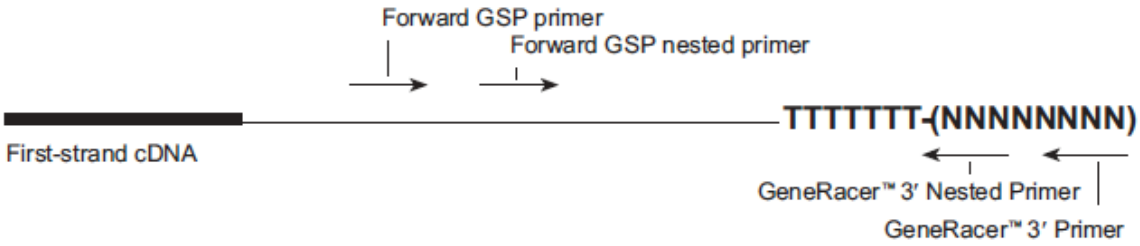

Figure 29: The kit is designed to obtain the 3′ ends by amplifying the first-strand cDNA using a forward gene specific primer (GR3'_C_GSP2506) and homologous GeneRacer™ 3′ Primer (GR3'P), (complimentary to the GeneRacer™ Oligo dT Primer).

The first strand sculpin NHE2c cDNA was mixed in a 50µl 3' reaction. The PCR was prepared as previously described. The initial denaturing step was performed at 95°C for 3 minutes. Next 59°C for 30 seconds annealed the primers to the cDNA with high specificity. Elongation of the first cDNA copy was made at 72°C for 1 minute 30 seconds. During the second PCR stage, 35 cycles of 95°C denaturation for 30 seconds, annealing at 54°C for 30 seconds, and extension at 72°C for 1 minute 15 seconds were repeated. When the PCR product sequence came back with nonspecific sequence for NHE2c, a temperature gradient from 56°C to 72°C was established in the columns of the PCR hot plate in order to increase the specificity of the PCR products.

Results

The full-nested, GeneRacer 3' RACE PCR product was obtained using a homologous GeneRacer 3' primer (GR3'P) with GeneRacer gene specific primer (GR3'_C_GSP2506) and nested with nested GeneRacer 3' primer (NGR3'P) plus nested GeneRacer gene specific primer (N_GR3'_C_GSP2580). An annealing temperature of 54°C seemed to amplify a RACE product that was of the right size to be from the NHE2c 3' transcript, approximately 738 bp (Figure 30, Lane 9). There were at least 3 bands stacked on top of each other in lane 9, distinguished as high, medium and low bands. So these bands were resolved with low-meltelectrophoresis, excised from the gel, and cloned. Colonies of bacteria with the gel-purified, RACE inserts were picked for simultaneous PCR amplification and overnight growth in LB media. GeneRacer 3' Nested Primer and N_GR3'_C_GSP2580 were used in PCR to see if the target sequence could be obtained from the cloned inserts (Figure 31).

At least two colonies picked from the high, medium, and low-melt gel transformants were PCR amplified and had a fragment that could possibly have been from the 3' NHE2c. Two bacteria colonies from each the low band (Figure 31, Lane 5 & 7), the middle band (Lane 13 & 14), and the high band (Lane 17 & 18) from gel electrophoresis were checked for cDNA purity with a spectrophotometer. The 260/280-absorbance ratios for the bands were 1.86, 1.87, 1.84, 1.85, 1.85, and 1.88, respectively. The bacteria

cultures were then plasmid purified and sent off to the Mount Desert Island Biological Laboratory (MDIBL) for sequencing.

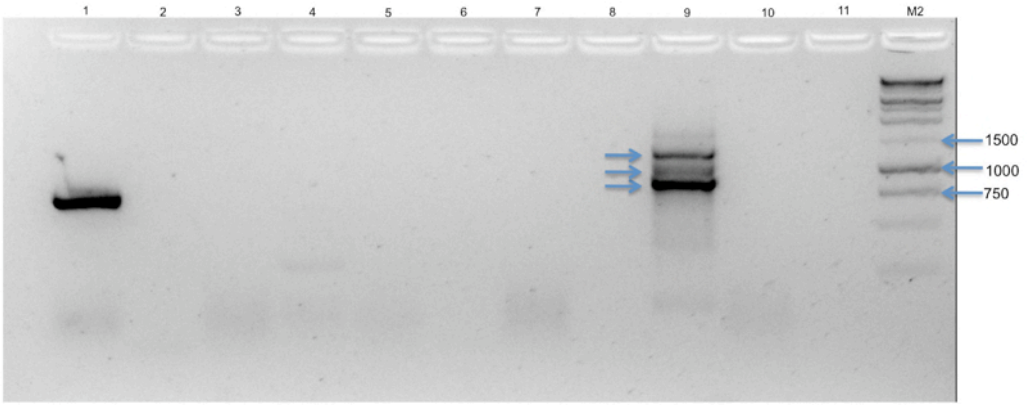

Figure 30: 2% agarose gel stained with ethidium bromide showing results for GeneRacer nestedRACE reaction. In lane 9, the putative NHE2c GeneRacer 3' RACE PCR product amplified with a homologous GeneRacer 3' Primer (GR3'P) and GeneRacer gene specific primer (GR3'_C_GSP2506), and then nested with a homologous Nested GeneRacer 3' Primer (NGR3'P) and nested GeneRacer gene specific primer (N_GR3'_C_GSP2580). The 3 bands indicated by arrows (low, medium and high) were resolved and extracted with low-melt gel electrophoresis and sent off for sequencing at MDIBL. Lane 1: positive control with NHE2c cDNA amplified with CC572 and CC573 primers; Lane 2: negative NHE2c cDNA; Lane 3-8: Negative GeneRacer products; Lane 9: 3' GeneRacer PCR product that was resolved with low-meltgel electrophoresis; Lane 10: negative control GeneRacer 3' RACE with NHE2c RNA;Lane 11: negative control without cDNA.

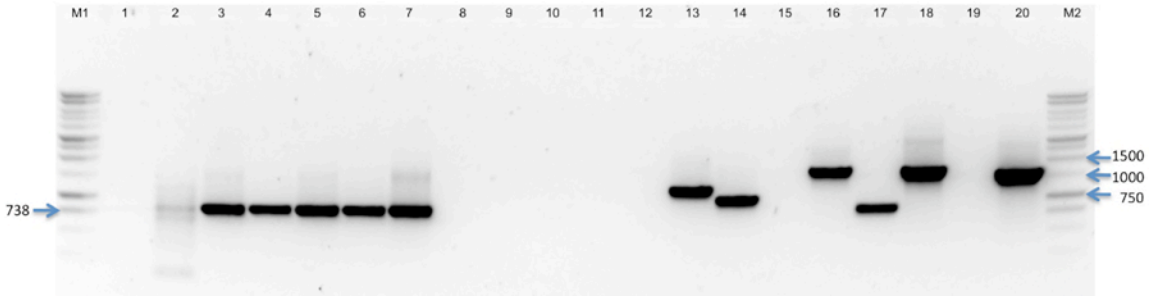

Figure 31: 2% agarose gel stained with 0.01% ethidium bromide showing colonies transformed with GeneRacer 3' RACE gel purified PCR product. All controls and colonies were amplified with homologous Nested GeneRacer 3' primer (NGR3'P) and nested GeneRacer gene specific primer (N_GR3'_C_GSP2580). Bacterial cultures that corresponded to the low band (Lane 5 & 7), the middle band (Lane 13 & 14), and the high band (Lane 17 &18) were plasmid purified and sent to MDIBl for sequencing. Lane 2: positive control with gel purified GeneRacer full-nested PCR product; Lane 2-9: low band from low-meltgel purified GeneRacer 3' product; Lane 10-15: middle band; Lane 16-20; high band.

The returned sequence trace file did not match the *G. aculeatus* NHE2c nucleotide sequence when compared in Pustell DNA Matrix, a dot-plot function in MacVector. So to try to resolve this issue, the same GeneRacer nested PCR was repeated but this time at various annealing temperatures of 56°C, 59.4, 63.1, 65.9, and 68.2, so that the primers would bind specifically to the cDNA template. The PCR products returned streaked bands which we did not try to resolve and sequence.

Appendix C: IHC controls

Secondary Antibody Only (MOC 37)

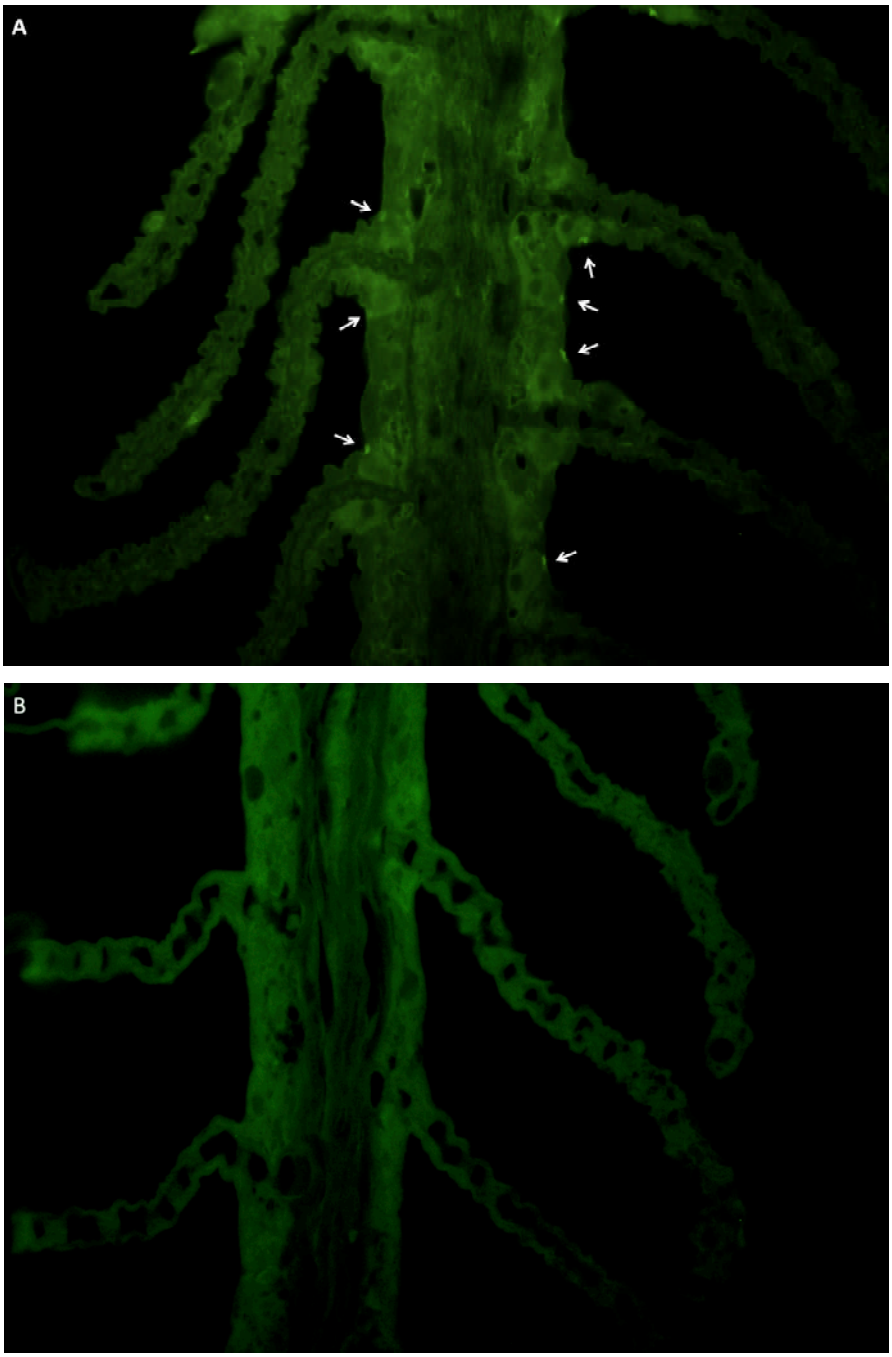

Figure 32: Color-contrast micrograph images of consecutive gill slices from sculpin #37 that shows the background staining from an Invitrogen Alexa-Fluor 488 goat, anti-rabbit secondary antibody when used alone as a negative control (B). This fluorescence occurs when the secondary antibody is applied to the tissue without a primary antibody to bind. This indicates that either the gill tissue of sculpin is autofluroscent, or the mass manufactured antibody is not suited for sculpin tissue.

Pre-Immune Controls (MOC 1009 & MOC 37)

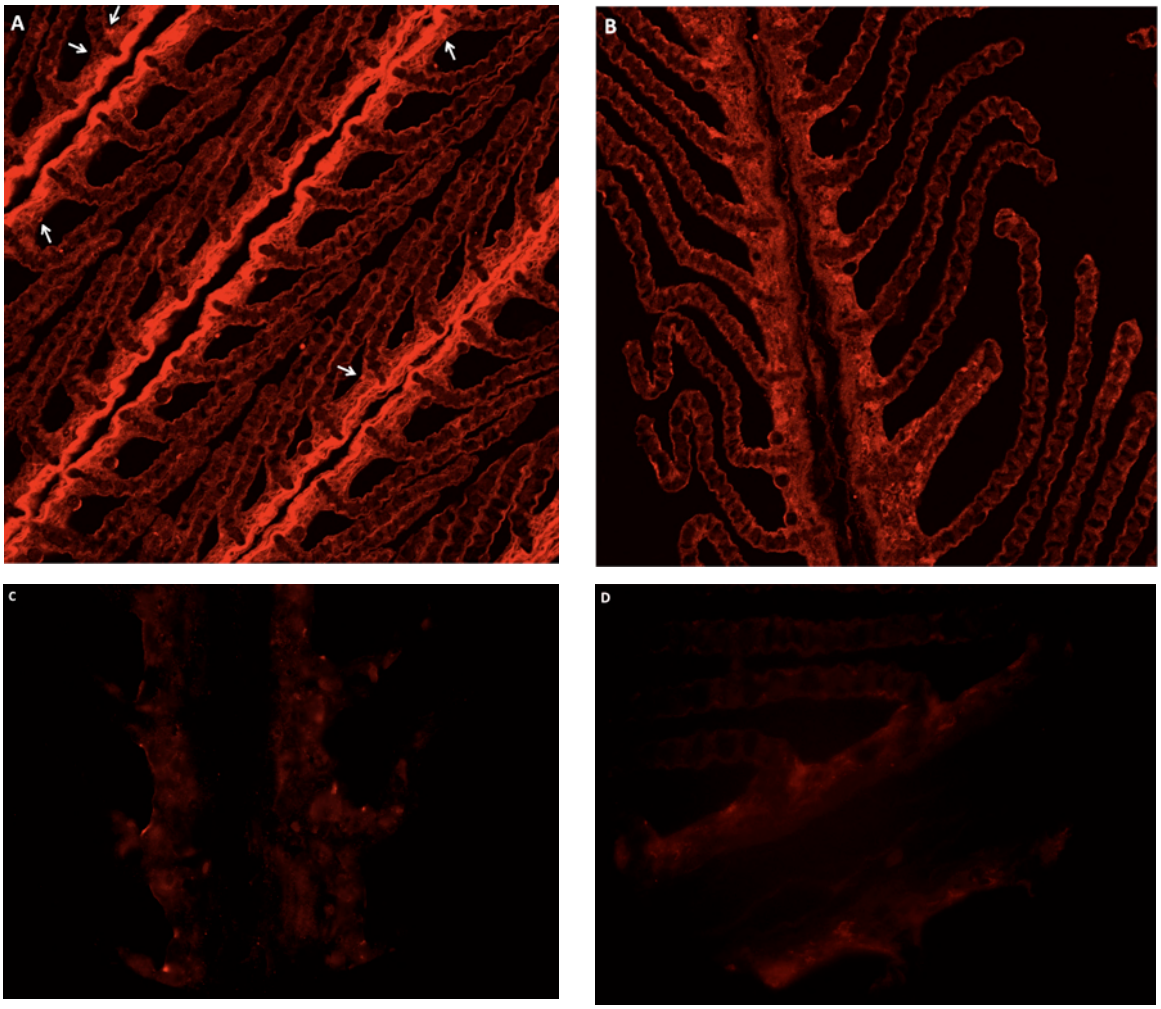

Figure 33: Pre-immune NHE2c controls of branchial tissue from sculpin MOC1009 (B & D) and MOC37 (C). The tissue was incubated at the same concentration as the anti-NHE2c antibody concentration but with plasma from rabbits prior to immunization with the NHE2c peptide. Panel A and B are confocal laser scanning micrographs of M1009 tissue that was incubated with the anti-NHE2c antibody and the pre-immune serum, respectively. Panel C, sculpin MOC37, and D, MOC1009, are images taken with a fluorescent microscope that are also labeled with pre-immune serum. In some cases, the pre-immune serum seems to have bound to areas similar to the NHE2c location, however, pre-immune binding does not appear to have the same pattern as NHE2c. This does not affirm false-positive antibody specificity, as the peptide-competition control is the real assurance that the antibody is specific for its peptide.The pre-immune serum could have a good amount of pre-existing, natural antibodies that recognize antigenic determinants, not molecules (Tips et al., 1997).

Work-cited

Argos, P., J. K. M. Rao and P. A. Hargrave (1982). "Structural Prediction of Membrane-Bound Proteins." European Journal of Biochemistry **128**(2-3): 565-575.

Aronson, P. S. (1983). "Mechanisms of active H+ secretion in the proximal tubule." American Journal of Physiology - Renal Physiology **245**(6): F647-F659.

Aronson, P. S., J. Nee and M. A. Suhm (1982). "Modifier role of internal H^+ in activating the Na^+-H^+ exchanger in renal microvillus membrane vesicles." Nature **299**(5879): 161-3.

Bailey, M. A., G. Giebisch, T. Abbiati, P. S. Aronson, L. R. Gawenis,G. Shull and T. Wang (2004). "NHE2-mediated bicarbonate reabsorption in the distal tubule of NHE3 null mice." Journal of Physiology **561**(3): 765-775.

Bentley, P. J., J. Maetz and P. Payan (1976). "A study of the unidirectional fluxes of Na^+ and Cl^- across the gills of the dogfish *Scyliorhinus canicula* (Chondrichthyes)." Journal of Experimental Biology **64**(3): 629-637.

Bookstein, C., Y. Xie, K. Rabenau, M. W. Musch, R. L. McSwine, M. C. Rao and E. B. Chang (1997). "Tissue distribution of Na^+ /H^+ exchanger isoforms NHE2 and NHE4 in rat intestine and kidney." American Journal of Physiology - Cell Physiology **273**(5): C1496-C1505.

Borson, N. D., W. L. Salo and L. R. Drewes (1992). "A lock-docking oligo(dT) primer for 5' and 3' RACE PCR." Genome Research **2**(2): 144-148.

Brett, C. L., M. Donowitz and R. Rao (2005). "Evolutionary origins of eukaryotic sodium/proton exchangers." American Journal of Physiology and Cell Physiology **288**(2): C223-239.

Brett, C. L., Y. Wei, M. Donowitz and R. Rao (2002). "Human Na^+/H^+ exchanger isoform 6 is found in recycling endosomes of cells, not in mitochondria." American Journal of Physiology - Cell Physiology **282**(5): C1031-C1041.

Catches, J. S., J. M. Burns, S. L. Edwards and J. B. Claiborne (2006). "Na^+ /H^+ antiporter, V-H^+ -ATPase and Na^+/K^+-ATPase immunolocalization in a marine teleost (*Myoxocephalus octodecemspinosus*)." Journal of Experimental Biology **209**(17): 3440-3447.

Cavet, M. E., S. Akhter, F. S. de Medina, M. Donowitz and C.-M. Tse (1999). "Na^+/H^+ exchangers (NHE1-3) have similar turnover numbers but different percentages on the cell surface." American Journal of Physiology - Cell Physiology **277**(6): C1111-C1121.

Chambrey, R. g., P. L. St. John, D. Eladari, F. Quentin, D. G. Warnock, D. R. Abrahamson, R.-A. Podevin and M. Paillard (2001). "Localization and functional characterization of Na^+/H^+ exchanger isoform NHE4 in rat thick ascending limbs." American Journal of Physiology - Renal Physiology **281**(4): F707-F717.

Choe, K. P., A. Kato, S. Hirose, C. Plata, A. Sindic, M. F. Romero, J. B. Claiborne and D. H. Evans (2005). "NHE3 in an ancestral vertebrate: primary sequence, distribution, localization, and function in gills." American Journal of Physiology - Regulatory, Integrative and Comparative Physiology **289**(5): R1520-R1534.

Choe, K. P., S. O'Brien, D. H. Evans, T. Toop and S. L. Edwards (2004). "Immunolocalization of Na^+ /K+-ATPase, carbonic anhydrase II, and vacuolar H^+ -ATPase in the gills of freshwater adult lampreys, Geotria australis." Journal of Experimental Zoology Part A: Comparative Experimental Biology **301A**(8): 654-665.

Chow, C. W. (1999). Regulation and intracellular localization of the epithelial isoforms of the Na[+]/H[+] exchangers NHE2 and NHE3. Toronto, ON, CANADA, Canadian Medical Association.

Claiborne, J. B., C. R. Blackston, K. P. Choe, D. C. Dawson, S. P. Harris, L. A. Mackenzie and A. I. Morrison-Shetlar (1999). "A mechanism for branchial acid excretion in marine fish: identification of multiple Na^+/H^+ antiporter (NHE) isoforms in gills of two seawater teleosts." Journal of Experimental Biology **202**(Pt 3): 315-24.

Claiborne, J. B., K. P. Choe, A. I. Morrison-Shetlar, J. C. Weakley, J. Havird, A. Freiji, D. H. Evans and S. L. Edwards (2008). "Molecular detection and immunological localization of gill Na^+/H^+ exchanger in the dogfish (*Squalus acanthias*)." American Journal of Physiology - Regulatory, Integrative and Comparitive Physiology **294**(3): R1092-102.

Claiborne, J. B., S. L. Edwards and A. I. Morrison-Shetlar (2002). "Acid-base regulation in fishes: cellular and molecular mechanisms." Journal of Experimental Zoology **293**(3): 302-19.

Claiborne, J. B. and N. Heisler (1986). "Acid-base regulation and ion transfers in the carp (*Cyprinus carpio*): pH compensation during graded long- and short-term environmental hypercapnia, and the effect of bicarbonate infusion." Journal of Experimental Biology **126**: 41-61.

Claiborne, J. B., E. Perry, S. Bellows and J. Campbell (1997). "Mechanisms of acid-base excretion across the gills of a marine fish." Journal of Experimental Zoology **279**(5): 509-520.

Claiborne, J. B., J. Walton and D. Compton-Mccullough (1994). " Acid-base regulation, branchial transfers and renal output in a marine teleost fish (the long-horned sculpin *Myoxocephalus octodecimspinosus*) during exposure to low salinities " Journal of Experimental Biology **193**(1): 79-95.

Coupaye-Gerard, B., C. Bookstein, P. Duncan, X. Y. Chen, P. R. Smith, M. Musch, S. A. Ernst, E. B. Chang and T. R. Kleyman (1996). "Biosynthesis and cell surface delivery of the NHE1 isoform of Na^+ /H^+ exchanger in A6 cells." American Journal of Physiology - Cell Physiology **271**(5): C1639-C1645.

Cutler, C. P., S. Brezillon, S. Bekir, I. L. Sanders, N. Hazon and G. Cramb(2000). "Expression of a duplicate Na,K-ATPase beta (1)-isoform in the European eel (*Anguilla anguilla*)." American Journal of Physiology - Regulatory, Integrative and Comparative Physiology **279**(1): R222-R229.

Cutler, C. P. and G. Cramb (2001). "Molecular physiology of osmoregulation in eels and other teleosts: the role of transporter isoforms and gene duplication." Comparative Biochemistry and Physiology - Part A: Molecular & Integrative Physiology **130**(3): 551-564.

Diamanduros, A., M. Foster, G. Luchini, C. Lanier and J. Claiborne(2006). "Nucleotide repeats in gill NHE3 of longhorn sculpin (Myoxocephalus octodecimspinosus)." The Bulletin, MDI Biological Laboratory **45**: 49.

de Silva, M. G., K. Elliott, H.-H. Dahl, E. Fitzpatrick, S. Wilcox, M. Delatycki, R. Williamson, D. Efron, M. Lynch and S. Forrest (2003). "Disruption of a novel member of a sodium/hydrogen exchanger family and DOCK3 is associated with an attention deficit hyperactivity disorder-like phenotype." Journal of Medical Genetics **40**(10): 733-740.

Edwards, S. L., C. M. Tse and T. Toop (1999). "Immunolocalisation of NHE3-like immunoreactivity in the gills of the rainbow trout (*Oncorhynchus mykiss*) and the blue-throated wrasse (Pseudolabrus tetrious)." Journal of Anatomy **195**(3): 465-469.

Edwards, S. L., B. P. Wall, A. Morrison-Shetlar, S. Sligh, J. C. Weakley and J. B. Claiborne (2005). "The effect of environmental hypercapnia and salinity on the expression of NHE-like isoforms in the gills of a euryhaline fish (*Fundulus heteroclitus*)." Journal of Experimental Zoology Part A: Comparative and Experimental Biology **303**(6): 464-75.

Edwards, S. L., J. C. Weakley, A. W. Diamanduros and J. B. Claiborne (2010). "Molecular identification of Na^+ –H^+ exchanger isoforms (NHE2) in the gills of the euryhaline teleost *Fundulus heteroclitus*." Journal of Fish Biology **76**(2): 415-426.

Evans, D. E. (1982). "Mechanisms of Acid Extrusion by Two Marine Fishes: The Teleost, *Opsanus Beta*, and the Elasmobranch, *Squalus Acanthias* " Journal of Experimental Biology **97**: 289-299.

Evans, D. H. (2008). "Teleost fish osmoregulation: what have we learned since August Krogh, Homer Smith, and Ancel Keys." American Journal of Physiology - Regulatory, Integrative and Comparative Physiology **295**(2): R704-R713.

Evans, D. H., J. B. Claiborne, L. Farmer, C. Mallery and E. J. Krasny, JR. (1982). " Fish gill ionic transport: methods and models " Biological Bulletin **163**(1): 108-130.

Evans, D. H., P. M. Piermarini and K. P. Choe (2005). "The Multifunctional Fish Gill: Dominant Site of Gas Exchange, Osmoregulation, Acid-Base Regulation, and Excretion of Nitrogenous Waste." Physiological Reveiw **85**(1): 97-177.

Evans, D. H., P. M. Piermarini and W. T. W. Potts (1999). "Ionic transport in the fish gill epithelium." Journal of Experimental Zoology **283**(7): 641-652.

Fliegel, L. and J. R. B. Dyck (1995). "Molecular biology of the cardiac sodium/hydrogen exchanger." Cardiovascular Research **29**(2): 155-159.

Force, A., M. Lynch, F. B. Pickett, A. Amores, Y.-l. Yan and J. Postlethwait (1999). "Preservation of Duplicate Genes by Complementary, Degenerative Mutations." Genetics **151**(4): 1531-1545.

Foskett, J. and C. Scheffey (1982). "The chloride cell: definitive identification as the salt-secretory cell in teleosts." Science **215**(4529): 164-166.

Fukura, N., R. Ohgaki, M. Matsushita, N. Nakamura, K. Mitsui and H. Kanazawa (2010). "A Membrane-Proximal Region in the C-Terminal Tail of NHE7 Is Required for Its Distribution in the Trans-Golgi Network, Distinct from NHE6 Localization at Endosomes." Journal of Membrane Biology **234**(3): 149-158.

Gilfillan, G. D., K. K. Selmer, I. Roxrud, R. Smith, M. Kyllerman, K. Eiklid, M. Kroken, M. Mattingsdal, T. Egeland, H. Stenmark, H. Sj¯holm, A. Server, L. Samuelsson, A. Christianson, P. Tarpey, A. Whibley, M. R. Stratton, P. A. Futreal, J. Teague, S. Edkins, J. Gecz, G. Turner, F. L. Raymond, C. Schwartz, R. E. Stevenson, D. E. Undlien and P. Str¯mme (2008). "SLC9A6 Mutations Cause X-

Linked Mental Retardation, Microcephaly, Epilepsy, and Ataxia, a Phenotype Mimicking Angelman Syndrome." American journal of human genetics **82**(4): 1003-1010.

Goyal, S., G. Vanden Heuvel and P. S. Aronson (2003). "Renal expression of novel Na^+ /H^+ exchanger isoform NHE8." American Journal of Physiology - Renal Physiology **284**(3): F467-F473.

Gunning, D. L., J. B. Claiborne and A. I. M-Sheltar (2001). "Molecular identification and cloning of the first full-length fish NHE2-like sequence from the gills of the long-horned sculpin, *Myoxocephalus octodecimspinosus.*" Bulletin of the Mount Desert Island Biological Laboratory **40**: 71-72.

He, P. and C. C. Yun (2010). "Mechanisms of the Regulation of the Intestinal Na^+ /H^+ Exchanger NHE3." Journal of Biomedicine and Biotechnology **2010**.

Hinegardner, R. (1968). "Evolution of Celular DNA Content in Teleost Fish " The American Naturalist **102**(928): 517-523.

Hirata, T., T. Kaneko, T. Ono, T. Nakazato, N. Furukawa, S. Hasegawa, S. Wakabayashi, M. Shigekawa, M. Chang, M. F. Romero and S. Hirose (2003). "Mechanism of acid adaptation of a fish living in a pH 3.5 lake." American Journal of Physiology - Regulatory, Integrative and Comparartive Physiology **284**(5): R1199-1212.

Hunte, C., E. Screpanti, M. Venturi, A. Rimon, E. Padan and H. Michel (2005). "Structure of a Na^+ /H^+ antiporter and insights into mechanism of action and regulation by pH." Nature **435**(7046): 1197-1202.

Hyndman, K. A. and D. H. Evans (2009). "Short-term low-salinity tolerance by the longhorn sculpin, *Myoxocephalus octodecimspinosus.*" Journal of Experimental Zoology Part A: Ecological Genetics and Physiology **311A**(1): 45-56.

Invitrogen GeneRacer TOPO TA Cloning® Kit for Sequencing. U.S. .

Ivanis, G., A. J. Esbaugh and S. F. Perry (2008). "Branchial expression and localization of SLC9A2 and SLC9A3 sodium/hydrogen exchangers and their possible role in acid-base regulation in freshwater rainbow trout (*Oncorhynchus mykiss*)." Journal of Experimental Biology **211**(15): 2467-2477.

Jameson, B. A. and H. Wolf (1988). "The antigenic index: a novel algorithm for predicting antigenic determinants " Computer Applications in the Biosciences **4**(1): 181-186.

Janis, C. M. and C. Farmer (1999). "Proposed habitats of early tetrapods: gills, kidneys, and the water-land transition." Zoological Journal of the Linnean Society **126**(1): 117-126.

Johnson, J. D., D. Epel and M. Paul (1976). "Intracellular pH and activation of sea urchin eggs after fertilisation." Nature **262**(5570): 661-664.

Karnaky, K., K. Degnan and J. Zadunaisky (1977). "Chloride transport across isolated opercular epithelium of killifish: a membrane rich in chloride cells." Science **195**(4274): 203-205.

Karnaky, K. J., L. B. Kinter, W. B. Kinter and C. E. Stirling (1976). "Teleost chloride cell. II. Autoradiographic localization of gill Na,K-ATPase in killifish Fundulus heteroclitus adapted to low and high salinity environments." The Journal of Cell Biology **70**(1): 157-177.

Kazuo, M. and S. Sumio (1994). "Oligo-capping: a simple method to replace the cap structure of eukaryotic mRNAs with oligoribonucleotides." Gene **138**(1-2): 171-174.

Key, R. M., A. Kozyr, C. L. Sabine, K. Lee, R. Wanninkhof, J. L. Bullister, R. A. Feely, F. J. Millero, C. Mordy and T. H. Peng (2004). "A global ocean carbon climatology: Results from Global Data Analysis Project (GLODAP)." Global Biogeochem. Cycles **18**.

Keys, A. and E. N. Willmer (1932). "“Chloride secreting cells” in the gills of fishes, with special reference to the common eel." Journal of Physiology **76**(3): 368-378.

Khatiwala, S., F. Primeau and T. Hall (2009). "Reconstruction of the history of anthropogenic CO2 concentrations in the ocean." Nature **462**(7271): 346-349.

Knauf, P. A., F.-Y. Law, T.-W. V. Leung, A. U. Gehret and M. L. Perez (2002). "Substrate-dependent reversal of anion transport site orientation in the human red blood cell anion-exchange protein, AE1." Proceedings of the National Academy of Sciences **99**(16): 10861-10864.

Kozak, M. (1984). "Compilation and analysis of sequences upstream from the translational start site in eukaryotic mRNAs." Nucleic Acids Research **12**(2): 857-872.

Kratochvilova, H., S. Edwards and J. B. claiborne (2009). "Expression of Na^+ /H^+ exchanger paralogs in skin of the marine longhorn sculpin (*Myoxocephalus octodecemspinosus*)." The Bulletin, MDI Biological Laboratory **48**: 77-78.

Krogh, A. (1937). "Osmotic regulation in fresh water fishes by active absorption of chloride ions." Journal of Comparative Physiology A: Neuroethology, Sensory, Neural, and Behavioral Physiology **24**(5): 656-666.

Lanier, C. (2007). CHARACTERIZATION OF Na^+ /H^+ EXCHANGER-3 (NHE3) IN THE GILLS OF
LONGHORN SCULPIN (*MYOXOCEPHALUS OCTODECEMSPINOSUS*). Department of Biology. Statesoboro, Georgia Southern University. **M.S. :** 91.

LaRue, K., Tarley, M., Wilbur, B., Diamanduros, A., Claiborne, J. (2009). "Tissue distribution of NHE isoform transcripts in the longhorn sculpin, *Myoxocephalus octodecemspinosus* " The Bulletin, MDI Biological Laboratory **48**: 48-49.

Ledoussal, C., J. N. Lorenz, M. L. Nieman, M. Soleimani, P. J. Schultheis and G. E. Shull (2001). "Renal salt wasting in mice lacking NHE3 Na^+ /H^+ exchanger but not in mice lacking NHE2." American Journal of Physiology - Renal Physiology **281**(4): F718-F727.

Lewis, E. and W. R. Wallace (1998). Program developed for CO2 System Calculations. . Oak Ridge, TE, Carbon Dioxide Information Analysis Center, Oak Ridge National Laboratory, U.S. Department of Energy.

Liu, Z., P. Li, A. Kocabas, A. Karsi and Z. Ju (2001). "Microsatellite-Containing Genes from the Channel Catfish Brain: Evidence of Trinucleotide Repeat Expansion in the Coding Region of Nucleotide Excision Repair Gene RAD23B." Biochemical and Biophysical Research Communications **289**(2): 317-324.

Maetz, J. (1971). "Fish Gills: Mechanisms of Salt Transfer in Fresh Water and Sea Water." Philosophical Transactions of the Royal Society of London. B, Biological Sciences **262**(842): 209-249.

Malo, M. E. and L. Fliegel (2006). "Physiological role and regulation of the Na^+ /H^+ exchanger." Canadian Journal of Physiology and Pharmacology **84**(11): 1081-1095.

Mandoiu, I., G. Narasimhan, Y. Zhang, A. Muñoz and D. Sankoff (2009). Rearrangement Phylogeny of Genomes in Contig Form. Bioinformatics Research and Applications, Springer Berlin / Heidelberg. **5542:** 160-172.

Marshall, W. S. and M. Grosell (2006). The Physiology of Fishes Boca Raton, CRC Press

McCormick, S. D., A. M. Regish and A. K. Christensen (2009). "Distinct freshwater and seawater isoforms of Na^+ /K+-ATPase in gill chloride cells of Atlantic salmon." Journal of Experimental Biology **212**(24): 3994-4001.

McDonald, D. G., R. L. Walker, P. R. Wilkes and C. M. Wood (1982). "H^+ excretion in the marine teleost Parophrys vetulus." Journal of Experimental Biology **98**(1): 403-414.

Millero, F. (2006). Chemical Oceanography Boca Raton, FL, CRC Press

Miyazaki, E., M. Sakaguchi, S. Wakabayashi, M. Shigekawa and K. Mihara (2001). "NHE6 Protein Possesses a Signal Peptide Destined for Endoplasmic Reticulum Membrane and Localizes in Secretory Organelles of the Cell." Journal of Biological Chemistry **276**(52): 49221-49227.

Morgan, I., W. Potts and K. Oates (1994). "Intracellular ion concentrations in branchial epithelial cells of brown trout (*Salmo Trutta L.*) determined by x-ray microanalysis " Journal of Experimental Biology **194**(1): 139-151.

Munoz, A. and D. Sankoff (2009). Rearrangement Phylogeny of Genomes in Contig Form. Proceedings of the 5th International Symposium on Bioinformatics Research and Applications. Fort Lauderdale, FL, Springer-Verlag.

Nakamura, N., S. Tanaka, Y. Teko, K. Mitsui and H. Kanazawa (2005). "Four Na^+ /H^+ Exchanger Isoforms Are Distributed to Golgi and Post-Golgi Compartments and Are Involved in Organelle pH Regulation." Journal of Biological Chemistry **280**(2): 1561-1572.

Ohgaki, R., S. C. D. van Ijzendoorn, M. Matsushita, D. Hoekstra and H. Kanazawa (2010). "Organellar Na^+ /H^+ Exchangers: Novel Players in Organelle pH Regulation and Their Emerging Functions." Biochemistry **50**(4): 443-450.

Ohno, S. (1970). Evolution by gene duplication. New York, Springer-Verlag.

Olkhova, E., C. Hunte, E. Screpanti, E. Padan and H. Michel (2006). "Multiconformation continuum electrostatics analysis of the NhaA Na^+ /H^+ antiporter of Escherichia coli with functional implications." Proceedings of the National Academy of Sciences of the United States of America **103**(8): 2629-2634.

Orlowski, J. and S. Grinstein (2004). "Diversity of the mammalian sodium/proton exchanger SLC9 gene family." Pflügers Archiv European Journal of Physiology **447**: 549-565.

Orr, J. C., V. J. Fabry, O. Aumont, L. Bopp, S. C. Doney, R. A. Feely, A. Gnanadesikan, N. Gruber, A. Ishida, F. Joos, R. M. Key, K. Lindsay, E. Maier-Reimer, R. Matear, P. Monfray, A. Mouchet, R. G. Najjar, G. Plattner, K. B. Rodgers, C. L. Sabine, J. L. Sarmiento, R. Schlitzer, R. D. Slater, I. J. Totterdell, M. Weirig, Y. Yamanaka and A. Yool (2005). "Anthropogenic ocean acidification over the twenty-first century and its impact on calcifying organisms." Nature **437**(7059): 681-686.

Palmer, M. R., P. N. Pearson and S. J. Cobb (1998). "Reconstructing Past Ocean pH-Depth Profiles." Science **282**(5393): 1468-1471.

Patel, H. and D. L. Barber (2005). "A developmentally regulated Na-H exchanger in *Dictyostelium discoideum* is necessary for cell polarity during chemotaxis." Journal of Cell Biology **169**(2): 321-329.

Pelis, R. M., J. Zydlewski and S. D. McCormick (2001). "Gill Na^+ -K+-2Cl¸àícotransporter abundance and location in Atlantic salmon: effects of seawater and smolting." American Journal of Physiology - Regulatory, Integrative and Comparative Physiology **280**(6): R1844-R1852.

Piermarini, P. M., D. Weihrauch, H. Meyer, M. Huss and K. W. Beyenbach (2009). "NHE8 is an intracellular cation/H^+ exchanger in renal tubules of the yellow fever mosquito Aedes aegypti." American Journal of Physiology - Renal Physiology **296**(4): F730-F750.

Putney, L. K. and D. L. Barber (2003). "Na-H Exchange-dependent Increase in Intracellular pH Times G2/M Entry and Transition." Journal of Biological Chemistry **278**(45): 44645-44649.

Riebesell, U., V. Fabry and J. Gattuso. (2009). "Guide to Best Practices in Ocean Acidification Research and Data Reporting " Retrieved Septmeber 19 2009, from http://www.epoca-project.eu/index.php/Home/Guide-to-OA-Research/.

Sardet, C., A. Franchi and J. Pouyssegur (1989). "Molecular cloning, primary structure, and expression of the human growth factor-activatable Na^+ H^+ antiporter." Cell **56**(2): 271-280.

Schultheis, P. J., L. L. Clarke, P. Meneton, M. Harline, G. P. Boivin, G. Stemmermann, J. J. Duffy, T. Doetschman, M. L. Miller and G. E. Shull (1998). "Targeted disruption of the murine Na^+ /H^+ exchanger isoform 2 gene causes reduced viability of gastric parietal cells and loss of net acid secretion." The Journal of clinical investigation **101**(6): 1243-53.

Sherwood, L., H. Klandorf and P. H. Yancy (2005). Fluid and Acid-Base Balance. Animal Physiology: From Genes to Organisms. M. Julet. China, Brooks/Cole**:** 608.

Silva, P., R. Solomon, K. Spokes and F. H. Epstein (1977). "Ouabain inhibition of gill Na-K-ATPase: Relationship to active chloride transport." Journal of Experimental Zoology **199**(3): 419-426.

Smith, H. W. (1930). "The absorption and excretion of water and salts by marine teleosts. " American Journal of Physiology -- Legacy Content **93**(2): 480-505.

Soleimani, M., G. Singh, G. L. Bizal, S. R. Gullans and J. A. McAteer (1994). "Na^+ /H^+ exchanger isoforms NHE-2 and NHE-1 in inner medullary collecting duct cells. Expression, functional localization, and differential regulation." Journal of Biological Chemistry **269**(45): 27973-27978.

Solomon, S., D. Qin, M. Manning, Z. Chen, M. Marquis, K. B. Averyt, M. Tignor and H. L. Miller (2007). Climate change 2007: the physical science basis. Contribution of Working Group I to the Fourth Assessment Report of the Intergovernmental Panel on Climate Change. Cambridge, United Kingdom and New York, NY, USA 996.

Sullivan, M. (2006). Recovery strategy for boreal felt lichen (*Erioderma pedicellatum*) in New Brunswick, Canada. . Fredericton, New Brunswick Department of Natural Resources.

Tips, A., L. Schoofs, L. Paemen, K. Hendrickx and A. De Loof (1997). "False Positive Immunostaining ofLocustaNeurosecretory Cells with a Variety of Preimmune Sera." General and Comparative Endocrinology **106**(2): 231-240.

Toews, D., G. Holeton and N. Heisler (1983). "Regulation of the acid-base status during environmental hypercapnia in the marine teleost fish Conger conger." Journal of Experimental Biology **107**(1): 9-20.

Tse, C. M., S. R. Brant, M. S. Walker, J. Pouyssegur and M. Donowitz (1992). "Cloning and sequencing of a rabbit cDNA encoding an intestinal and kidney-specific Na^+ /H^+ exchanger isoform (NHE-3)." Journal of Biological Chemistry **267**(13): 9340-9346.

Tse, C. M., S. A. Levine, C. H. Yun, M. H. Montrose, P. J. Little, J. Pouyssegur and M. Donowitz (1993). "Cloning and expression of a rabbit cDNA encoding a serum-activated ethylisopropylamiloride-resistant epithelial Na^+ /H^+ exchanger isoform (NHE-2)." Journal of Biological Chemistry **268**(16): 11917-11924.

Uniprot (2007). S9A11_HUMAN.

Vallon, V., J.-R. Schwark, K. Richter and M. Hropot (2000). "Role of Na^+/H^+ exchanger NHE3 in nephron function: micropuncture studies with S3226, an inhibitor of NHE3." American Journal of Physiology - Renal Physiology **278**(3): F375-F379.

Volff, J. N. (2004). "Genome evolution and biodiversity in teleost fish." Heredity **94**(3): 280-294.

Wakabayashi, S., P. Fafournoux, C. Sardet and J. Pouyss√©gur (1992). "The Na^+/H^+ antiporter cytoplasmic domain mediates growth factor signals and controls "H(+)-sensing"." Proceedings of the National Academy of Sciences **89**(6): 2424-2428.

Wakabayashi, S., T. Pang, X. Su and M. Shigekawa (2000). "A Novel Topology Model of the Human Na^+/H^+ Exchanger Isoform 1." Journal of Biological Chemistry **275**(11): 7942-7949.

Wakabayashi, S., M. Shigekawa and J. Pouyssegur (1997). "Molecular physiology of vertebrate Na^+/H^+ exchangers." Physiological Reviews **77**(1): 51-74.

Wall, B. P., A. Morrison-Shetlar and J. B. Claiborne (2001). "Effect of environmental salinity and hypercapnia on NHE2-like and NHE3-like protein expression in the gill of mummichog (*Fundulus heteroclitus*) " The Bulletin, MDI Biological Laboratory **40**: 58-59.

Wang, D., S. M. King, T. A. Quill, L. K. Doolittle and D. L. Garbers(2003). "A new sperm-specific Na^+/H^+ Exchanger required for sperm motility and fertility." Nat Cell Biol **5**(12): 1117-1122.

Wang, T., C.-L. Yang, T. Abbiati, P. J. Schultheis, G. E. Shull, G. Giebisch and P. S. Aronson (1999). "Mechanism of proximal tubule bicarbonate absorption in NHE3 null mice." American Journal of Physiology - Renal Physiology **277**(2): F298-F302.

Wang, Z., J. Orlowski and G. E. Shull (1993). "Primary structure and functional expression of a novel gastrointestinal isoform of the rat Na/H exchanger." Journal of Biological Chemistry **268**(16): 11925-11928.

Weiss, R. F. (1970). "The solubility of nitrogen, oxygen and argon in water and seawater." Deep Sea Research and Oceanographic Abstracts **17**(4): 721-735.

Wilson, J. M. and P. Laurent (2002). "Fish gill morphology: inside out." Journal of Experimental Zoology **293**(3): 192-213.

Wilson, J. M., P. Laurent, B. L. Tufts, D. J. Benos, M. Donowitz, A. W. Vogl andD. J. Randall (2000). "NaCl uptake by the branchial epithelium in freshwater teleost fish:

an immunological approach to ion-transport protein localization." Journal of Experimental Biology **203**(15): 2279-2296.

Wootton, J. T., C. A. Pfister and J. D. Forester (2008). "Dynamic patterns and ecological impacts of declining ocean pH in a high-resolution multi-year dataset." Proceedings of the National Academy of Sciences.

Wood, C. M. (1991). "Branchial ion and acid-base transfer in freshwater teleost fish: environmental hyperoxia as a probe " Physiological zoology **64**(1): 68-102.

Yun, C. H., C. M. Tse, S. Nath, S. L. Levine and M. Donowitz(1995). "Structure/function studies of mammalian Na-H exchangers--an update." Journal of Physiology **482**(P): 1S-b-6.

Zeebe, R. and D. Wolf-Gladrow (2009). Carbon dioxide, dissolved (ocean). Encyclopedia of paleoclimatology and ancient environments V. Gornitz. Dordrecht, Springer**:** 123-127.

Zizak, M., M. E. Cavet, D. Bayle, C. M. Tse, S. Hallen, G. Sachs and M. Donowitz (2000). "Na^+ /H^+ Exchanger NHE3 Has 11 Membrane Spanning Domains and a Cleaved Signal Peptide:Topology Analysis Using In Vitro Transcription/Translation." Biochemistry **39**(27): 8102-8112.